Monitoring of greenhouse gases and aerosols at Svalbard and Birkenes in 2013

Annual report

COLOPHON

Author(s)

C.L. Myhre, O. Hermansen, M. Fiebig, C. Lunder, A.M. Fjæraa, K. Stebel, T. Svendby, N. Schmidbauer, T. Krognes, W. Aas

Title – Norwegian and English

Monitoring of greenhouse gases and aerosols at Svalbard and Birkenes in 2013 - Annual report
Overvåking av klimagasser og partikler på Svalbard og Birkenes i 2012: Årsrapport

Summary – sammendrag

The report summaries the activities and results of the greenhouse gas monitoring at the Zeppelin Observatory situated on Svalbard in Arctic Norway during the period 2001-2013 and the greenhouse gas monitoring and aerosol observations from Birkenes for 2009-2013.

Rapporten presenterer aktiviteter og måleresultater fra klimagassovervåkingen ved Zeppelin observatoriet på Svalbard for årene 2001-2013 og klimagassmålinger og klimarelevant partikkelmålinger fra Birkenes for 2009 2013.

4 emneord

Drivhusgasser, partikler, Arktis, halokarboner

4 subject words

Greenhouse gases, aerosols, Arctic, halocarbons

Front page photo

Svalbard, Ny-Ålesund. Photo: Kjetil Tørseth, NILU.

Preface

This report presents results from the monitoring of greenhouse gases and aerosol properties in 2013. The aerosol results are focusing on the understanding of the interactions between aerosols and radiation. The observations are done at two atmospheric supersites; one regional background site in southern Norway and one Arctic site. The observations made are part of the national monitoring programme conducted by NILU on behalf of The Norwegian Environment Agency.

The monitoring programme includes measurements of 23 greenhouse gases at the Zeppelin Observatory in the Arctic; and this includes also a long list of halocarbons, which are not only greenhouse gases but also ozone depleting substances. In 2009, NILU upgraded and extended the observational activity at the Birkenes Observatory in Aust-Agder and from 2010, the national monitoring programme was extended to also include the new greenhouse gas observations from Birkenes and selected aerosol observations particularly relevant for the understanding of the interactions between aerosols and radiation.

The present report is one out of a series of four annual reports for 2013, which all cover the national monitoring of atmospheric composition in the Norwegian rural background environment. The other three reports are published separately, of which the first focuses on atmospheric composition and deposition of air pollution of particulate and gas phase of inorganic constituents, particulate carbonaceous matter, ground level ozone and particulate matter. The second one focuses on persistent organic pollutants and heavy metals, the third covers the monitoring of the ozone layer and UV, whereas this is the final one covering climate gases and aerosol particles influence on climate.

Data and results from the national monitoring programme are also included in various international programmes, including: EMEP (European Monitoring and Evaluation Programme) under the CLTRAP (Convention on Long-range Transboundary Air Pollution), AGAGE (Advanced Global Atmospheric Gases Experiment), CAMP (Comprehensive Atmospheric Monitoring Programme) under OSPAR (the Convention for the Protection of the marine Environment of the North-East Atlantic) and AMAP (Arctic Monitoring and Assessment Programme). Data from this report are also contributing to European Research Infrastructure networks ACTRIS (Aerosols, Clouds, and Trace gases Research InfraStructure Network) and ICOS (*Integrated Carbon Observation System*).

All measurement data presented in the current report can be received by contacting NILU, or they can be downloaded directly from the database: http://ebas.nilu.no.

A large number of persons at NILU have contributed to the current report, including those responsible for sampling, technical maintenance, chemical analysis and quality control and data management. In particular Cathrine Lund Myhre (coordinating the program), Ove Hermansen, Chris Lunder, Terje Krognes, Norbert Schmidbauer, Ann Mari Fjæraa, Kerstin Stebel, Markus Fiebig, and Tove Svendby. Berit Modalen is especially acknowledged for compiling this report.

Kjeller, November 2014

Cathrine Lund Myhre
Senior Scientist,
Dep. Atmospheric and Climate Research

Content

Summary

This annual report describes the activities and main results of the programme "*Monitoring of greenhouse gases and aerosols at the Zeppelin Observatory, Svalbard, and Birkenes Observatory, Aust-Agder, Norway*". This is a part of the Governmental programme for monitoring pollution in Norway. The report comprises the 2013 measurements of all natural well mixed greenhouse gases, the most important anthropogenic greenhouse gases and various particle's properties with high relevance to climate and climate change. Many of the gases do also have strong ozone depleting effect. For the 23 greenhouse gases included, The report include the development and trends for the period 2001-2013, in addition to daily and annual mean observations.

The measurements at Zeppelin Observatory characterises the development in the Arctic region, and Birkenes Observatory is located in an area in southern Norway most affected by long-range transport of pollutants. The observations of CO_2 and CH_4 at Birkenes is also highly influenced by the local vegetation and terrestrial interactions, important for the understanding of the carbon cycle.

The results and measurements show that the concentration in the atmosphere of the main greenhouse gases with high anthropogenic emissions has been increasing over the period of investigation since 2001, except for Chlorofluorocarbons (CFCs) and a few halogenated gases. In 2013 there were new record concentrations of all the main greenhouse gases CO_2, CH_4 and N_2O at Zeppelin Observatory, and also in CO_2, and CH_4, the only well-mixed greenhouse gases measured at Birkenes. The development is in accordance with the global development as well.

The development in the CFCs and a few of the replacement gases are promising. These gases have strong ozone depleting effect and are regulated through the successful Montreal protocol. The positive effect of this regulation on the recovery of the ozone layer is well documented, and the CFCs measured at Zeppelin is now declining or at least stabilised. For the Hydrochlorofluorocarbons (HCFC) which are CFC replacement gases, this is the first year we detected a reduction in the development of the concentration for one of these components, HCFC-142b. Furthermore it is worth to note that both dichloromethane (CH_2Cl_2) and methyl chloride (CH_3Cl) have a strong increase from 2012 to 2013, ca 20% in both compounds. These gases have both natural and anthropogenic sources and also short lifetime thus the compounds respond rapidly to emission changes. A larger focus on the understanding of the sources and recent development of these compounds are important now.

Aerosol properties at Birkenes are mainly determined by long-range transport of air pollution from continental Europe, Arctic air, as well as regional sources like biogenic particle formation and regional pollution events. These two regional sources show distinct and opposite annual cycles. Being controlled by photochemical reactions, biogenic particle formation peaks in summer, whereas regional pollution events occur most often in winter time. Occurrence of regional pollution events is associated with a higher fraction of absorbing aerosol particles. The time series of aerosol properties are still too short for trend analysis.

Sammendrag (Norwegian)

Denne årsrapporten beskriver aktiviteter og hovedresultater fra programmet "Overvåking av klimagasser og aerosoler på Zeppelin-observatoriet, Svalbard og Birkenes-observatoriet, Aust-Agder, Norge". Programmet er en del av det statlige programmet for overvåking av forurensning i Norge. Rapporten inkluderer 2013-målingene av alle naturlige godt blandede drivhusgasser (WMGHGs), de viktigste klimagassene med utelukkende menneskeskapte kilder, og ulike partiklers egenskaper som har høy relevans for stråling og klimaendringer. Mange av klimagassene som rapporteres har også sterk ozonreduserende effekt. Rapporten omfatter utvikling og trender for perioden 2001-2013 for alle de 23 inkluderte klimagassene, i tillegg til daglige og årlige gjennomsnittsobservasjoner.

Målingene på Zeppelin-observatoriet karakteriserer utviklingen i Arktis, og Birkenes-observatoriet ligger i det området i Sør-Norge som er mest berørt av langtransportert forurensning. Observasjonene av CO_2 og CH_4 på Birkenes er også sterkt påvirket av den lokale vegetasjonen og terrestriske vekselvirkninger, noe som er viktig for forståelsen av karbonkretsløpet.

Resultater og målinger viser at konsentrasjonen av de viktigste klimagassene med høye menneskeskapte utslipp i atmosfæren har økt i løpet av overvåkningsperioden siden 2001. Unntakene er klorfluorkarboner (KFK) og noen halogenerte gasser. I 2013 ble det observert nye rekordkonsentrasjoner av alle de viktigste klimagassene; CO_2, CH_4 og N_2O ved Zeppelin-observatoriet, og på Birkenes CO_2 og CH_4. Dette er de eneste godt blandede drivhusgassene som måles på Birkenes. Utviklingen er forøvrig i samsvar med den globale utviklingen.

Utviklingen for KFK-er og noen av erstatningsgassene er lovende. Disse gassene har sterk ozonreduserende effekt, og er regulert gjennom den vellykkede Montreal-protokollen. Den positive effekten av denne forskriften om styrking av ozonlaget er godt dokumentert, og KFK-nivåene målt ved Zeppelin er nå fallende eller i det minste stabilisert. For hydroklorfluorkarboner (HKFK-er), som er erstatningsgasser for KFK-er, er dette det første året vi har registrert en reduksjon i utviklingen av konsentrasjonen for en av disse komponentene, HKFK-142b. Videre er det verdt å merke seg at både diklormetan (CH_2Cl_2) og metylklorid (CH_3Cl) øker kraftig fra 2012 til 2013, ca 20% i begge forbindelser. Disse gassene har både naturlige og menneskeskapte kilder, i tillegg til kort levetid, dermed reagerer forbindelsene raskt på utslippsendringer. Det er viktig å legge større vekt på å forstå kildene til og den nye utviklingen av disse forbindelsene i kommende år.

Aerosolegenskapene ved Birkenes er i hovedsak bestemt av den langtransporterte luftforurensningen fra det kontinentale Europa, den arktiske lufta, samt regionale kilder som biogen partikkeldannelse og regionale forurensningshendelser. Disse to regionale kildene viser distinkte og motsatte årlige sykluser. Siden de kontrolleres av fotokjemiske reaksjoner, når den biogene partikkeldannelsen sin topp om sommeren, mens regionale forurensningshendelser oftest oppstår om vinteren. Forekomsten av regionale forurensningshendelser assosieres med en høyere andel av absorberende aerosolpartikler. Tidsseriene med aerosolegenskaper er fortsatt for korte for trendanalyse.

1. The monitoring programme in 2013

The atmospheric monitoring programme presented in this report focuses on the level of greenhouse gases and aerosols properties relevant for the interaction of aerosols and radiation in the Norwegian background air and in the Arctic. The main objectives are to quantify the levels of greenhouse gases including ozone depleting substances, describe the relevant optical and physical properties of aerosols, and document the development over time. Measurements of the amount of greenhouse gases and aerosol properties are core data for studies and assessments of climate change, and also crucial in order to evaluate if mitigation strategies work as expected. The Norwegian monitoring sites are located in areas where the influence of local sources are minimal, and thus the sites are representative for a wider region and long-term atmospheric changes.

Figure 1: Location of NILU's atmospheric supersites measuring greenhouse gases and aerosol properties.

The Norwegian greenhouse gas and aerosol monitoring programme is set up to meet national and international needs for greenhouse gas and aerosol measurement data, both for the scientific community, environmental authorities and stakeholders. The targets set by the Kyoto protocol first and second commitment periods is to reduce the total emissions of greenhouse gases from the industrialized countries. To follow up on this, negotiations under the UNFCCC are under way to develop a new international climate change agreement that will cover all countries. The new agreement is expected to be adopted in 2015, at the Paris climate conference. As preparation for this, EU Heads of State and Governments agreed in October 2014 on the headline targets and the architecture for the EU framework on climate and energy for 2030. The agreed targets include a cut in greenhouse gas emissions by at least 40% by 2030 compared to 1990 levels.

In 1987 the Montreal Protocol was signed and entered into force in 1989 in order to reduce the production, use and eventually emission of the ozone-depleting substances (ODS). The amount of most ODS in the troposphere is now declining slowly and is expected to be back to pre-1980 levels around year 2050. It is central to follow the development of the concentration of these ozone depleting gases in order to verify that the Montreal Protocol and its amendments work as expected. The development of the ozone layer above Norway is monitored closely, and the results of the national monitoring of ozone and UV is presented in "*Monitoring of the atmospheric ozone layer and natural ultraviolet radiation: Annual report 2013*" (Svendby et al, 2014). The ozone depleting gases and their replacement gases are strong greenhouse gases making it even more important to follow the development of their concentrations.

As a response to the need for monitoring of greenhouse gases and ozone depleting substances, the Norwegian Environment Agency and NILU – Norwegian Institute for Air Research signed a

contract commissioning NILU to run a programme for monitoring greenhouse gases at the Zeppelin Observatory, close to Ny-Ålesund in Svalbard in 1999. This national programme includes now monitoring of 23 greenhouse gases at the Zeppelin Observatory in the Arctic, many of them also ozone depleting substances. In 2009, NILU upgraded and extended the observational activity at the Birkenes Observatory in Aust-Agder. From 2010, the Norwegian Environment Agency/NILU monitoring programme was extended to also include the new observations from Birkenes of the greenhouse gases CO_2 and CH_4 and selected aerosol observations particularly relevant for the understanding of climate change. Relevant components are also reported in "*Monitoring of long-range transported air pollutants in Norway, annual report 2013*" (Aas et al, 2014), this incudes particulate and gaseous inorganic constituents, particulate carbonaceous matter, ground level ozone and particulate matter for 2013. This report also includes a description of the weather in Norway in 2013 in Chap. 2, which is relevant for the observed concentrations of greenhouse gases and aerosols.

The location of both sites are shown in Figure 1, and a picture of the sites are shown in Figure 2.

The unique location of the Zeppelin Observatory at Svalbard, together with the infrastructure of the scientific research community in Ny-Ålesund, makes it ideal for monitoring the global changes of concentrations of greenhouse gases and aerosols in the atmosphere. There are few local sources of emissions, and the Arctic location is also important as the Arctic is a particularly vulnerable region. The observations at the Birkenes Observatory complement the Arctic site. Birkenes Observatory is located in a forest area with few local sources. However, the Observatory often receives long-range transported pollution from Europe and the site is ideal to analyse the contribution of long range transported greenhouse gases and aerosol properties.

Figure 2: The two atmospheric supersites included in this programme, Zeppelin above and Birkenes to the left

Data and results from the national monitoring programme are also included in various international regional programmes. Both sites are contributing to EMEP (European Monitoring and Evaluation Programme) under the CLTRAP (Convention on Long-range Transboundary Air

Pollution). Data from the sites are also reported to CAMP (Comprehensive Atmospheric Monitoring Programme) under OSPAR (the Convention for the Protection of the marine Environment of the North-East Atlantic, http://www.ospar.org); AMAP (Arctic Monitoring and Assessment Programme http://www.amap.no), WMO/GAW (The World Meteorological Organization, Global Atmosphere Watch programme, http://www.wmo.int) and AGAGE (Advanced Global Atmospheric Gases Experiment)

Zeppelin and Birkenes are integrated into two central EU research infrastructures focusing on climate forcers. One is ICOS (Integrated Carbon Observation System) focusing on the understanding of carbon cycle and the other is ACTRIS (Aerosols, Clouds, and Trace gases Research InfraStructure Network, www.actris.net) focusing on clouds and the short-lived aerosol climate forcers and related reactive gases. International collaboration and harmonisation of these types of observations are crucial for improved processes understanding and satisfactory quality to assess trends.

NILU host the data centres of the European Monitoring and Evaluation Programme (EMEP), ACTRIS (Aerosols, Clouds, and Trace gases Research InfraStructure Network) and the WMO Global Atmosphere Watch (GAW) World Data Centre for Aerosol (WDCA) and numerous other projects and programs (e.g. AMAP, HELCOM) and all the data reported are found in the EBAS data base: http://ebas.nilu.no. All data from these frameworks are reported to this data base.

Compiled key information on the national monitoring programme at the sites are listed in Table 1. More detailed information on the monitoring program and measurement frequencies are provided in Appendix II. For the measurements of aerosol properties more details are also presented in table 6 in chapter 4.

Table 1: Summary of the ongoing relevant measurement program run under NILU responsibility at Birkenes and Zeppelin Observatory 2013.

Component	Birkenes Start	Zeppelin Start	Report to international networks	Comment
CO_2	2009	2012	ICOS (establishes in 2014 - 2015)	Measured at Zeppelin since 1988 by Univ. Stockholm. NILU measure CO2 at Zeppelin since 2009[1]
CH_4	2009	2001	EMEP, ICOS (establishes in 2014-2015)	
N_2O	-	2009	ICOS establishes in 2014-2015)	
CO	-	2001	ICOS (establishes in 2014-2015)	
Ozone (surface)	1985	1989	EMEP	Reported in M-203/2014, Aas et al, 2014.
CFC-11*				
CFC-12*				
CFC-113*				
CFC-115*				
HCFC-22				
HCFC-141b				
HCFC-142b				
HFC-125				
HFC-134a				
HFC-152a				*The measurements of "*" these components are not within the required precision of AGAGE, but a part of the AGAGE quality assurance program. Other components are also measured (like new replacements), but lack funding and calibration issues need to be solved.
H-1211	2001	2001	AGAGE	
H-1301				
CH_3Cl				
CH_3Br				
CH_2Cl_2				
$CHCl_3$				
CH_3CCl_3				
$CHClCCl_2$				
CCl_2CCl_2				
SF_6,				
NMHC and VOC	1994 (carbonyls)	2010	AGAGE, ACTRIS (ethane, propane, benzene, toluene)	Other components are also measured, but lack funding and calibration issues need to be solved.
Aerosol measurements				
Absorption properties	2009	-	EMEP, ACTRIS	Measured by Univ. of Stockholm at Zeppelin
Scattering properties	2009	-	EMEP, ACTRIS	Measured by Univ. of Stockholm at Zeppelin
Number Size Distribution	2009	-	EMEP, ACTRIS	Measured by Univ. of Stockholm at Zeppelin
Cloud Condensation Nuclei	2012	-	ACTRIS	Zeppelin: In collaboration with Korean Polar Research Institute
Aerosol Optical depth	2010	2007	AERONET (Birkenes), GAW-PFR (Ny-Ålesund)	
PM_{10}	2001		EMEP	
$PM_{2.5}$	2001		EMEP	
Chemical composition -inorganic	1978	1979	EMEP	Reported in M-203/2014, Aas et al, 2014.
Chemical composition - carbonaceous matter	2001		EMEP	

---

[1] CO2 at Zeppelin is not included in the national monitoring program, but the results are included in the report due to the high relevance.

2. Introduction to greenhouse gases, aerosols and their climate effects

The IPCC's Fifth Assessment Report and the contribution from Working Group I "*Climate Change 2013: The Physical Science Basis*" was published in September 2013. This substantial climate assessment report presents new evidence of past and projected future climate change from numerous independent scientific studies ranging from observations of the climate system, paleoclimate archives, theoretical studies on climate processes and simulations using climate models. Their main conclusion is that:

> "*Warming of the climate system is unequivocal, and since the 1950s, many of the observed changes are unprecedented over decades to millennia. The atmosphere and ocean have warmed, the amounts of snow and ice have diminished, sea level has risen, and the concentrations of greenhouse gases have increased*"
> (*IPCC, Summary for policy makers, WG I, 2013*)

Their conclusions are based on a variety of independent indicators, some of them are observations of atmospheric compositional change. The overall conclusion with respect to the development of the concentrations of the main greenhouse gases is:

> "*The atmospheric concentrations of carbon dioxide, methane, and nitrous oxide have increased to levels unprecedented in at least the last 800,000 years. Carbon dioxide concentrations have increased by 40% since pre-industrial times, primarily from fossil fuel emissions and secondarily from net land use change emissions. The ocean has absorbed about 30% of the emitted anthropogenic carbon dioxide, causing ocean acidification*"
> (*IPCC, Summary for policy makers, 2013*)

In particular chapter 2, "*Observations: Atmosphere and Surface*", presents all types of atmospheric and surface observations, including observations of greenhouse gases since the start of the observations in mid-1950s and changes in aerosols since the 1980s. This was the first time long term changes of aerosols are included in the report, based on global and regional measurement networks and satellite observations. The main conclusion with respect to development of the aerosol levels is that **"*It is very likely that aerosol column amounts have declined over Europe and the eastern USA since the mid 1990s and increased over eastern and southern Asia since 2000*"** (Hartmann et al, 2013). This is important since the total effect of aerosols is atmospheric cooling, counteracting the effect of greenhouse gases. The changes in Europe and USA is mainly due to mitigation strategies of e.g. sulphur, while the emissions are increasing rapidly in Asia, including increasing emissions of the warming component black carbon.

The basic metric to compare the effect of the various climate change drivers is radiative forcing (RF), as in previous reports. Most other metrics include this concept. RF is the net change in the energy balance of the Earth system due to some imposed perturbation. RF provides a quantitative basis for comparing some aspects of the potential climate response to different imposed agents. Forcing is often presented as the radiative change from one time-period to

another, such as pre-industrial to present-day. In the last report it was also introduced a new concept, the effective radiative forcing (ERF). For many forcing agents the RF is an appropriate way to compare the relative importance of their potential climate effect. However, rapid adjustments in the troposphere can either enhance or reduce the perturbations, leading to large differences in the forcing driving the long-term climate change. The ERF concept aims to take this into account and is the change in net TOA (Top Of Atmosphere) downward radiative flux after allowing for atmospheric temperatures, water vapour and clouds to adjust, but with surface temperature or a portion of surface conditions unchanged (*Myhre et al*, 2013b). Figure 3 shows the RF and ERF of the main components referring to a change in the atmospheric level since 1750, pre-industrial time.
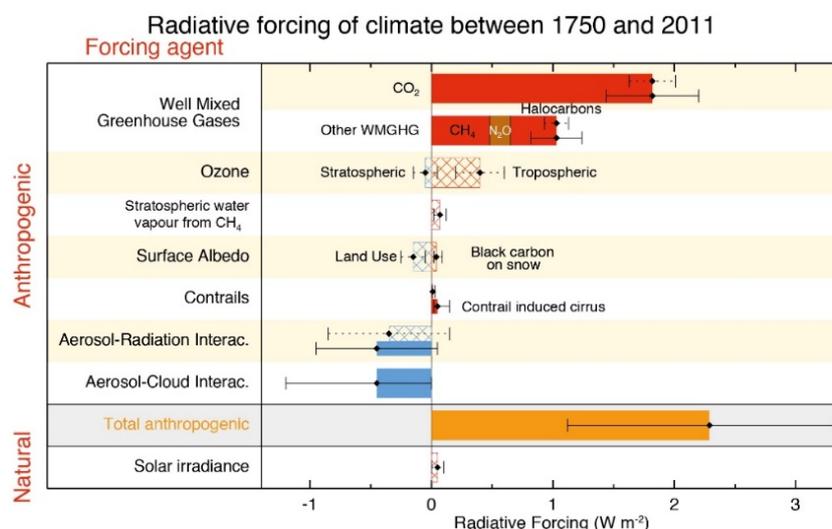
Figure 3: Bar chart for RF (hatched) and ERF (solid) for the period 1750-2011. Uncertainties (5 to 95% confidence range) are given for RF (dotted lines) and ERF (solid lines). (Taken from Myhre et al, 2013b).

Total adjusted anthropogenic forcing is 2.29 W m^{-2}, [1.13 to 3.33], and the main anthropogenic component driving this is CO_2 with a total RF of 1.82 W m^{-2}. The direct and indirect effect of aerosols are cooling and calculated to -0.9 W m^{-2}. The diagram in Figure 4 shows a comparison in percent % of the various contribution from the long-lived greenhouse gases to the total forcing of the well-mixed greenhouse gases, based on 2011 levels.

Figure 4: The contribution (in %) of the well-mixed greenhouse gases to the total forcing of the well-mixed greenhouse gases for the period 1975-2011 based on estimate in Table 8.2, Chap 8, IPCC (Myhre et al, 2013b).

Figure 5: RF bar chart for the period 1750-2011 based on emitted compounds (gases, aerosols or aerosol precursors) or other changes. Red (positive RF) and blue (negative forcing) are used for emitted components which affect few forcing agents, whereas for emitted components affecting many compounds several colours are used as indicated in the inset at the upper part the 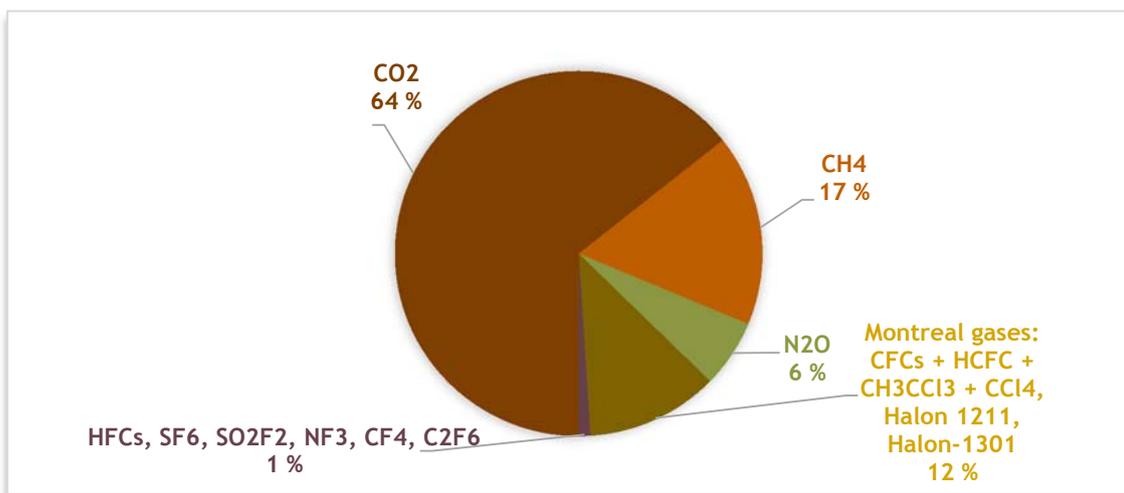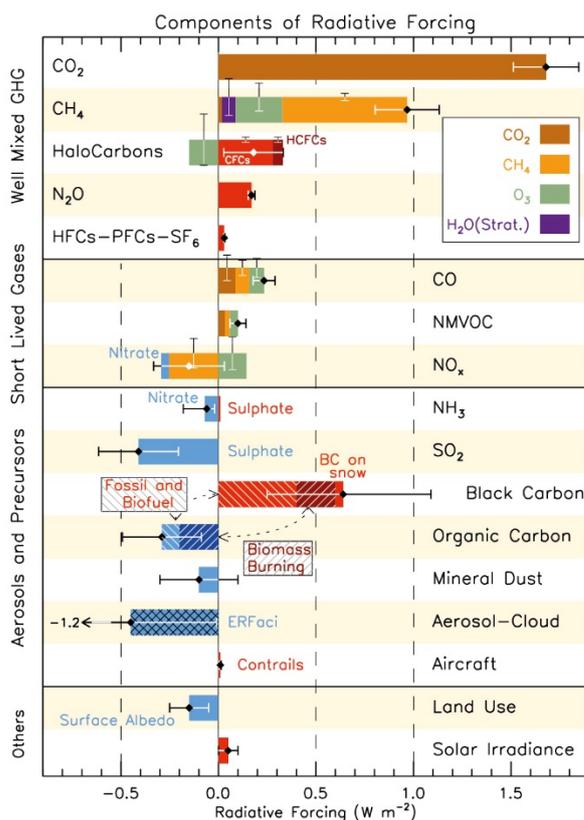figure. The vertical bars indicate the relative uncertainty of the RF induced by each component. Their length is proportional to the thickness of the bar, that is, the full length is equal to the bar thickness for a ±50% uncertainty. The net impact of the individual contributions is shown by a diamond symbol and its uncertainty (5 to 95% confidence range) is given by the horizontal error bar. ERFaci is ERF due to aerosol-cloud interaction. BC and OC are co-emitted, especially for biomass burning emissions (given as Biomass Burning in the figure) and to a large extent also for fossil and biofuel emissions (given as Fossil and Biofuel in the figure where biofuel refers to solid biomass fuels) (The Figure is taken from Myhre et al, 2013b).

An interesting and more detailed picture of the influence of variouss emissions on the RF is illustrated in Figure 5. This Figure shows the forcing since 1750 by emitted compounds, to better illustrate the effects of emissions and potential impact of mitigations. As seen, the number of emitted compounds and changes leading to RF is larger than the number of compounds causing RF directly. This is due to indirect effects, in particular components involved in atmospheric chemistry that affects e.g. CH_4 and ozone. Emissions of CH_4, CO, and NMVOC all lead to excess CO_2 as one end product if the carbon is of fossil origin, and this is the reason why the RF of direct CO_2 emissions is slightly lower than the RF of abundance change of CO_2 in Figure 3. Note also that for CH_4, the contribution from emission is estimated to be almost twice as large as that from the CH_4 concentration change, 0.97 W m^{-2} versus 0.48 W m^{-2} shown in Figure 3 and Figure 5 respectively. This is because emission of CH_4 leads to ozone production (shown in green colour in the CH_4 bar in Figure 5), stratospheric water vapour, CO_2 (as mentioned above), and importantly affects its own lifetime. As seen from the Figure, there is also a particularly complex picture of the effects of aerosols. Black carbon heats the atmosphere, originating from both fossil fuel, biofuel and biomass burning. The direct effect of black carbon from fossil and biofuel is +0.4 W m^{-2}, while black carbon from biomass burning is 0 in total due to co-emitted effects of organic carbon, cooling the atmosphere and cancelling out the heating effect.

In addition there is a small heating effect of black carbon on snow (0.04 W m^{-2} since 1750). The effect of black carbon on snow since 1750 is currently in the order of one year increase of CO_2 concentration in the atmosphere (around 2 ppm).

3. Observations of greenhouse gases at the Birkenes and Zeppelin Observatories

NILU measures 23 climate gases at the Zeppelin Observatory at Svalbard and 2 at Birkenes, in addition to surface ozone reported in Aas et al (2014). The results from these measurements, and analysis are presented in this chapter. Also observations of CO_2 since 1989 at Zeppelin performed by the Stockholm University - Department of Applied Environmental Science (ITM), are included in the report.

Table 2 summarize the main results for 2013 and the trends over the period 2001-2013. Also a comparison of the main greenhouse gas concentrations at Zeppelin and Birkenes compared to annual mean values given in the 5th Assessment Report of the IPCC (Myhre et al. 2013b) is included.

Table 2: Greenhouse gases measured at Zeppelin and Birkenes; lifetimes in years, global warming potential (GWP) for 100 year horizon, and global mean for 2011 is taken from 5th Assessment Report of the IPCC, Chapter 8 (Myhre et al, 2013b).Global mean is compared to annual mean values at Zeppelin and Birkenes for 2011. Annual mean for 2013, change last year, the trends per year over the period 2001-2013 is included. All concentrations are mixing ratios in ppt, except for methane, nitrous oxide and carbon monoxide (ppb) and carbon dioxide (ppm).

Component		Life-time	GWP	Global mean 2011	Annual mean 2011	Annual mean 2013	Absolute change last year	Trend /yr
Carbon dioxide - Zeppelin	CO_2	-	1	391 ±0.2	392.5	397.3	2.5	-
Carbon dioxide - Birkenes					397.4	400.7	2.8	-
Methane - Zeppelin	CH_4	12.4	28	1803 ±2	1879.6	1897.8	6.0	4.5
Methane - Birkenes					1895.5	1902.3	1.8	-
Carbon monoxide	CO	few months	-	-	115.4	113.1	-7.5	-1.3
Nitrous oxide	N_2O	121	265	324 ±0.1	324.2	326.1	1.1	-
Chlorofluorocarbons								
CFC-11*	CCl_3F	45	4 660	238 ±0.8	238.3	234.9	-1.7	-2.1
CFC-12*	CF_2Cl_2	640	10 200	528 ±1	531.5	525.2	-3.1	-1.9
CFC-113*	CF2ClCFCl2	85	13 900	74.3 ±0.1	74.6	73.4	-0.7	-0.7
CFC-115*	CF_3CF_2Cl	1 020	7 670	8.37	8.4	8.4	0.0	0.0
Hydrochlorofluorocarbons								
HCFC-22	$CHClF_2$	11.9	1 760	213 ±0.1	226.0	236.6	5.1	6.8
HCFC-141b	$C_2H_3FCl_2$	9.2	782	21.4 ±0.1	23.0	25.0	1.0	0.6
HCFC-142b	CH_3CF_2Cl	17.2	1 980	21.2 ±0.2	22.7	23.3	0.2	0.8
Hydrofluorocarbons								
HFC-125	CHF_2CF_3	28.2	3 170	9.58 ±0.04	10.9	15.6	2.0	1.1

* The measurements of these components have higher uncertainty. See Appendix I for more details

Component		Life-time	GWP	Global mean 2011	Annual mean 2011	Annual mean 2013	Absolute change last year	Trend /yr
HFC-134a	CH_2FCF_3	13.4	1 300	62.7 ±0.3	68.4	78.9	5.4	4.7
HFC-152a	CH_3CHF_2	1.5	506	6.4 ±0.1	10.1	10.2	-0.1	0.7
Halons								
H-1211	$CBrClF_2$	16	1 750		4.2	4.0	-0.1	0.0
H-1301	$CBrF_3$	65	7 800		3.3	3.4	0.0	0.0
Halogenated compounds								
Methylchloride	CH_3Cl	1	12	-	508.2	540.5	27.1	0.0
Methylbromide	CH_3Br	0.8	2	-	7.04	7.02	0.0	-0.2
Dichloromethane	CH_2Cl_2	0.4	9	-	41.2	54.1	19.1	1.6
Chloroform	$CHCl_3$	0.4	16	-	11.9	12.7	8.7	1.6
Methylchloroform	CH_3CCl_3	5	160	6.32 ±0.07	6.48	4.48	-0.93	-2.60
Trichloroethylene	$CHClCCl_2$	-	-	-	0.55	0.57	0.1	1.6
Perchloroethylene	CCl_2CCl_2	-	-	-	2.8	2.54	-0.2	-0.1
Sulphurhexafluoride	SF_6	3 200	23 500	7.28 ±0.03	7.49	8.12	0.33	0.3

Greenhouse gases have numerous sources, both anthropogenic and natural. Trends and future changes in concentrations are determined by their sources and the sinks, and in section 3.1 are observations and trends of the monitored greenhouse gases with both natural and anthropogenic sources presented in more detail. In section 3.2 are the detailed results of the ozone depleting substances with purely anthropogenic sources presented.

We have used the method described in Appendix II in the calculation of the annual trends, and also include a description of the me Dichloromethane asurements at Zeppelin at Svalbard and Birkenes Observatory in southern Norway in more details. Generally, Zeppelin Observatory is a unique site for observations of changes in the background level of atmospheric components. All peak concentrations of the measured gases are significantly lower here than at other sites at the Northern hemisphere, due to the station's remote location. Birkenes is closer to the main source areas. Further, the regional vegetation is important for regulating the carbon cycle, resulting in much larger variability in the concentration level compared to the Arctic region.

3.1 Greenhouse gases with natural and anthropogenic sources

The annual mean concentrations for all gases included in the program for all years are given in Appendix I, Table A1 at page 65. All the trends, uncertainties and regression coefficients are found in Table A 2 at page 66. Section 3.1 focuses on the measured greenhouse gases that have both natural and anthropogenic sources.

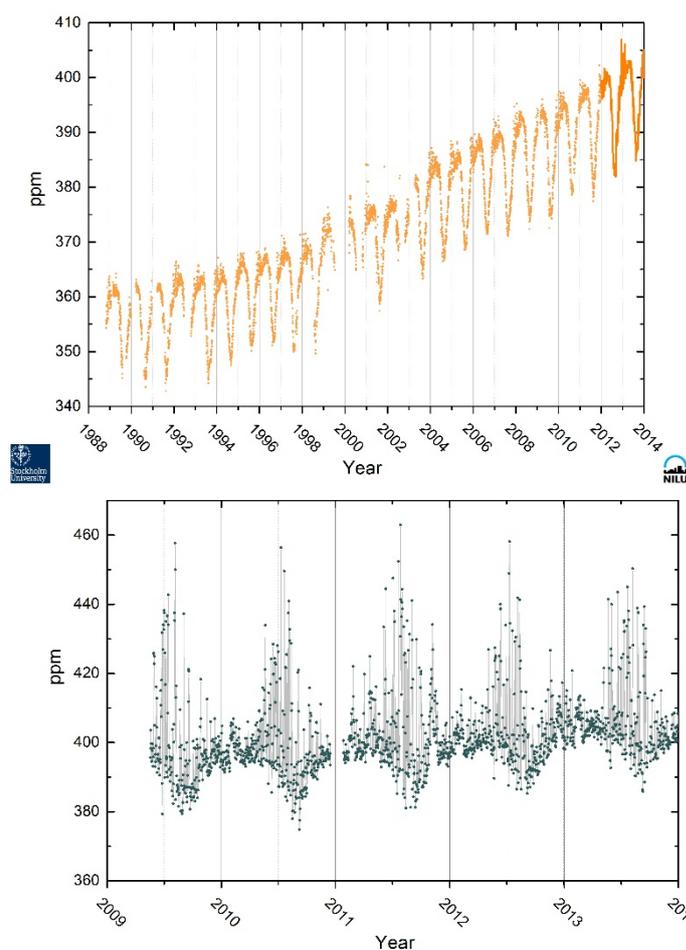## 3.1.1 Carbon dioxide at the Birkenes and Zeppelin Observatories

Carbon dioxide (CO_2) is the most important greenhouse gas with a radiative forcing of 1.82 W m^{-2} since the year 1750, and an increase since the previous IPCC report (AR4, 2007) of 0.16 Wm^{-2} (Myhre et al., 2013b). The increase in forcing is due to the increase in concentrations over these last years. CO_2 is the end product in the atmosphere of the oxidation of all main organic compounds, and it has shown an increase of as much as 40 % since the pre industrial time (Hartmann et al, 2013). This is mainly due to emissions from combustion of fossil fuels and land use change. CO_2 emissions from fossil fuel burning and cement production increased by 2.3% in 2013 since 2012, with a total of 9.9±0.5 GtC (billion tonnes of carbon) equal to 36 GtCO$_2$ emitted to the atmosphere, 61% above 1990 emissions (the Kyoto Protocol reference year). Emissions are projected to increase by a further 2.5% in 2014 according to Global Carbon Project estimates

Figure 6: The atmospheric daily mean CO_2 concentration measured at Zeppelin Observatory for the period mid 1988-2013 is presented in the upper panel. Prior to 2012, ITM University of Stockholm provides all data, shown as dots and the solid line is from the Picarro instrument installed by NILU in 2012. The measurements for Birkenes is shown in the lower panel.

http://www.globalcarbonproject.org.

NILU started CO_2 measurements at the Zeppelin Observatory in 2012. These measurements are not a part of the national monitoring programme, but the results are presented in this report and in Figure 6, together with the time series provided by ITM, University of Stockholm. ITM

provides all data up till 2012 and we acknowledge the effort they have been doing in monitoring CO_2 at the site. Note that the data from ITM are preliminary, and have not undergone full quality assurance. Until 2009 the only Norwegian site measuring well-mixed greenhouse gases (LLGHG) greenhouse gases was Zeppelin, but after upgrading Birkenes there are continuous measurements of CO_2 and CH_4 from mid May 2009 also at this site.

The atmospheric daily mean CO_2 concentration measured at Zeppelin Observatory for the period mid 1988-2013 is presented in **Figure 6** upper panel, together with the shorter time series for Birkenes in the lower panel.

The results show continuous increase since the start of the observations at both sites. As can be seen there are much stronger variability at Birkenes than Zeppelin. At Zeppelin the largest variability is during winter/spring. For Birkenes (green dots in the lower panel) it is clear that the variations are largest during the summer months. In this period, there is a clear diurnal variation with high values during the night and lower values during daytime. This is mainly due to changes between plant photosynthesis and respiration, but also the general larger meteorological variability, particularly during summer contributes to larger variations in the concentrations. In addition to the diurnal variations, there are also episodes with higher levels at both sites due to transport of pollution from various regions. In general, there are high levels when the meteorological situation results in transport from Central Europe or United Kingdom at Birkenes, and central Europe or Russia at Zeppelin. The maximum daily mean value for CO_2 in 2013 was 450.3 ppm at the 8th of August at Birkenes, and at Zeppelin the highest daily mean value was 406 ppm the 6th February.

Figure 7 shows the development of the annual mean concentrations of CO_2 measured at Zeppelin Observatory for the period 1988-2013 in orange together with the values from Birkenes in green since 2010. The global mean values as given by WMO in black. The yearly annual change is shown in the lower panel.

The time series for CO_2 at Birkenes are too short to be used for trend calculations, but the annual change shown in the lower panel show an increase of ca 2 ppm both at Zeppelin, and slightly higher at Birkenes the last years, comparing well with the global mean growth from 2012-2013 which was 2.9 ppm.

3.1.2 Methane at the Birkenes and Zeppelin Observatories

Methane (CH_4) is the second most important greenhouse gas from human activity after CO_2. The radiative forcing is 0.48 W m^{-2} since 1750 and up to 2011 (Myhre et al., 2013b), but as high as 0.97 W m^{-2} for the emission based radiative forcing (Figure 5) due to complex atmospheric effects. In addition to be a dominating greenhouse gas, methane also plays central role for the atmospheric chemistry. The atmospheric lifetime of methane is approx. 12 years when indirect effects are included, as explained in section 2.

The main sources of methane include boreal and tropical wetlands, rice paddies, emission from ruminant animals, biomass burning, and extraction and combustion of fossil fuels. Further, methane is the principal component of natural gas and e.g. leakage from pipelines; off-shore and on-shore installations are a known source of atmospheric methane. The distribution between natural and anthropogenic sources is approximately 40% natural sources, and 60% of the sources are direct a result of anthropogenic emissions. Of natural sources there is a large unknown potential methane source at the ocean floor, so called methane hydrates. Further, a
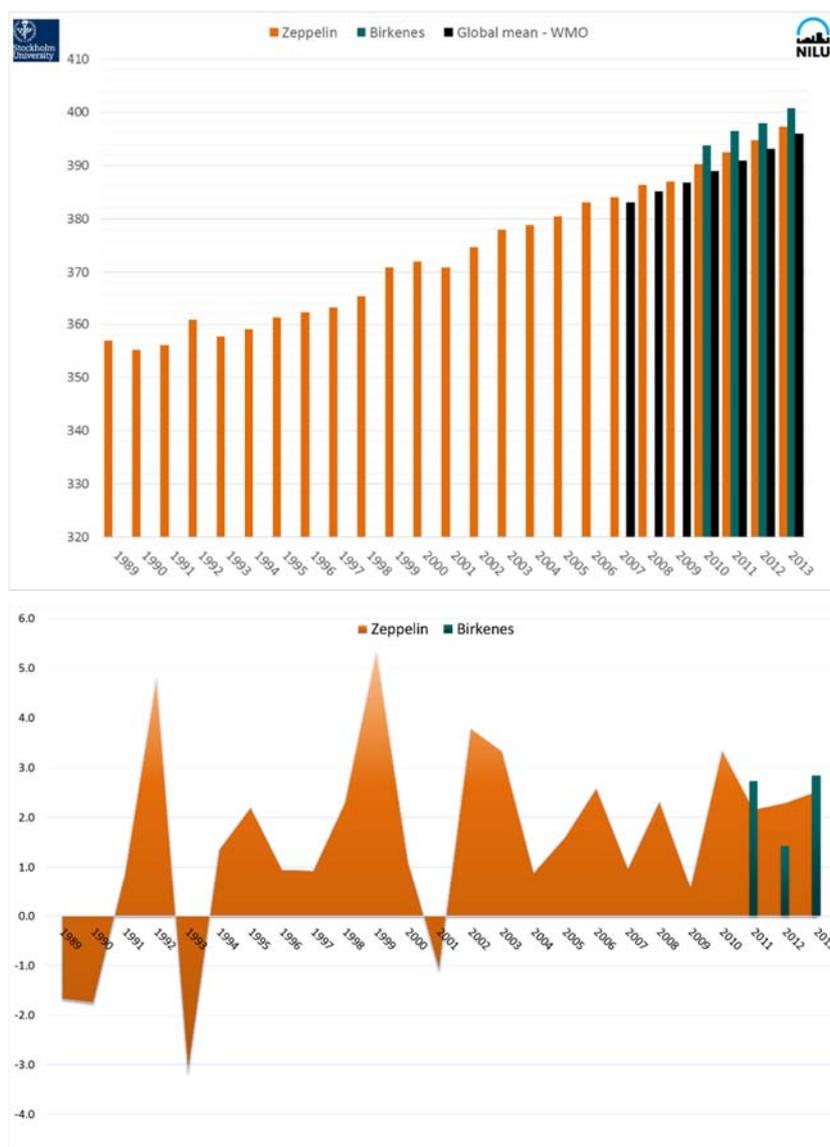
Figure 7: Upper panel: the annual mean concentrations of CO₂ measured at Zeppelin Observatory for the period 1988-2013 shown in orange. Prior to 2012, ITM University of Stockholm provides all data. The annual mean values from Birkenes is shown in green. The global mean values as given by WMO is included in black. The yearly annual change is shown in the lower panel, orange for Zeppelin, green for Birkenes.

large unknown amount of carbon is bounded in the permafrost layer in Siberia and North America and this might be released as methane if the permafrost layer melts as a feedback to climate change.

The average CH_4 concentration in the atmosphere is determined by a balance between emission from the various sources and reaction and removal by free hydroxyl radicals (OH) in the troposphere. In the atmosphere, methane is destroyed by reaction with OH giving water vapour and CO_2. A small fraction is also removed by surface deposition. Since the reaction with OH also represents a significant loss path for the oxidant OH, additional CH_4 emission will suppress OH and thereby increase the CH_4 lifetime, implying further increases in atmospheric CH_4 concentrations (Isaksen and Hov, 1987; Prather et al., 2001). The OH radical has a crucial role in the tropospheric chemistry by reactions with many emitted components and is responsible for the cleaning of the atmosphere (like removal of CO, hydrocarbons, HFCs, and others). A

stratospheric impact of CH$_4$ is due to the fact that CH$_4$ contributes to water vapour build up in this part of the atmosphere, influencing and reducing the stratospheric ozone amount.

The atmospheric mixing ratio of methane was, after a strong increase during the 20th century, relatively stable over the period 1998-2006. The global average change was close to zero for this period, also at Zeppelin. Recently an increase in the methane levels is evident from our observations both at Zeppelin and Birkenes as well as observations at other sites and in the global mean (see e.g. section 2.2.1.1.2 in Hartmann et al, 2013, WMO, 2014).

During 2012 the methane data series from Zeppelin has been revised as part of the EU project InGOS (Integrated non-CO2 Greenhouse gas Observing System) (see Appendix I). All original measurement signals have been processed with new improved software to recalculate every single measurement over the last 12 years as a part of harmonized quality assurance procedures across Europe. Figure 8 depict the daily mean observations of methane at Zeppelin since the start in 2001 in the upper panel and Birkenes since start in 2009 in the lower panel.
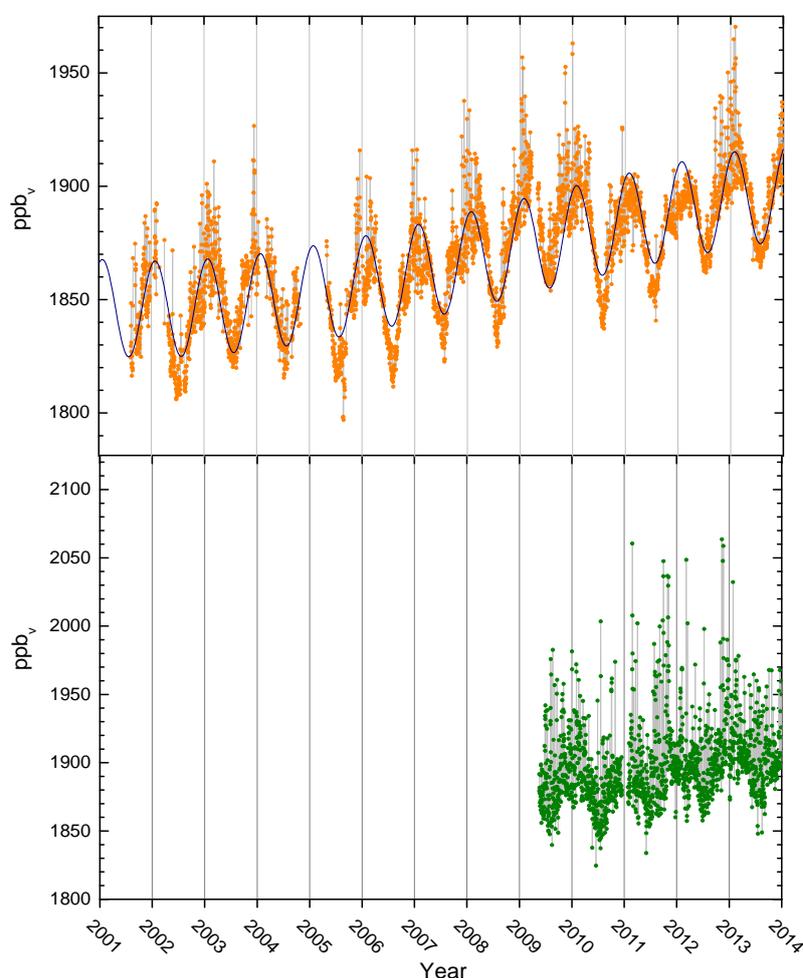
Figure 8: Observations of daily averaged methane mixing ratio for the period 2001-2013 at the Zeppelin Observatory in the upper panel. Orange dots: daily mean observations, blue solid line: empirical modelled background methane mixing ratio. Daily mean observations for Birkenes are shown in the lower panel as green dots.

As can be seen from the Figure there has been an increase in the concentrations of methane observed at both sites the last years, and in general the concentrations are much higher at

Birkenes than at Zeppelin. For both Zeppelin and Birkenes, the diurnal variations are clearly visible, although much stronger at Zeppelin than Birkenes. This is due longer distance to the sources at Zeppelin, and thus the sink through reaction of OH is dominating this and the atmospheric background levels of the compound is detected. The larger variations at Birkenes is explained by the regional sources, both in Norway, as well as episodes of long range transport of pollution from Europe.

At Zeppelin there is now almost 13 years of data, and the trend is calculated. To retrieve the annual trend in the methane for the entire period, the observations have been fitted by an empirical equation. The empirical modelled methane values are shown as the blue solid line in Figure 8. Only the observations during periods with clean air arriving at Zeppelin are used in the model, thus the model represents the background level of methane at the site (this is described in Appendix I). This corresponds to an increasing trend of 4.5 ppb per year, or ca 0.2% per year. The pronounced increase started in November/December 2005 and continued throughout the years 2007 - 2009, and is particularly evident in the late summer-winter 2007, and summer-autumn 2009. The year 2013 showed new record globally, and at Zeppelin (see Figure 9). For the daily mean in Figure 8, the measurements show very special characteristics in 2010 and 2011 at Zeppelin. As can be seen there is remarkable lower variability in the daily mean in 2011 with fewer episodes than the typical situation previous years, and also after summer/autumn 2012. The reason for this is intensively investigated as part of various national and international research programmes, also at NILU. A conclusion is however still not possible to draw. The highest daily mean for CH_4 in 2013 was 6th February, the same day as for CO and CO_2. The right panel in Figure 15 at page 27 show the transport of air this day.

For Birkenes shown in the lower panel, the time series is too short for trend calculations, but a yearly increase is evident since the start 2009. There are also episodes with higher levels due to transport of pollution from various regions. In general, there are high levels when the meteorological situation results in transport from Central Europe.

The annual mean increase in the methane levels the last years is visualized in Figure 9 showing the CH_4 annual mean mixing ratio for the period 2001-2013 from Zeppelin and for Birkenes from 2010-2013. Also the global mean value given by WMO (WMO, 2014) is included for comparison, together with the IPCC global mean value for 2011.
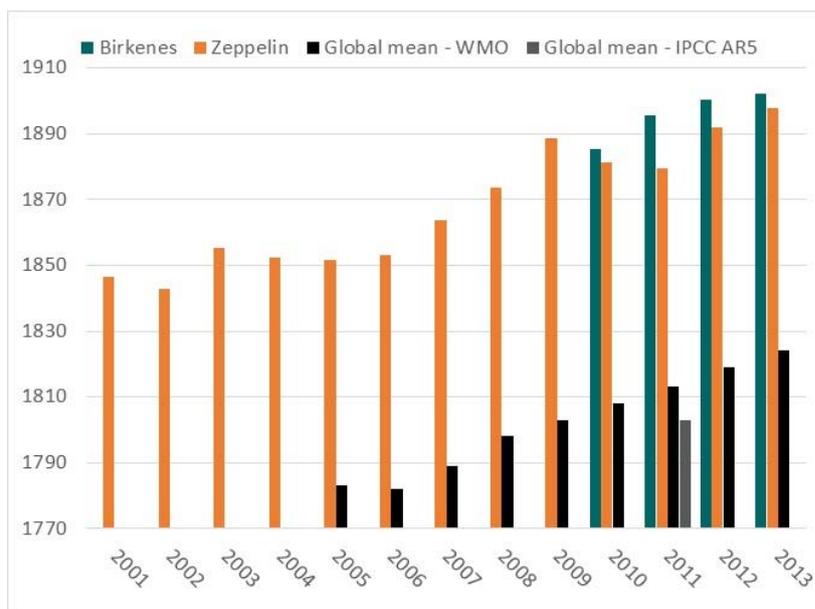
Figure 9: Development of the annual mean mixing ratio of methane in ppb measured at the Zeppelin Observatory (orange bars) for the period 2001-2013, Birkenes for the period 2010-2013 in green bars, compared to global mean provided by WMO as black bars (WMO, 2014). The global annual mean in 2011 as given in IPCC, Chapter 8 (Myhre et al, 2013b) are included as grey bar.

The annual means are based on the measured methane values. Modelled empirical background values are used, when data is lacking in the calculation of the annual mean.

The diagram in Figure 9 clearly illustrates the increase in the concentrations of methane at Zeppelin since 2005 a small decrease in 2010 and 2011, and then a new record level in 2012 and now in 2013. The annual mean mixing ratio for 2013 was 1898 ppb while the level was 1892 ppb in 2012, an increase of 6 ppb which is the same increase as the global mean. The increase since 2005 at Zeppelin is 46 ppb (approx. 2.5 %) which is considered as relatively large compared to the development of the methane mixing ratio in the period from 1999-2005 both at Zeppelin, Svalbard and globally. It is also slightly larger than the global mean increase since 2005, which is 41 ppb as published in the yearly bulletins by WMO (WMO, 2011, 2012, 2013, 2014). The global mean shows an increase since 2006 and the last 4 years of constantly 5-6 ppb per year, while larger fluctuations are evident at Zeppelin. This is explained by the distribution of the sources; there are more sources at the northern hemisphere, and thus larger interannual variations. For comparison, during 1980s when the methane mixing ratio showed a large increase, the annual global mean change was around 15 ppb per year.

Currently the observed increase the last years is not explained and well understood. The recent observed increase in the atmospheric methane concentrations has led to enhanced focus and intensified research to improve the understanding of the methane sources and changes particularly in responses to global and regional climate change. It is essential to find out if the increase since 2005 is due to emissions from large point sources, or if it is caused by newly initiated processes releasing methane to the atmosphere like e.g. the thawing of the permafrost layer. Recent and ongoing scientific discussions point in the direction of increased emissions from wetlands located both in the tropical region and in the Arctic region. Gas hydrates at the sea floor are widespread in thick sediments in this area between Spitsbergen and Greenland. If the sea bottom warms, this might initiate further emissions from this source. This is the core of the large polar research project *MOCA - Methane Emissions from the Arctic OCean to the*

Atmosphere: Present and Future Climate Effects[2], started at NILU October 2013, and is expected to be finalized by spring 2017 (see http://moca.nilu.no)

3.1.3 Nitrous Oxide at the Zeppelin Observatory

Nitrous Oxide (N_2O) is a greenhouse gas with both natural and anthropogenic sources. The sources include oceans, tropical forests, soil, biomass burning, cultivated soil and use of particular synthetic fertilizer, and various industrial processes. There are large uncertainties in the major soil, agricultural, combustion and oceanic sources of N_2O. Also frozen peat soils in Arctic tundra is reports as a potential source (Repo et al., 2009), but recent studies lead by NILU identify tropical and sub-tropical regions as the largest source regions (Thompson et al, 2013). N_2O is an important greenhouse gas with a radiative forcing of 0.17 W m^{-2} since 1750 contributing around 6 % to the overall well-mixed greenhouse gas forcing over the industrial era. N_2O is also the major source of the ozone-depleting nitric oxide (NO) and nitrogen dioxide (NO_2) in the stratosphere, thus the component is also influencing the stratospheric ozone layer. The Assessment of the ozone depletion (WMO, 2011) suggests that current emissions of N_2O are presently the most significant substance that depletes ozone.

N_2O has increased from around 270 ppb prior to industrialization and up to an average global mean of 325.9 ppb in 2013 (WMO, 2014). In 2009, NILU installed a new instrument at Zeppelin measuring N_2O with high time resolution; 15 minutes. The instrument was in full operation in April 2010 and the results for 2010 -2013 are presented in Figure 10, with the global mean included as horizontal lines for each year.
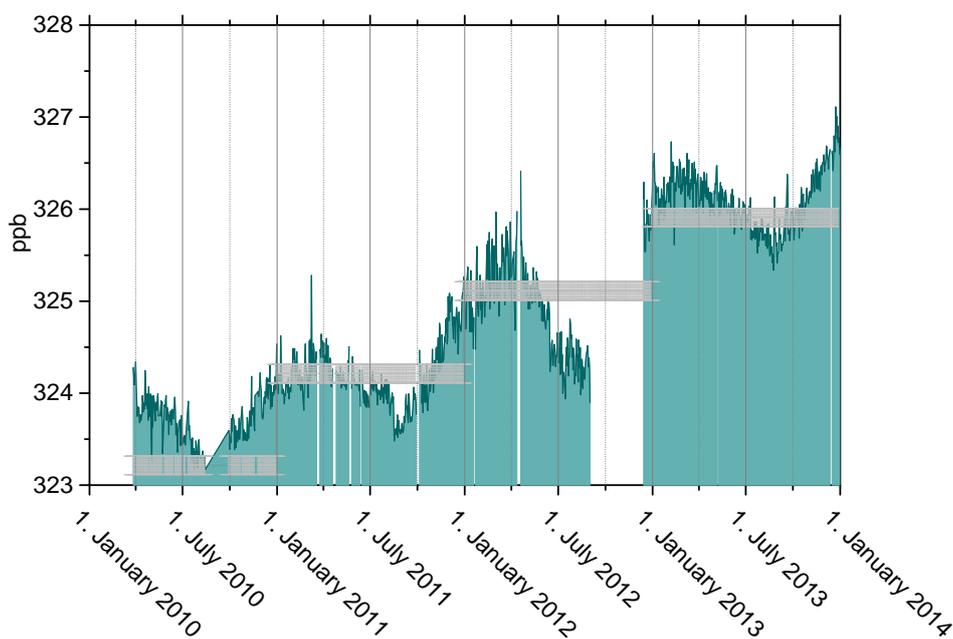

Figure 10: Measurements of N_2O at the Zeppelin Observatory for 2010-2013.The grey shaded areas are global annual mean, with the given uncertainty (WMO, 2011, 2012, 2013, 2014)

---

[2] http://moca.nilu.no/

The time series is too short for trend calculations, but according to WMO (WMO, 2014) the global mean value for 2013 was 325.9 with an increase of 0.8 ppb since 2012, similar as previous years. Annual mean for Zeppelin in 2013 was 326.1 with a standard deviation of 0.3 ppb.

3.1.4 Methyl Chloride at the Zeppelin Observatory

Methyl chloride (CH_3Cl) is the most abundant chlorine containing organic gas in the atmosphere, and it contributes approx. 16% to the total chlorine from the well-mixed gases in the troposphere (WMO, 2011). The main sources of methyl chloride are natural, and dominating source is thought to be emissions from warm coastal land, particularly from tropical islands are shown to be a significant source but also algae in the ocean, and biomass burning. Due to the dominating natural sources, this compound is not regulated through any of the Montreal or Kyoto protocols, but is an important natural source of chlorine to the stratosphere. To reach the stratosphere, the lifetime in general needs to be in the order of 2-4 years to have significant chorine contribution, but this is also dependant on the source strength and their regional distribution. Methyl chloride has relatively high mixing ratios, and contributes to the stratospheric chlorine burden.

The results of the observation of this substance for the period 2001-2013 are shown in Figure 11.
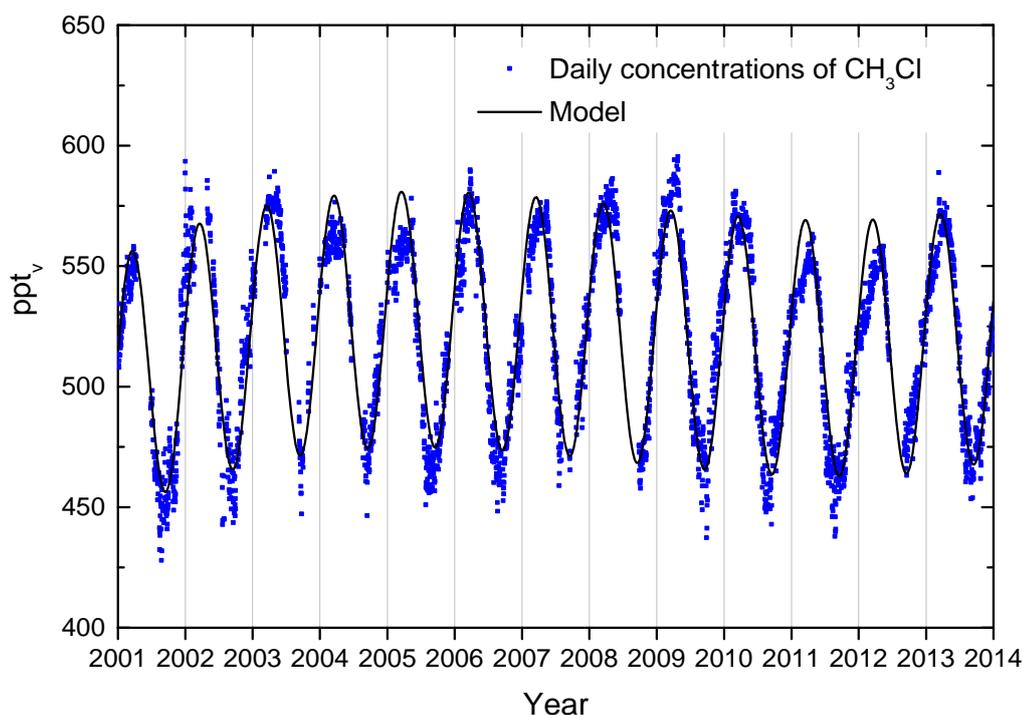
Figure 11: Observations of methyl chloride, CH_3Cl, for the period 2001-2013 at the Zeppelin Observatory. Dots: daily averaged concentrations from the observations, solid line: empirical modelled background mixing ratio.

The lifetime of the compound is only one year resulting in large seasonal fluctuations, as shown in the Figure, and rapid response to changes in sources. There is a decrease the last years, but this seems to have stopped in 2011-2012, and a large increase is detected in 2013, see also Figure 12 with the annual means.
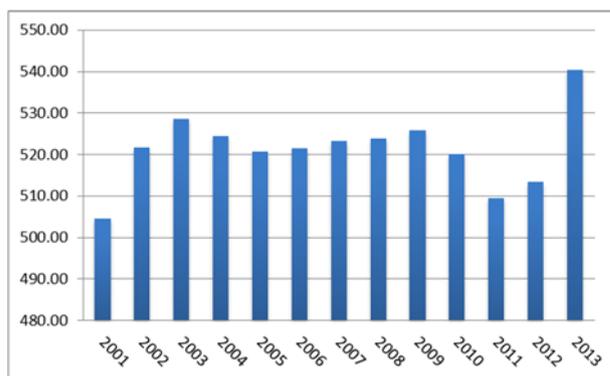
Figure 12: Development of the annual means methyl chloride measured at the Zeppelin Observatory for the period 2001-2013.

No annual trend over the period 2001-2013 is detected due to the large variability. The annual means of methyl chloride for the period 2001-2013 is presented in Figure 12. The period 2002-2009 was relatively stable, but since 2009 there is larger variability and from 2011 to 2013 there is an increase of more than 30 ppt in our data corresponding to an increase of ca 20%. The reasons to this is not clear, and will be investigated and discussed already within the AGAGE network and discussion meeting December 2014. A closer study of source variation for this compound is also recommended by WMO (WMO, 2011), as the sources are also related to atmospheric temperature change and ocean.

3.1.5 Methyl Bromide at the Zeppelin Observatory

The sources of methyl bromide (CH_3Br) are both from natural and anthropogenic activities. The natural sources such as the ocean, plants, and soil, can also be a sink for this substance. Additionally there are also significant anthropogenic sources; it is used in a broad spectrum of pesticides in the control of pest insects, nematodes, weeds, pathogens, and rodents. Biomass burning is also a source and it is used in agriculture primarily for soil fumigation, as well as for commodity and quarantine treatment, and structural fumigation. Even though methyl bromide is a natural substance, the additional methyl bromide added to the atmosphere by humans contributes to the man-made thinning of the ozone layer. Total organic bromine from halons and methyl bromide peaked in 1998 and has declined since. The tropospheric abundance of bromine is decreasing, and the stratospheric abundance is no longer increasing (WMO, 2011).

The results of the daily averaged observations of this compound for the period 2001-2013 are shown in Figure 13. A relatively large change is evident after the year 2007, a reduction of approx. 21% since the start of our measurements at Zeppelin. Methyl bromide is a greenhouse gas with a lifetime of 0.8 years and it is 2 times stronger greenhouse gas than CO_2 (Myhre et al, 2013b) if the amount emitted of both gases were equal. The short lifetime explains the large annual and seasonal variations of this compound.
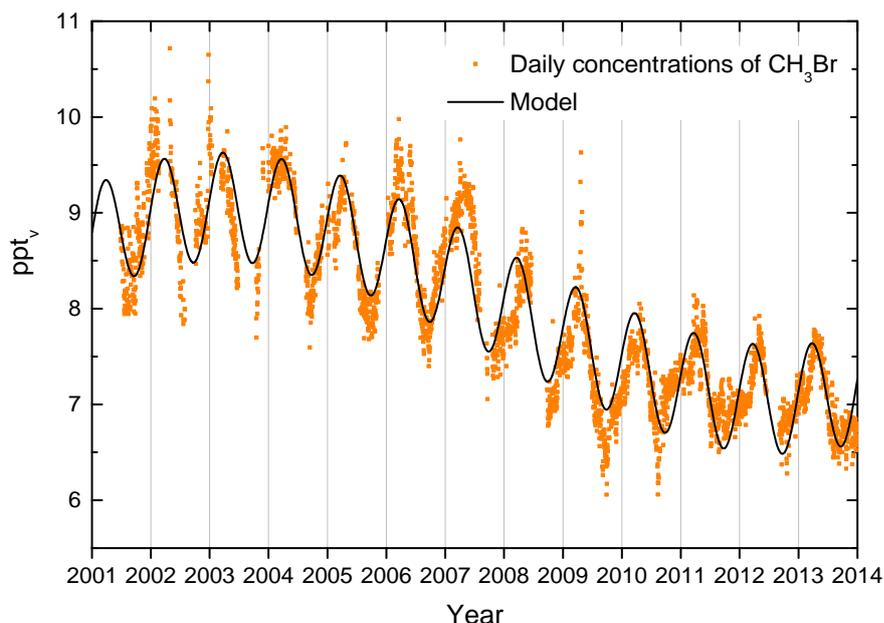
Figure 13: Observations of methyl bromide, CH₃Br, for the period 2001-2013 at the Zeppelin Observatory. Dots: daily averages mixing ratios from the observations, solid line: empirical modelled background mixing ratio.

For the period 2001-2013 there is a reduction in the mixing ratio of -0.2 ppt per year, with a relaxation in the trend the last years. However, note that the observed changes are small (approx. 1.6 ppt since 2005).

The development of the annual means for the period 2001-2013 is presented in Figure 14, clearly illustrating the decrease in the last years and a stabilisation of the level towards 7 ppt. In general atmospheric amounts of methyl bromide have declined since the beginning in 1999 when industrial production was reduced as a result
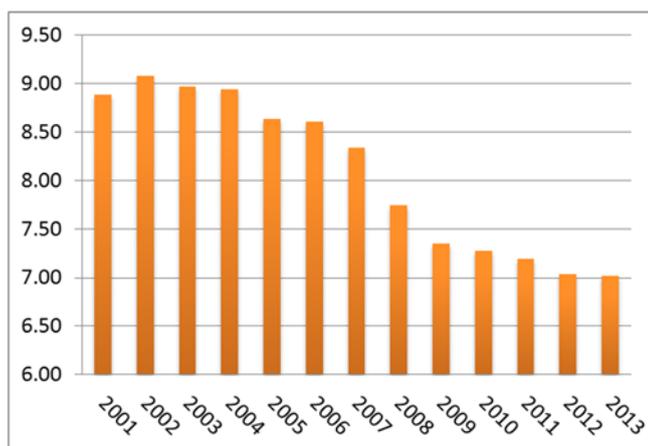
Figure 14: Development of the annual means of methyl bromide measured at the Zeppelin Observatory for the period 2001-2013.

of the Montreal protocol. The global mean mixing ratio was 7.3-7.5 ppt in 2011, slightly lower than at Zeppelin. The differences are explained by slower inter hemispheric mixing. The recent reduction is explained by considerable reduction in the use of this compound; in 2008 the use was 73% lower than the peak year in late 1990s (WMO, 2011).

3.1.6 Carbon monoxide at the Zeppelin Observatory

Atmospheric CO sources are oxidation of various organic gases (volatile organic compounds, VOC) from sources as fossil fuel, biomass burning, and also oxidation of methane is important. Additionally, emissions from plants and ocean are important sources. CO is also emitted from

biomass burning. Carbon monoxide (CO) is not considered as a direct greenhouse gas, mostly because it does not absorb terrestrial thermal IR energy strongly enough. However, CO is able to modulate the level of methane and production of tropospheric ozone, which are both very important climate components. CO is closely linked to the cycles of methane and ozone and, like methane; CO plays a key role in the control of the OH radical.

CO at Zeppelin is include in the national monitoring programme and the observed CO mixing ratios for the period September 2001-2013 are shown in Figure 15.
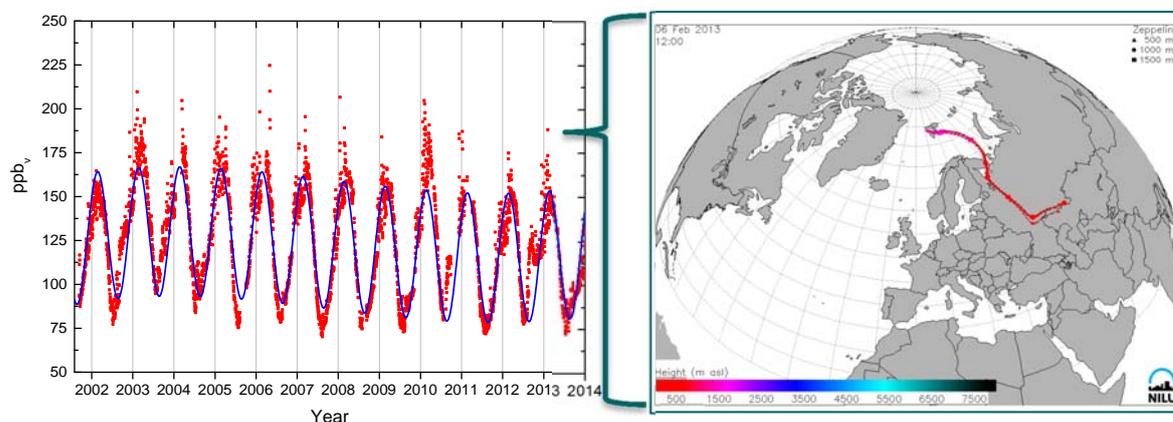
Figure 15: Observations of carbon monoxide (CO) from September 2001 to 31.12.2013 at the Zeppelin observatory. Red dots: daily averaged observed mixing ratios. The solid line is the modelled background mixing ratio. The right panel shows the transport of air to Zeppelin the 6th February.

The concentrations of CO show characteristic seasonal variations. This seasonal cycle is driven by variations in OH concentration as a sink, emission by industries and biomass burning, and transportation on a large scale. As seen from the Figure there are also peak values due to long-range transport of polluted air to Zeppelin and the Arctic. The highest mixing ratio of CO ever observed at Zeppelin; is 217.2 ppb on the 2nd of May 2006. These peak values are due to transport of polluted air from lower latitudes; urban pollution (e.g. combustion of fossil fuel). CO is an excellent tracer for transport of smoke from fires (biomass burning, agricultural- or forest fires). The compound is very valuable in the interpretation of other variables at Zeppelin. The maximum daily average value in 2013 was observed on the 6th February and was 188 ppb. The maximum value is caused by transport of pollution from Central Russia, and also CH_4 and CO_2 had yearly maximum value this day.

We calculated a trend at Zeppelin of -1.3 ppb per year for the period 2001-2013. The development of the annual means for the period 2001-2013 are presented in Figure 16, clearly illustrating a maximum in the year of 2003, and a decrease from 2003-2009.

In general the CO concentrations measured at Zeppelin show a decrease during the period 2003 to 2009, and stable values the last years with a small increase in 2010.

Figure 16: Development of the annual means of CO measured at the Zeppelin Observatory for the period 2001-2013.

3.2 Greenhouse gases with solely anthropogenic source

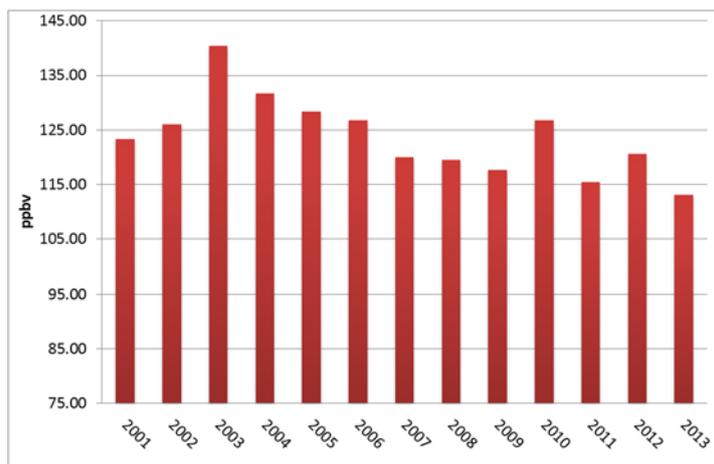All the gases presented in this chapter have solely anthropogenic sources. These are purely man-made greenhouse gases and are called CFCs, HCFCs, HFCs, SF_6 and halons, and most of the gases did not exist in the atmosphere before the 20th century. All these gases except for SF_6 are halogenated hydrocarbons. Although the gases have much lower concentration levels than most of the natural gases mentioned in the previous section, they are strong infrared absorbers, many of them with extremely long atmospheric lifetimes resulting in high global warming potentials; see Table 2. Together as a group, the gases contribute to around 12% to the overall global radiative forcing since 1750 (Myhre et al, 2013b). The annual mean concentrations for all the gases included in the monitoring program for all years are given in Appendix I, Table A1 at page 65, while all trends, uncertainties and regression coefficients are found in Table A 2 at page 66.

Some of these gases are ozone depleting, and consequently regulated through the Montreal protocol. Additional chlorine and bromine from CFCs, HCFCs and halons added to the atmosphere contributes to the thinning of the ozone layer, allowing increased UV radiation to reach the earth's surface, with potential impact not only to human health and the environment, but to agricultural crops as well. In 1987 the Montreal Protocol was signed in order to reduce the production and use of these ozone-depleting substances (ODS) and the amount of ODS in the troposphere reached a maximum around 1995. The amount of most of the ODS in the troposphere is now declining slowly and one expects to be back to pre-1980 levels around year 2050. In the stratosphere the peak is reached somewhat later, around the year 2000, and observations until 2004 confirm that the level of stratospheric chorine has not continued to increase (WMO, 2011).

The CFCs, consisting primarily of CFC-11, -12, and -113, accounted for ~62% of total tropospheric chlorine in 2004 and accounted for a decline of 9 ppt chlorine from 2003-2004 (or nearly half of the total chlorine decline in the troposphere over this period) (WMO, 2011).

There are two generations of substitutes for the CFCs, the main group of the ozone depleting substances. The first generation substitutes is now included in the Montreal protocol as they also influence the ozone layer. This comprises the components called HCFCs listed in Table 2. The second-generation substitutes, the HFCs, are included in the Kyoto protocol. The situation now is that the CFCs have started to decline, while their substitutes are increasing, and many of them have a steep increase.

3.2.1 Chlorofluorocarbons (CFCs) at Zeppelin Observatory

This section includes the results of the observations of the CFCs: CFC-11, CFC-12, CFC-113, and CFC-115. These are the main ozone depleting gases, and the anthropogenic emissions started around 1930s and were restricted in the first Montreal protocol. The main sources of these compounds were foam blowing, aerosol propellant, temperature control (refrigerators), solvent, and electronics industry. The highest production of the observed CFCs was around 1985 and maximum emissions were around 1987. The lifetimes of the compounds are long, as given in Table 2, and combined with strong infrared absorption properties, the GWP is high. Figure 17 shows the daily averaged observed mixing ratios of these four CFCs.

The instrumentation employed at Zeppelin is not in accordance with recommendations and criteria of AGAGE for measurements of CFCs, and there are relatively large uncertainties in the observations of these compounds, see also Appendix I. As a result, the trends are connected with large uncertainties. From September 2010, new and improved instrumentation was installed at Zeppelin providing more accurate observations of these compounds. The higher precisions are clearly visualised in Figure 17.

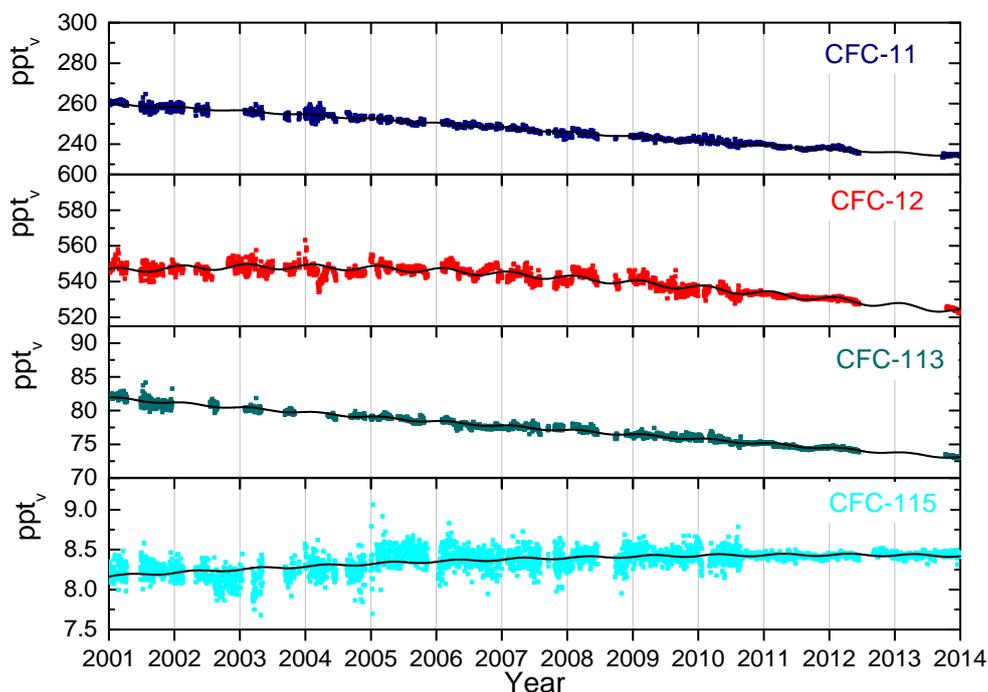*Figure 17: Daily averaged mixing ratios of the monitored CFCs: CFC-11 (dark blue), CFC-12 (red), CFC-113 (green) and CFC-115 (light blue) for the period 2001-2013 at the Zeppelin observatory. The solid lines are modelled background mixing ratio.*

The trends per year for the substances CFC-11, CFC12 and CFC-113 given in Table 2 are all negative, and the changes in the trends are also negative, indicating acceleration in the

decline[3]. For the compound CFC-115, the trend is still slightly positive, +0.02 ppt/year, but the change in trend is negative and thus we expect the trend to be negative in few years. In total, the development of the CFC levels at the global background site Zeppelin is now very promising.

The development of the annual means for all the observed CFCs is shown in Figure 18. The global annual mean of 2011 as given in IPCC (Chapter 8, Myhre et al, 2013b) is included as black bars for comparison. As can be seen, the concentrations at Zeppelin are very close to the global mean for these compounds, as the lifetimes are long and there are hardly any present-day emissions.
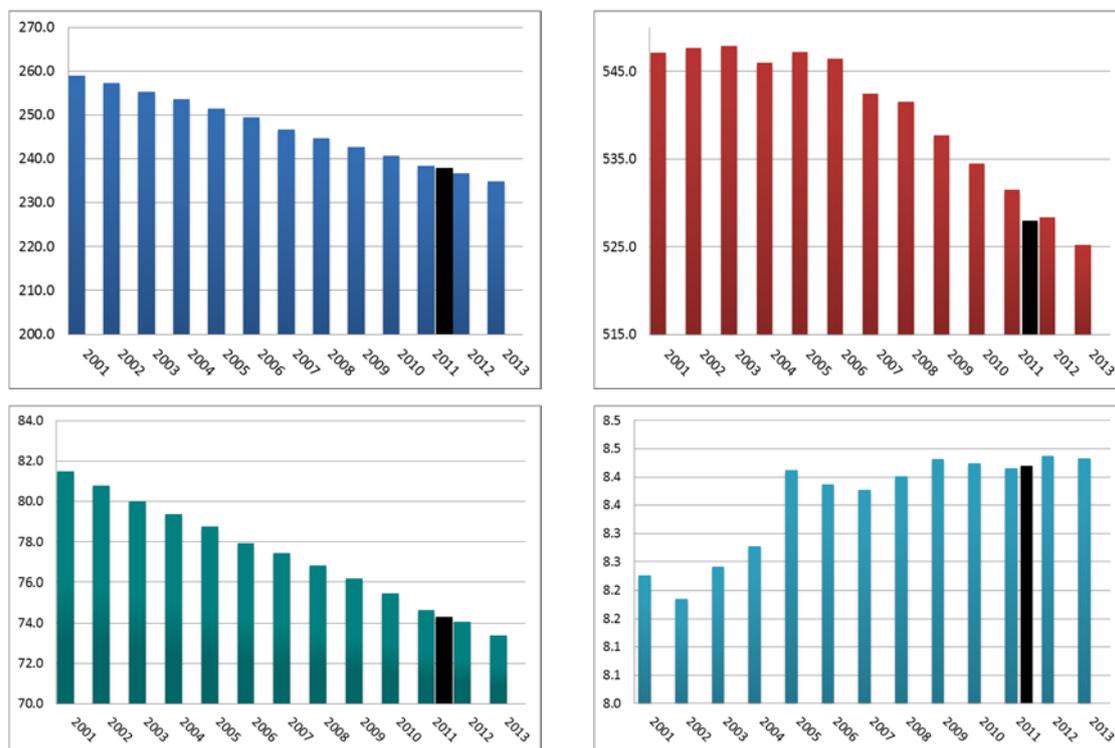
Figure 18: Development of the annual means all the observed CFCs at the Zeppelin Observatory for the period 2001-2013. Upper left panel: CFC-11, upper right panel: CFC-12, lower left panel: CFC-113, lower right panel: CFC-115. See Appendix I for data quality and uncertainty. The global annual mean as given in IPCC (Chapter 8, Myhre et al, 2013b) is included as grey bars. All units are ppt.

According to WMO (WMO, 2011) the global mean mixing ratios of CFC-11 are decreasing with approximately 2.0 ppt +/-0.01 ppt. This is in accordance with our results at Zeppelin (2.1 ppt/year). CFC-12 (the red diagram) has high GWP, 10200, the third highest of all gases observed at Zeppelin. The global averaged atmospheric mixing ratio of CFC-12 has been decreasing at a rate of 0.5% over the year 2004-2008 (WMO, 2011). This fits well with our

---

[3] *The current instrumentation is not in accordance with recommendations and criteria of AGAGE for measurements of the CFCs and there are larger uncertainties in the observations of this compound, see also Appendix I.*

observations as CFC-12 has the maximum in 2003-2004. There is a clear reduction the last years of -22 ppt since the maximum year 2005.

3.2.2 Hydrochlorofluorocarbons (HCFCs) at Zeppelin Observatory

This section includes the observations of the following components: HCFC-22, HCFC-141b and HCFC-142b. These are all first generation replacement gases for the CFCs and their lifetimes are rather long, see Table 2. The main sources of these gases are temperature control (refrigerants), foam blowing and solvents, as for the CFCs, which they are supposed to replace. All these gases are regulated through the Montreal protocol as they all contain chlorine. The use of the gases is now frozen, but they are not completely phased out. The gases they have potentially strong warming effects, depending on their concentrations and absorption properties; their GWPs are high (see Table 2). The compound HCFC-142b has the highest GWP, and the warming potential is 1980 times stronger than CO_2, per kg gas emitted. These gases do also contain chlorine, and thus are contributing to the depletion of the ozone layer.

The daily averaged observations of these gases are shown in Figure 19 for the period 2001-2013.

Figure 19: Daily average mixing ratios of the monitored HCFCs: HCFC-22 (red), HCFC-141b (dark blue) HCFC-142b (green) for the period 2001-2013 at the Zeppelin observatory. The solid lines are modelled background mixing ratios. All units are ppt.

The trends per year for the compounds HCFC-22, HCFC-141b and HCFC-142b are all positive. HCFC-22 is the most abundant of the HCFCs and is currently increasing at a rate of 6.8 ppt/year over the period 2001-2013. The concentration of the two other HCFCs included are a factor of ten lower, and also the annual increase is about a factor ten lower; HCFC-141b and HCFC-142b have increased by 0.6 ppt/yr and 0.8 ppt/year, respectively over the same period.

Figure 20 shows the annual means for the full period for the three compounds, clearly illustrating the development; a considerable increase over the period. With lifetimes in the

order of 10-20 years, it is central to continue monitoring the development of these compounds for many years to come as they have an influence both on the ozone layer and are strong climate gases. The global annual mean of 2011 as given in IPCC (Chapter 8, Myhre et al, 2013b) is included as black bars for comparison. As can be seen, the development and concentrations at Zeppelin are ca 2-3 ppt ahead of the global mean, indicating the development of the global mean values the next years.

3.2.3   Hydrofluorocarbons (HFCs) at Zeppelin Observatory

The substances called HFCs are the so called second generation replacements of CFCs, which means that they are considered as better alternatives to the CFCs with respect to the ozone layer than HCFCs. This sub-section includes the following components: HFC-125, HFC-134a, and HFC-152a with lifetimes in the order of 1.5-29 years. These substances do not contain chlorine thus they do not have a direct influence on the ozone layer, but they are infrared absorbers and contribute to the global warming. The three main HFCs are HFC-23 (not part of the national monitoring program, but measured at Zeppelin from 2010), HFC-134a and HFC152a. HFC-134a is the most widely used refrigerant for temperature control, and also in air conditioners in cars. Since 1990, when it was almost undetectable in the atmosphere, concentrations of HFC-134a have risen massively, and it is the one with the highest concentration of these compounds.

Even if these compounds are better alternatives for the protection of the ozone layer as they do not contain chlorine or bromine, they are still problematic as they are highly potent greenhouse gases. 1 kg of the gas HFC-125 is as much as 3170 times more powerful greenhouse gas than CO_2 (See Table 2). However, their mixing ratios are currently rather low, but the background mixing ratios are increasing steeply, except for HFC-152a, see Figure 21.

The seasonal cycle in the observed mixing ratios of these substances is caused by the variation in the incoming solar radiation and is clearly visible in the time series shown in Figure 21 for HFC-152a. HFC-152a has the shortest lifetime and is mainly destroyed in the lowest part of the atmosphere by photolysis and

Figure 20: Development of the annual means the observed HCFCs at the Zeppelin Observatory for the period 2001-2013. Red: HCFC-22, Blue: HCFC-141b, and green: HCFC-142b. All units are ppt. The global annual mean in 2011 as given in IPCC, Chapter 8 (Myhre et al, 2013b) are included as black bars.

reactions with OH. This is the first year we detected a reduction of the development of the concentration for one of these components. This is clearly illustrated in Figure 22 showing the development of the annual means.
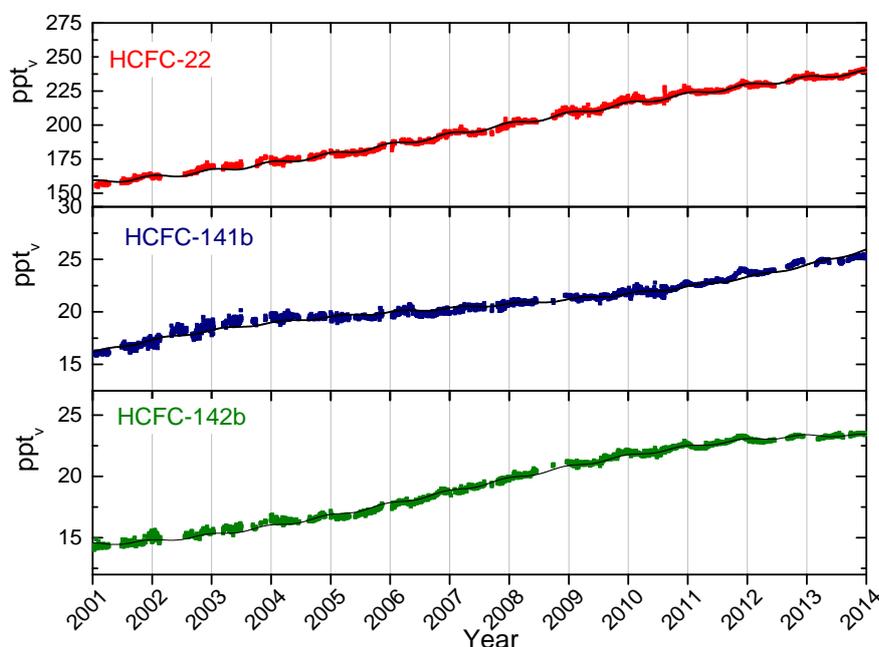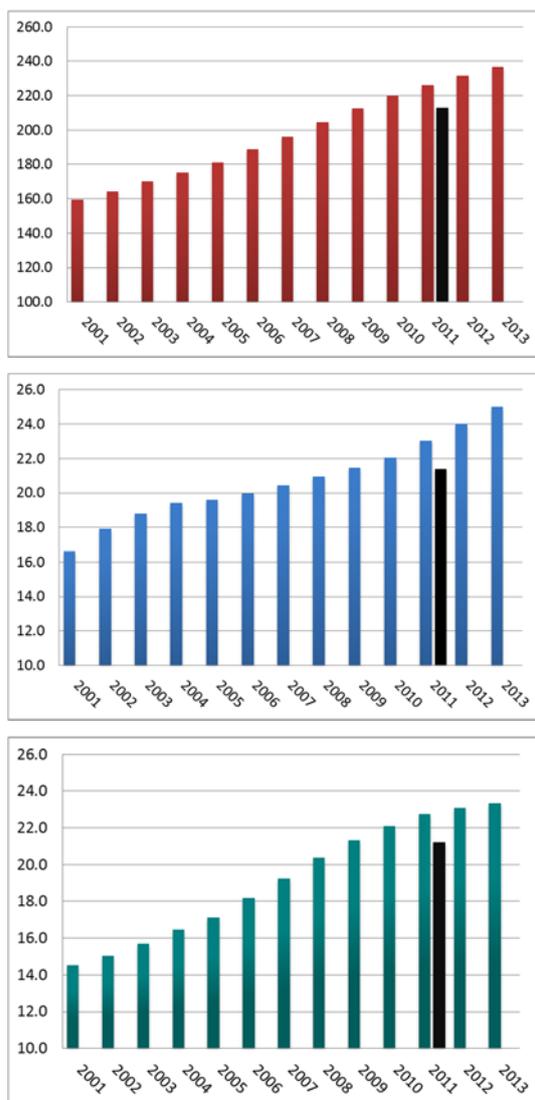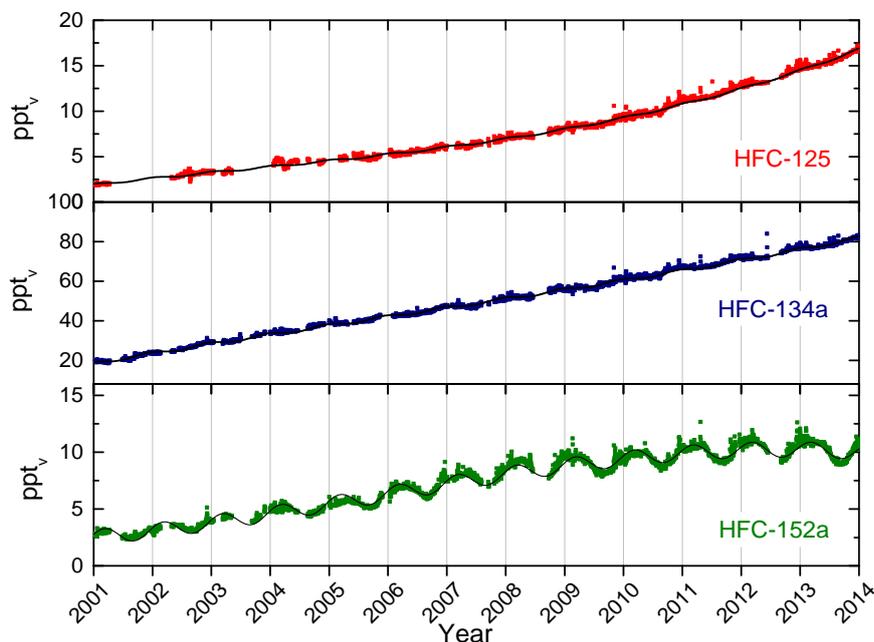

Figure 21: Daily average concentrations of the monitored HFCs: HFC-125 (red), HFC-134a (dark blue), and HFC-152a (green) for the period 2001-2013 at the Zeppelin observatory. The solid lines are empirical modelled background mixing ratio.

HFC-152a reveals a reduction since last year. For the period 2001-2013, we find an increasing trend of 4.8 ppt per year for HFC-134a which leaves this compound as the one with the second highest change per year of the all the halocarbons measured at Zeppelin, after HCFC-22. The mixing ratios of HFC-125, HFC-134a and HFC-152a have increased by as much as 695%, 280% and 263% respectively since 2001, and HFC-125 show even an acceleration on the development and trend. The global annual means of 2011 as given in IPCC (Chapter 8, Myhre et al, 2013b) are included as black bars for comparison. As for HCFCs the development and concentrations at Zeppelin is ca 2-3 years ahead of the global mean, indicating the development of the global mean values the next years. HFC-152a is an exception from this. This compound has much shorter lifetime, and is thus more sensitive to emission strength.
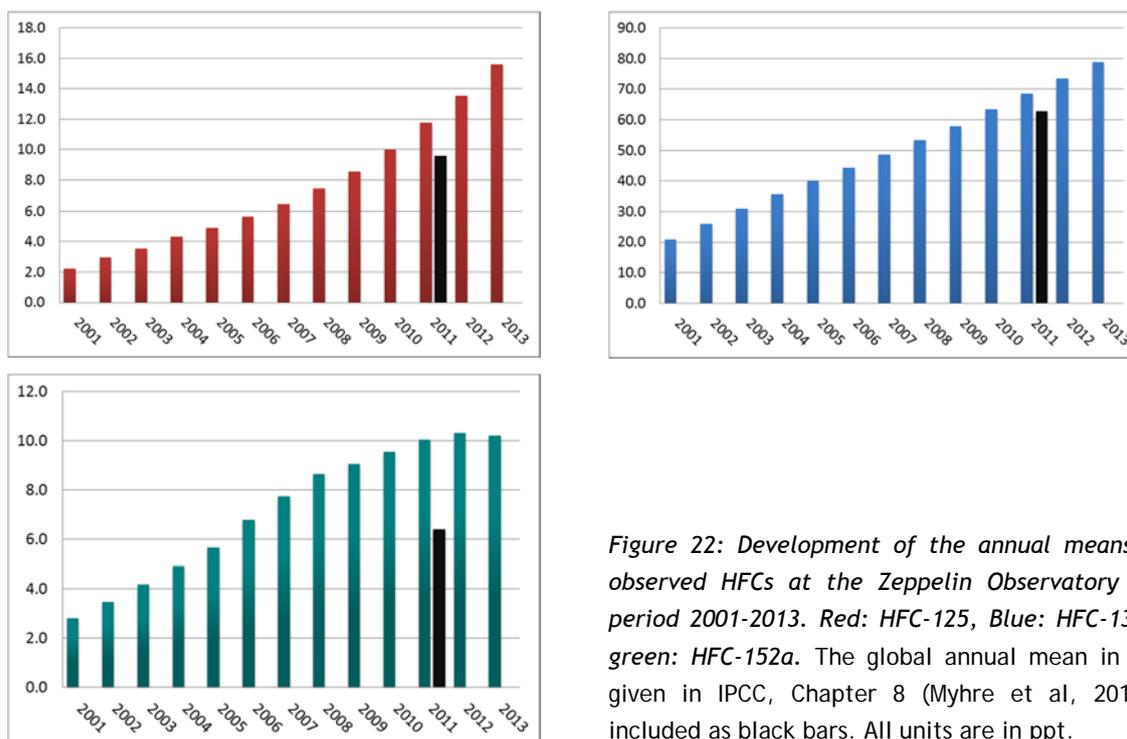
Figure 22: Development of the annual means of the observed HFCs at the Zeppelin Observatory for the period 2001-2013. Red: HFC-125, Blue: HFC-134a, and green: HFC-152a. The global annual mean in 2011 as given in IPCC, Chapter 8 (Myhre et al, 2013b) are included as black bars. All units are in ppt.

3.2.4 Halons measured at Zeppelin Observatory

Of the halons, H-1301 and H-1211 are measured at the Zeppelin Observatory. These greenhouse gases contain bromine, thus also contributing to the depletion of the ozone layer. Actually, bromine is even more effective in destroying ozone than chlorine. The halons are regulated trough the Montreal protocol, and are now phased out. The main source of these substances was fire extinguishers. The ambient concentrations of these compounds are very low, both below 4 ppt. Figure 23 presents the daily average concentrations of the monitored halons at Zeppelin.
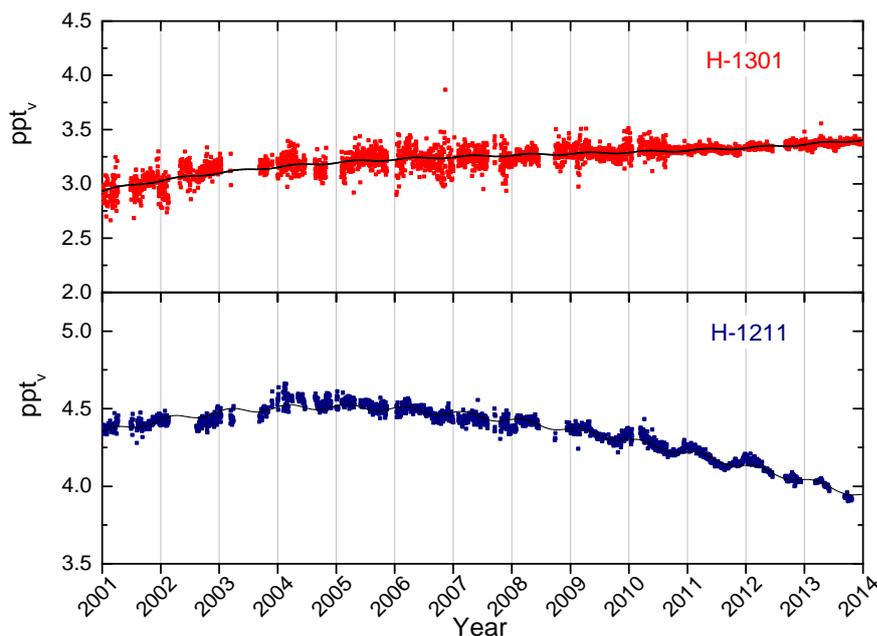
Figure 23: Daily average concentrations of the monitored halons: H-1301 (red in the upper panel) and H-1211 (blue in the lower panel) for the period 2001-2013 at the Zeppelin Observatory. The solid lines are empirical modelled background mixing ratio.

The trends of the compounds given in Table 2 shows that for the period 2001-2013 there is an increase for H-1301, and a relaxation for H1211. The concentration of the compound H-1211 is considerable lower now than when we started the measurements, almost 10% as also depicted in the development of the annual means in Figure 24.
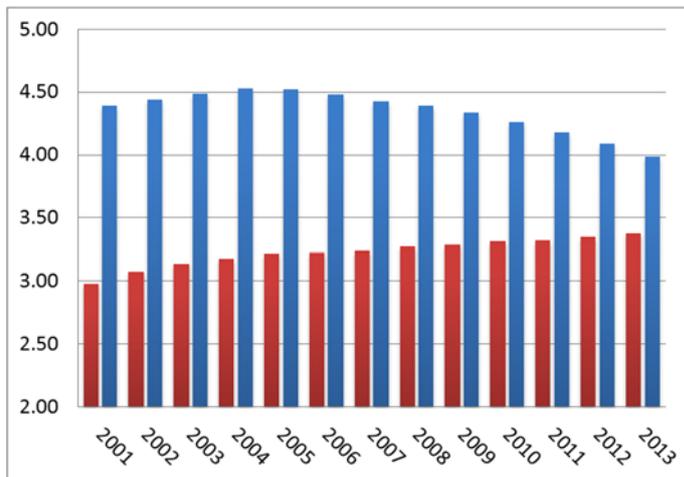
Figure 24: Development of the annual means of the observed Halons at the Zeppelin Observatory for the period 2001-2013. Red: Halon-1301, Blue: H-1211. All units are in ppt.

The development of the annual means are shown in Figure 24 to the left, and the mixing ratios are relatively stable over the measured period, explained by low emissions and relatively long lifetimes (11 years for H-1211 and 65 years for H-1301). However, a clear reduction is evident in Halon-1211, with the shortest lifetime. According to the last Ozone Assessment (WMO, 2011), the total stratospheric bromine concentration is no longer increasing, and bromine from halons stopped increasing during the period 2005-2008. H-1211 decreased for the first time in this period, while H-1301 continued to increase, but at a slower rate than previously.

3.2.5 Other chlorinated hydrocarbons at Zeppelin Observatory

This section includes observations of the components: trichloromethane (also called methyl chloroform, CH_3CCl_3), dichloromethane (CH_2Cl_2), chloroform ($CHCl_3$), trichloroethylen ($CHClCCl_2$), perchloroethylene (CCl_2CCl_2). The main sources of all these substances are solvents. Chloroform do also has natural sources, and the largest single source being in offshore seawater. The daily averaged concentrations are shown in Figure 25.
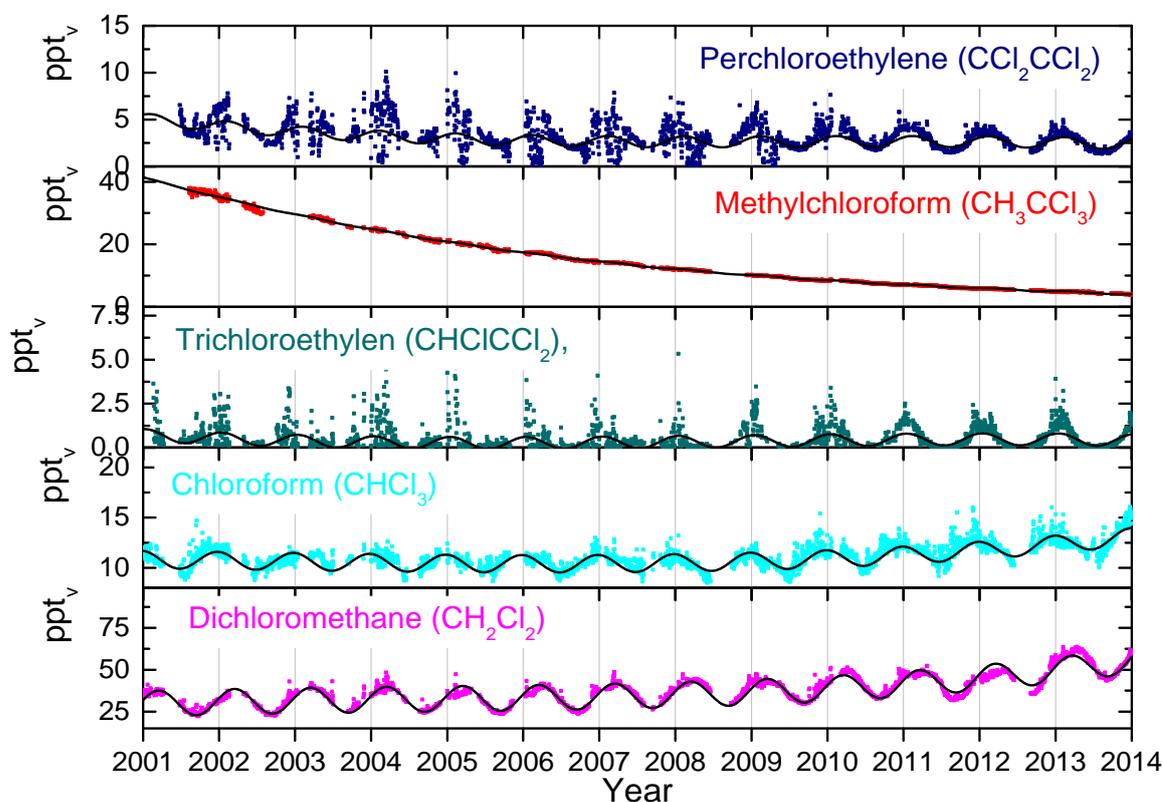
Figure 25: Daily average concentrations chlorinated hydrocarbons: From the upper panel: perchloroethylene (dark blue) methylchloroform (red), trichloroethylen (green), chloroform (light blue) and dichloromethane (pink) for the period 2001-2013 at the Zeppelin observatory. The solid lines are the empirical modelled background mixing ratio.

Methylchloroform (CH_3CCl_3) has continued to decrease, and accounted only for 1% of the total tropospheric chlorine in 2008, a reduction from a mean contribution of 10% in the 1980s (WMO, 2011). Globally averaged surface mixing ratios were around 10.5 ppt in 2008 (WMO, 2011) versus 22 ppt in 2004 (WMO, 2011). The measurements at Zeppelin show that the component has further decreased to 6.5 ppt, a reduction of almost 90% since 2001.
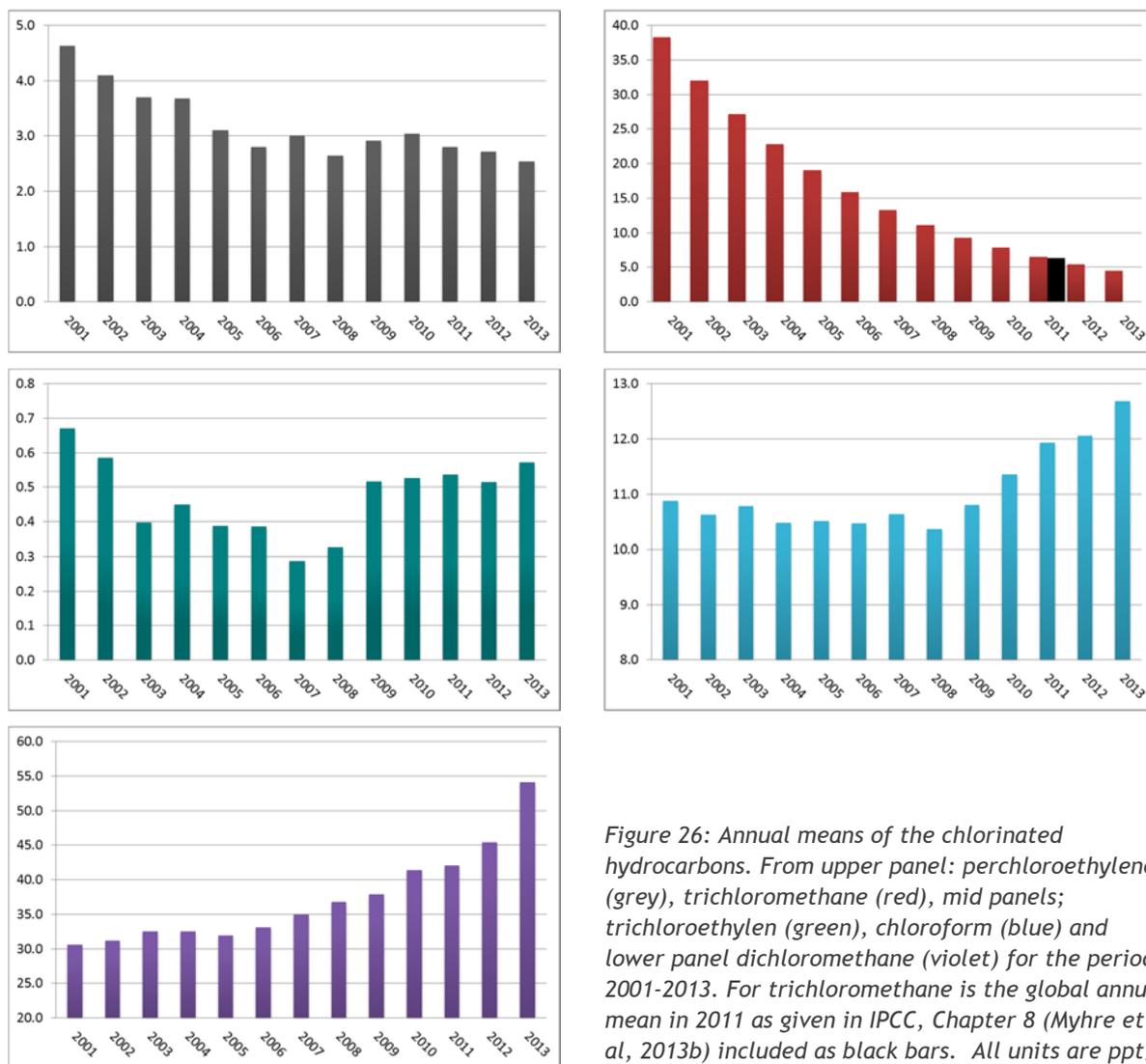
Figure 26: Annual means of the chlorinated hydrocarbons. From upper panel: perchloroethylene (grey), trichloromethane (red), mid panels; trichloroethylen (green), chloroform (blue) and lower panel dichloromethane (violet) for the period 2001-2013. For trichloromethane is the global annual mean in 2011 as given in IPCC, Chapter 8 (Myhre et al, 2013b) included as black bars. All units are ppt.

It is worth noting the recent increase in dichloromethane (violet), and chloroform (light blue)**.** Dichloromethane, has a lifetime of less than 6 months, and respond rapidly to emissions changes, about 90 % has industrial origin. Its main applications include use in paint strippers, degreasers and solvents; in foam production and blowing applications; and as an agricultural fumigant (WMO et al., 2011). The most recent estimation for its natural components suggests it is comprised of a 10% combined biomass burning and marine source. At Zeppelin, the increase since 2001 is about 75%, and as much as 20% since last year. The concentration is currently almost 55 ppt.

Large seasonal variations are observed for chloroform due to a relatively short lifetime of 1 year, thus the response to emission changes are also for this compound rapid. The annual mean value of chloroform has increased with as much as 22% since 2008 at Zeppelin, this is also observed at other sites (e.g. Mauna Loa at Hawaii and Barrow in Alaska). From known emissions of this compound this increase is not expected, and the reason for this increase is not yet clear, it might also be related to natural sources.

The concentration of trichloroethylene is very low and the annual variability is quite high, this

may partly be due to uncertainty in the measurements and missing data

3.2.6   Perfluorinated compounds at Zeppelin Observatory

The only perfluorinated compound measured and included in the monitoring programme at Zeppelin is sulphurhexafluoride, SF_6. This is an extremely strong greenhouse gas emitted to the atmosphere mainly from the production of magnesium and electronics industry. The atmospheric lifetime of this compound is as much as 3200 years, and the global warming potential is 23500, which means that the emission of 1 kg of this gas has a warming potential which is 23500 times stronger than 1 kg emitted CO_2 (Myhre et al, 2013b).

The other perfluorinated compounds are also very powerful greenhouse gases thus NILU has from 2010 extended the monitoring with carbon tetrafluoride (CF_4) and hexafluoroethane (C_2F_6), as we have new and improved instrumentation installed at Zeppelin. However, these compounds are not yet a part of the national monitoring programme.

The daily averaged concentration of SF_6 is presented in Figure 27.
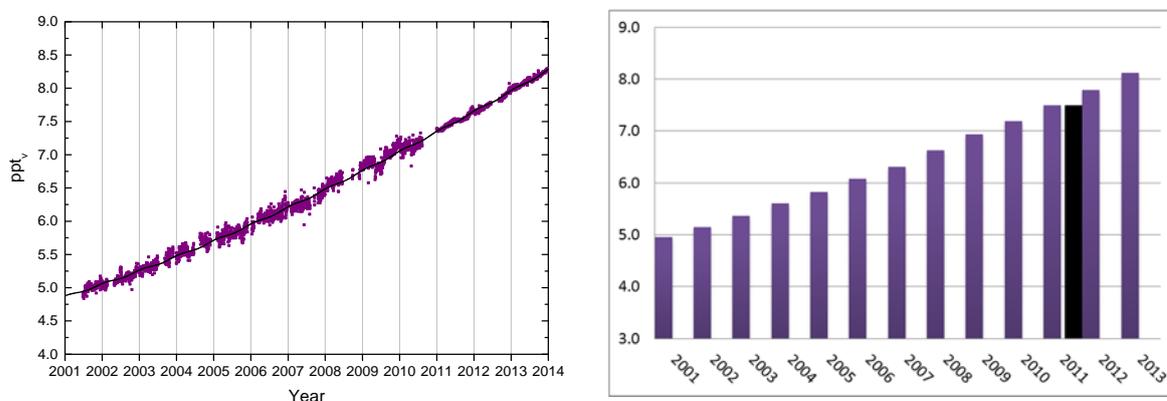
Figure 27: Daily average concentrations of SF_6 for the period 2001-2013 to the left, and the development of the annual mean concentrations in the right panel.

The compound is increasing with a rate of 0.26 ppt/year, and has increased by more than 60% since the start of our measurements in 2001. The instrumentation before 2010 is not the best suited for measurements of SF_6 thus there are larger uncertainties for this compound's mixing ratios than for most of the other compounds reported (see Appendix I). The diurnal variations through the years are not due to seasonal variations, but rather to instrumental adjustments. The improvement with the new instrumentation in 2010 is very easy to see for this component.

3.3 Satellite observations of methane above Norway and the Norwegian Arctic region

Satellite products can, in their current state, not replace the ground-based monitoring of greenhouse gases, but they give an important contribution to regional and global GHG mapping. Earlier studies (Vik et al., 2011, Stebel et al., 2013) have shown that the uncertainty in most satellite products, particularly in polar areas, are too large to be used alone in reporting to national authorities and international projects and programs. However, the satellite products make it possible to investigate the geographical extent of e.g. enhanced methane concentrations, emissions and long-range transport. In the project "Bridge to Copernicus", jointly financed by the Norwegian Space Center (Norsk Romsenter) and NILU, various methane satellite products have been investigated, particularly focusing on Norway and the Norwegian Arctic region. Results from the project are summarized in this chapter.

Figure 28 gives an overview of the various methane measuring satellites and their time of operation, together with the duration of in-situ measurements at Zeppelin and Birkenes. The ground-based (GB) observations at Zeppelin started in 2001, two years prior to the starting date in Figure 28.
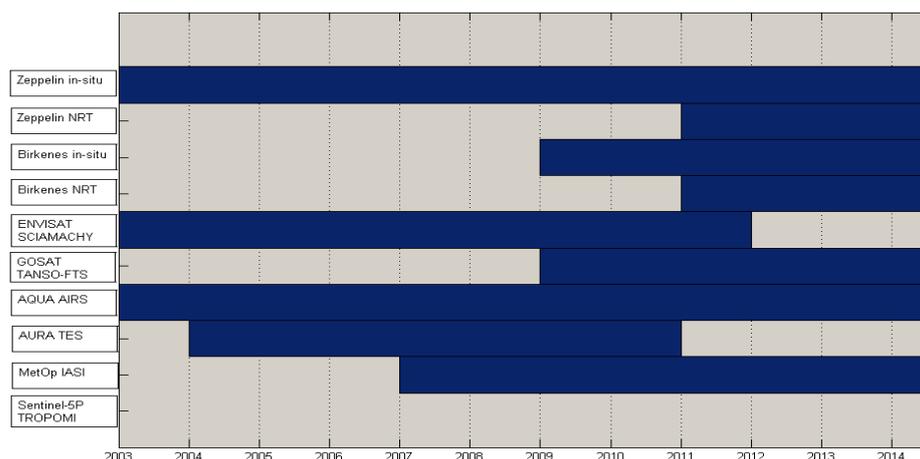
Figure 28: Overview of methane measuring satellites and their time of operation. The duration of Norwegian ground-based measurements are also marked.

In this chapter we describe the methane products from three satellites: AIRS (onboard AQUA), TES (on AURA), and GOSAT. The satellite data have been compared to ground-based data from the two Norwegian stations. Note that the Near Real Time GB methane data for 2013 and 2014 are preliminary and minor adjustments might occur after data finalization.

For the methane GB/satellite inter-comparison an area of 2x2 degrees around Zeppelin and Birkenes are defined, and the satellite pixels closest to the observational sites (within the 2x2° area) are selected from all the gridded satellite data files.

3.3.1 Atmospheric Infrared Sounder - AIRS

Atmospheric Infrared Sounder, AIRS, on board the AQUA satellite (NASA) was launched in 2002 and is still in operation. Monthly mean data, product AIRX3STM, are available for the period

2007-2014. AIRS provides both total column and methane profile data. Figure 29a (left panel) shows monthly mean methane data from the CH4_VMR_A ascending product (orange dots) and ground based observations (blue dots) at Birkenes. The correlation and bias between satellite and GB measurements are 0.62 and 22 ppb, respectively, the satellite data being higher than the GB observations. For Zeppelin (Figure 29b, right) the deviation between AIRS satellite values and GB observations are larger. Since the Zeppelin observatory is located at an altitude of 474 m, satellite data at the two lowest layers are used in the study; Altitude level 0 (L0: 0-750 m.a.s.l.) and level 1 (L1: ~750-1450 m.a.s.l.), marked as orange and grey lines, respectively. The correlations between AIRS and GB measurements at Zeppelin are 0.65 for L0 and 0.73 for L1. However, the corresponding biases are quite large: 68 and 56 ppb for L0 and L1, respectively.

Figure 29: a) Left: Monthly mean ground-based CH₄ measurements at Birkenes (blue) and the corresponding satellite observations from AIRS surface layer (orange), b) Right: Monthly mean CH₄ data at Zeppelin. Blue line represents GB observations, orange line is AIRS data from surface layer L0, grey line is AIRS data from layer L1, whereas yellow line is CH₄ total column values from AIRS.
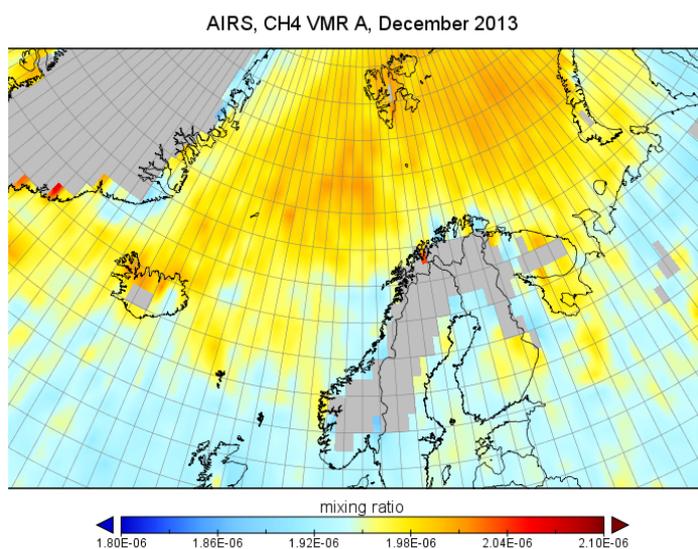
Figure 30: AIRS average methane concentrations (L0 surface layer) in December 2013.

AIRS sensitivity in the polar region is usually smaller than in the midlatitude and tropics. Large sensitivities suggest the variability of CH₄ is better retrieved, while smaller sensitivities indicate that the retrieved CH₄ will be closer to the first-guess (Xiong, 2008). Figure 30 shows monthly mean methane from AIRS L0 in December 2013. The high AIRS methane concentrations in the polar region are probably caused by the reduced sensitivity and uncertain retrieval algorithms at high latitudes, also evident from Figure 29b.

Total column methane data from AIRS, product XCH4_A, is shown as yellow line in Figure 29b. As expected the correlation between total column data and ground-based surface concentrations are not as good as for L0 and L1. A summary of the AIRS statistics, compared to in-situ measurements, are presented in Table 3.

Table 3: Bias, scatter and correlation (R) between AIRS AQUA satellite and ground-based methane data.

Monthly	Bias	Scatter	R	N
Zeppelin (L0)	67.5	17.3	0.65	85
Zeppelin (L1)	56.4	14.5	0.73	85
Zeppelin (total column)			0.23	85
Birkenes (L0)	22.1	18.7	0.62	42

3.3.2 Tropospheric Emission Spectrometer - TES

The Tropospheric Emission Spectrometer, TES, onboard the AURA satellite (NASA) was launched in 2004 and is still in operation. Data are available from September 2004 to October 2012. The data coverage has varied significantly over time, and since mid 2009 no observations have been available at high latitudes. Consequently, we have not enough Birkenes in-situ measurements for a proper satellite/GB inter-comparison.
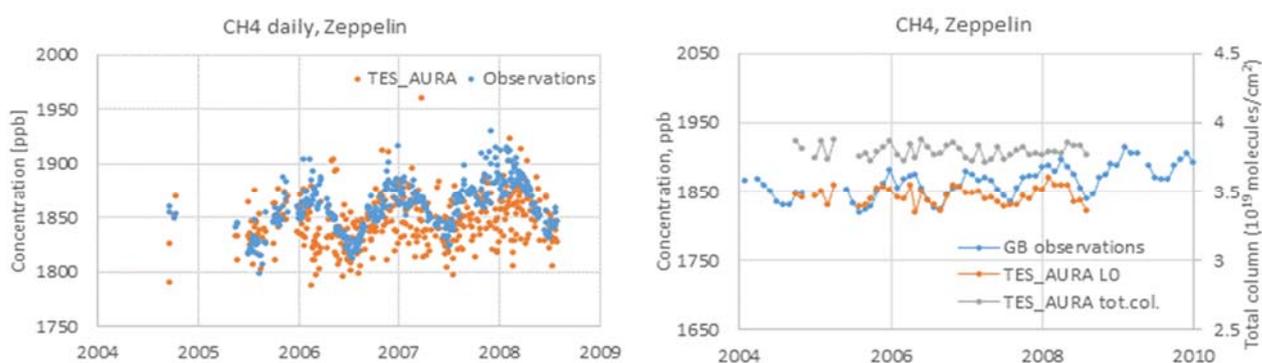
Figure 31: a) Left: Daily ground-based CH4 measurements at Zeppelin (blue dots) and the corresponding satellite observations from TES (AURA) surface layer (orange dots), b) Right: Monthly mean CH4 data at Zeppelin.

Figure 31a (left) shows daily TES AURA methane measurements (orange dots) and GB observations (blue dots) during days of simultaneous TES/GB measurements. The correlations and biases are listed in Table 4. Contrary to AIRS, the TES satellite data are in general lower than the GB observations. The bias between AIRS daily data (surface level, L0) and GB observations is -13 ppb and the correlation is 0.33. For the monthly mean data (Figure 31b, right) the correlation is significantly higher: 0.61 for the lowest TES level (L0) and 0.64 for the second lowest level (L1). The bias between satellite and GB observations are around -15 and -19 ppb for L0 and L1, respectively.

Table 4: Bias, scatter and correlation (R) between TES AURA satellite and ground-based methane data.

Daily	Bias	Scatter	R	N
Zeppelin (L0)	-12.9	26.5	0.33	423
Monthly	Bias	Scatter	R	N
Zeppelin (L0)	-15.4	15.9	0.61	39
Zeppelin (L1)	-18.8	16.3	0.64	39
Zeppelin (Total column)			0.1	39

3.3.3 Greenhouse Gases Observing Satellite - GOSAT

Greenhouse Gases Observing Satellite, GOSAT, was launched in 2009 and is still in operation. The GOSAT project is a joint effort of Japanese institutes (Japan). For comparison between GOSAT and the Norwegian GB measurements, we have used GOSAT Level 4 Data Product of CH_4. This product consists of the Level 4A (L4A) surface CH4 flux data estimated with GOSAT and a number of ground-based observations, and the Level 4B three-dimensional global CH4 distributions predicted with the estimated L4A fluxes. The data content is described in more detail in the GOSAT (L4) Data Product Format Description document (http://data.gosat.nies.go.jp/).

Figure 32a and b show comparisons of GOSAT satellite data (orange dots) and in-situ observations (blue dots) at Zeppelin and Birkenes. The correlations are very good: 0.78 and 0.72 for Zeppelin and Birkenes, respectively. The overall biases are also relatively small, within ±7 ppb. A summary of the GOSAT statistics, compared to the Norwegian in-situ measurements, are listed in

Table 5. The good agreement between GOSAT and GB measurements can probably be explained by the GOSAT L4 product, which takes global ground-based observations into account.

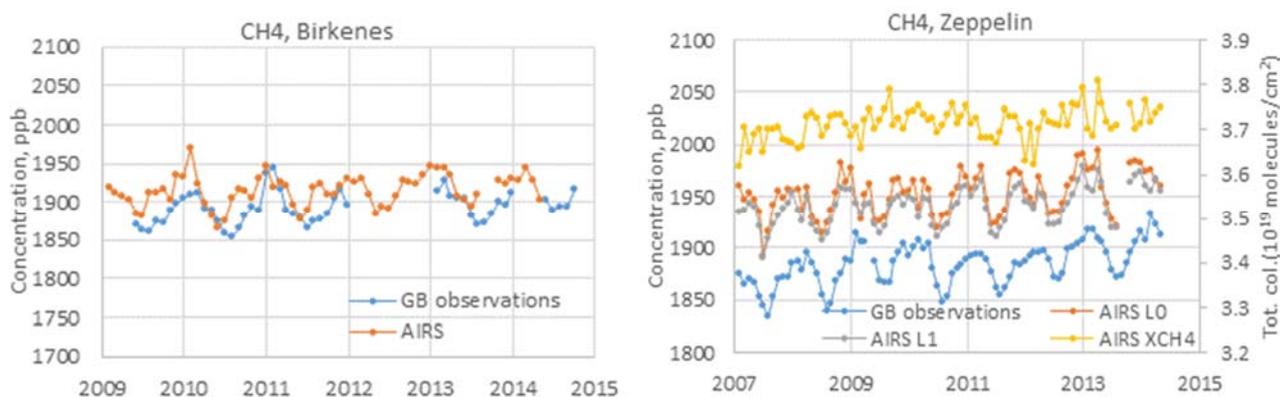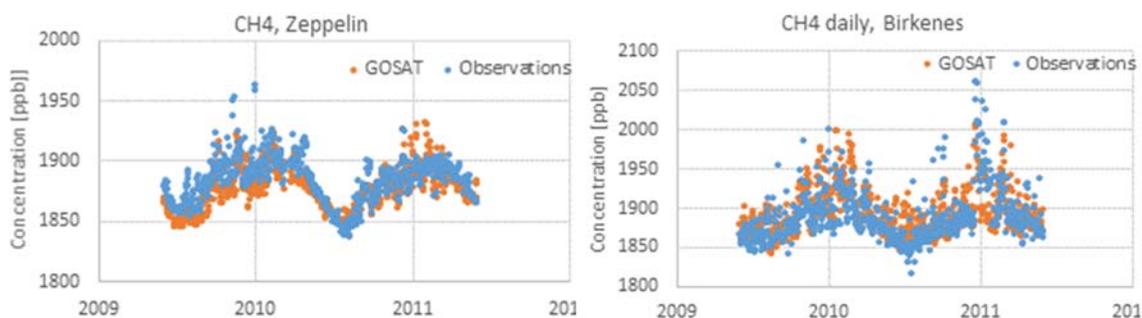*Figure 32: a) Left: Daily ground-based CH4 measurements at Zeppelin (blue) and the corresponding satellite observations from GOSAT surface layer (orange), b) Right: GOSAT and GB daily measurements at Birkenes.*

Table 5: Bias, scatter and correlation (R) between GOSAT and ground-based methane data

Daily	Bias	Scatter	R	N
Zeppelin (L0)	-6.5	12.5	0.77	682
Zeppelin (L1)	-6.7	12.1	0.78	682
Birkenes (L0)	4.8	24.3	0.72	724

4. Aerosols and climate: Observations from Zeppelin and Birkenes Observatories

Atmospheric aerosol influences climate by scattering incoming visible solar radiation back into space before it can reach the ground, be absorbed there and warm the earth surface. This so called direct aerosol climate forcing is mostly cooling, but can be moderated if the aerosol itself absorbs solar radiation, e.g. if it consists partly of light absorbing carbon or light absorbing minerals. In this case, the aerosol warms the surrounding atmosphere, the so-called semi-direct effect. Atmospheric aerosol particles also affect the reflectivity and lifetime of clouds, which is termed the indirect aerosol climate effect. Here as well, the effect can be cooling as well as warming for climate, but in most cases, the cloud reflectivity and lifetime are increased, leading again to a cooling effect (see chapter 2 at page 11).
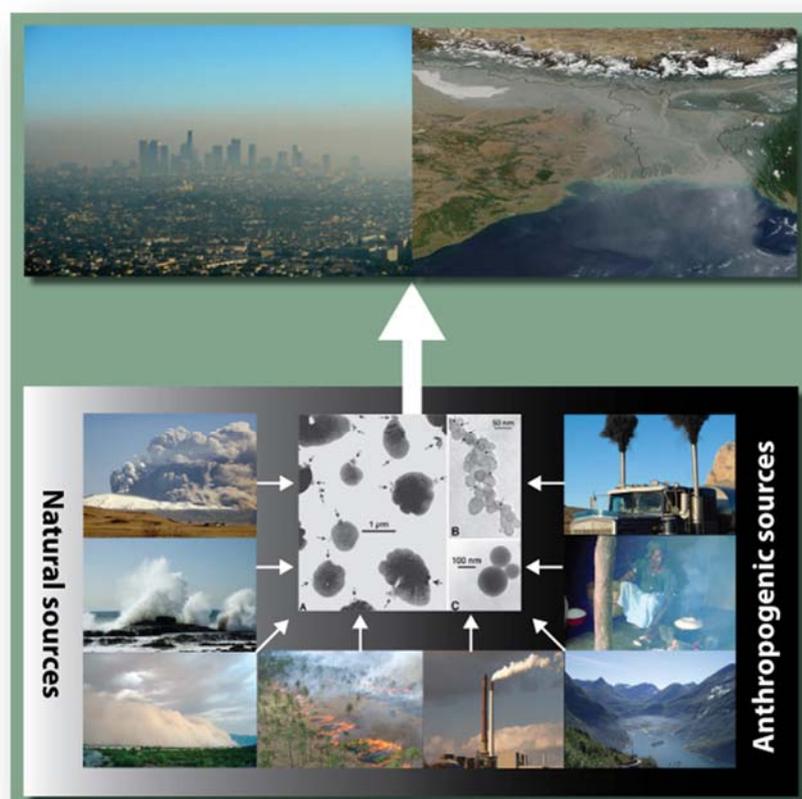
Figure 33: Illustration of the main natural and anthropogenic sources of atmospheric aerosols taken from Myhre et al (2013a). Top: local and large scale air pollution. Sources include (bottom, counter clockwise) volcanic eruptions (producing volcanic ash and sulphate), sea spray (sea salt and sulphate aerosols), desert storms (mineral dust), savannah biomass burning (BC and OC), coal power plants (fossil fuel BC and OC, sulphate, nitrate), ships (BC, OC, sulphates, nitrate), cooking* (domestic BC and OC), road transport (sulphate, BC, VOCs yielding OC). Center: Electron microscope images of (A) sulphates, (B) soot, (C) fly ash, a product of coal combustion (Posfai et al., 1999).

Uncertainties in assessing aerosol climate forcing hamper the attribution of changes in the climate system. IPCC AR5 (IPCC, 2013) has high confidence in stating that atmospheric aerosol in the past has offset a significant fraction of greenhouse gas radiative warming, although the magnitude is connected with uncertainty (see chapter 2). Due to the decline of aerosol concentrations as reported in Tørseth et al (2012), Coen et al, (2013), and Asmi et al, (2013), and summarized in Hartmann et al, 2013) the total anthropogenic radiative forcing will be even larger in the future.

IPCC AR5 mentions progress since AR4 concerning observations of climate relevant aerosol properties such as particle size distribution, particle hygroscopicity, chemical composition, mixing state, optical and cloud nucleation properties. This includes the parameters covered by the Norwegian monitoring programme, and underlines the importance of these observations. IPCC AR5 also mentions a lack of long time series on these parameters and stresses that existing time series need to be continued to maximise their informative value.

The aerosol measurements from this national monitoring program together with data from other national and international networks reported to the WMO world data centre of aerosols (WDCA) hosted at NILU, are very important together with atmospheric transport models for assessing and predicting the aerosol climate effects. An important and recognised modelling community is represented by AeroCom hosted by the Norwegian Meteorological Institute. In 2013, the AeroCom Phase III project, a collaboration between the Norwegian Meteorological Institute, Cicero and NILU funded by the Norwegian Research Council, has taken up its work. Ongoing activities include setting up facilities for data collection of coarse mode (D_p > 1 µm) particle size distribution data from stations a round the globe for making them accessible to climate models. This effort will have positive effects on the modelling accuracy of both, the direct and indirect aerosol climate effects. Data of this type have been measured at Birkenes observatory in Southern Norway since 2010, and are included in this report for the first time this year.

As presented in Chapter 1 and Table 1, the national monitoring program of aerosol properties are conducted at two Observatories (Zeppelin and Birkenes) In addition, NILU has similar measurements at the Troll Atmospheric Observatory in Antarctica funded through the NARE project and NILU. Recent relevant developments at these three Observatories include:

1. **Zeppelin Mountain**: Despite performing good quality assurance on the measurement programme within the WMO GAW programme, the collaboration partner Stockholm University who operates the respective instruments had some delay in delivering the quality assured data due to funding restrictions on the Swedish side. The process to remedy these problems is still ongoing.

2. **Birkenes Atmospheric Observatory:** Apart from resuming the operation of the extended aerosol instrument set at Birkenes according to the quality standards of WMO GAW and the European infrastructure project ACTRIS, a focus for 2013 and 2014 has been placed on workshop intercomparisons of selected instruments. Despite strictly following the operating procedures agreed within the networks, certain instrument malfunctions can pass unnoticed if the instruments within a network are not intercompared directly on the same sample. To this end, ACTRIS organised in 2013 intercomparison workshops for absorption photometers (measuring the aerosol absorption coefficient) and Differential or Scanning Mobility Particle Sizers (DMPS / SMPS, measuring the fine-mode particle number size distribution) in which the respective instruments from Birkenes participated successfully. In 2014, another workshop was organised, for the first time intercomparing instruments measuring the coarse mode (D_p > 1 µm) particle size distribution, also with instruments form Birkenes participating. For the Birkenes absorption photometer, in service since 2006, it was discovered that it overestimates aerosol absorption by a factor of 1.77 due to a design

problem, despite being operated correctly. This highlights the importance of such intercomparison workshops and facilitates the correction of the Birkenes aerosol absorption time series also in hindcast (the correction has already been applied for this report). For the Birkenes DMPS, it was found that its operation status is in full compliance with network quality objectives (sizing uncertainty <3%, counting uncertainty < 10%). The mode of operation could be optimised to extend the upper end of the measured particle size distribution from 550 nm to 800 nm, and the lower end from 15 nm to 10 nm. The optical particle spectrometer measuring the coarse mode particle number size distribution was among the instruments performing best at the workshop. Its data are for the first time included in this report, yielding, combined with the DMPS instrument, a particle number size distribution time series spanning 3 orders of magnitude in particle diameter (10 nm – 10 μm).

3. **Troll Atmospheric Observatory:** Funded by a base funding project controlled by the Norwegian Research Council (Strategisk Instituttsatsing, SIS), an article on the annual cycle of the baseline aerosol at Troll was published the past year (Fiebig et al., 2014). The article investigates the named annual cycle as observed in the particle number size distribution and aerosol scattering coefficient data collected at Troll. It is shown that the baseline aerosol annual cycles in both parameters have the same physical origin. A comparison with data collected at the Antarctic stations South pole and Dome C, yields that the baseline air annual cycle observed at Troll is common to the whole Central Antarctic plateau. Following the Troll baseline air masses backwards with the Lagrangian transport model FLEXPART, the article demonstrates that these air masses descend over Antarctica after being transported in the free troposphere and lower stratosphere from mid-latitudes (there uplifted in fronts) or from the inter tropical convergence zone (uplifted by convection). The article shows further that the aerosol particles contained in Antarctic baseline air are formed in situ by photochemical oxidation of precursor substances. The article draws a comprehensive picture of this natural aerosol process that will help climate models to distinguish better between natural and anthropogenic aerosol processes, and therefore between natural and anthropogenic aerosol climate effects. On the fieldwork side, it needs to be mentioned that the atmospheric Observatory has been moved in the past 2013/14 Antarctic summer season to a location virtually undisturbed by local contamination, after the necessary budget had been allocated. The previous location was only 200 m apart from the Troll station main building, which is in reach of turbulent diffusion. This led to typically 80% or more of the data collected at the previous location of the atmospheric Observatory to be locally contaminated and unsuitable for scientific use, which implied severe limitations on the kind of scientific questions possible to investigate. The first results from the new station location on top of a mountain south of the main station are rather promising, with the local contamination essentially eliminated.

An overview of all aerosol parameters currently measured at the three above mentioned Observatories can be found in Table 6. Parameters where observations funded by Miljødirektoratet (and which are covered in this report are written in green type.

Table 6: Aerosol observations at Zeppelin, Birkenes and Troll Observatories following the GAW recommendations. Parameters in green are funded by the Norwegian Environment Agency and included in this report.

	Zeppelin/Ny-Ålesund	Birkenes	Troll
Particle Number Size Distribution (fundamental to all aerosol processes)	fine mode (0.01 μm < D_p < 0.8 μm) in collaboration with Stockholm University	fine and coarse mode (0.01 μm < D_p < 10 μm)	fine mode (0.03 μm < D_p < 0.8 μm)
Aerosol Scattering Coefficient (addressing direct climate effect)	spectral at 450, 550, 700 nm, in collaboration with Stockholm University	spectral at 450, 550, 700 nm	spectral at 450, 550, 700 nm
Aerosol Absorption Coefficient (addressing direct climate effect)	single wavelength at 525 nm, in collaboration with Stockholm University	single wavelength (525 nm) and spectral	single wavelength at 525 nm
Aerosol Optical Depth (addressing direct climate effect)	spectral at 368, 412, 500, 862 nm in collaboration with WORCC	spectral at 340, 380, 440, 500, 675, 870, 1020, 1640 nm, in collaboration with Univ. Valladolid	spectral at 368, 412, 500, 862 nm
Aerosol Chemical Composition (addressing direct + indirect climate effect)	main components (ion chromatography), heavy metals (inductively-coupled-plasma mass-spectrometry)	main components (daily resolution, offline filter-based, ion chromatography), heavy metals (inductively-coupled-plasma mass-spectrometry)	main components (ion chromatography), discontinued from 2011 due to local contamination.
Aerosol Chemical Speciation (direct + indirect climate effect, source attribution, transport)	---	Particle main chemical species (hourly resolution, online mass spectrometry)	---
Particle Mass Concentration	---	$PM_{2.5}$, PM_{10}	PM_{10}, discontinued from 2011 due to local contamination
Cloud Condensation Nuclei (addressing indirect climate effect)	size integrated number concentration at variable supersaturation in collaboration with Korean Polar Research Institute	number concentration at variable supersaturation, installed in 2012	---

4.1 Physical and optical aerosol properties at Birkenes Observatory

4.1.1 Properties Measured In Situ at the Surface

Figure 34 summarises the optical aerosol properties measured at Birkenes since January 2010 when the upgraded station was in full routine operation. The optical aerosol properties quantify the direct climate effect of the aerosol, locally at the station and at the surface level. All panels of the figure depict time series of daily averages, the 2 topmost panels for the spectral scattering coefficient σ_{sp} and the absorption coefficient σ_{ap}. These properties are extensive properties, i.e. they scale with the total concentration of aerosol particles. The scattering coefficient quantifies the amount of light scattered by the aerosol particle population in a sample per distance a light beam travels through the sample. The absorption coefficient is the corresponding property quantifying the amount of light absorbed by the particle population in the sample. The two lower panels depict intensive optical aerosol properties, i.e. properties that don't scale with the particle concentration and that represent properties of the individual "average" particle in the aerosol. The scattering Ångström coefficient $å_{sp}$ parameterises the wavelength dependence of σ_{sp}. Normally, σ_{sp} decreases with wavelength. The stronger this decrease, the more positive $å_{sp}$ becomes. Higher values of $å_{sp}$ correlate with higher concentration ratios of particles in the fine size range ($D_p < 1$ μm) to those in the coarse size range ($D_p > 1$ μm). The single scattering albedo ϖ_0 depicted in the fourth panel quantifies the fraction of incident light interacting with the particles in an aerosol volume by scattering, rather than being absorbed by the particles. For a purely scattering aerosol, ϖ_0 is 1, and decreases with increasing fraction of light absorbing components in the aerosol particle phase. Since ϖ_0 is derived from σ_{sp} and σ_{ap}, the ϖ_0 wavelength plotted matches one of the wavelength of the integrating nephelometer, and is close to a wavelength of the filter absorption photometers. All panels include not only the time series of the daily averages, but also the 8-week running median centred around the data point, plotted as heavy line, to facilitate detection of possible seasonal variations. All properties are measured for particles with aerodynamic diameter $D_{p,aero} < 10$ μm and at relative humidity below 40%, thus avoiding water uptake by the aerosol particles, for best comparability between stations in the network. This protocol follows the recommendations of the WMO GAW aerosol network, and is identical with the recommendations of the relevant European networks (EUSAAR, ACTRIS). To facilitate an easier and quantitative comparison, Table 7 lists the annual and seasonal averages of the optical properties at Birkenes as well.
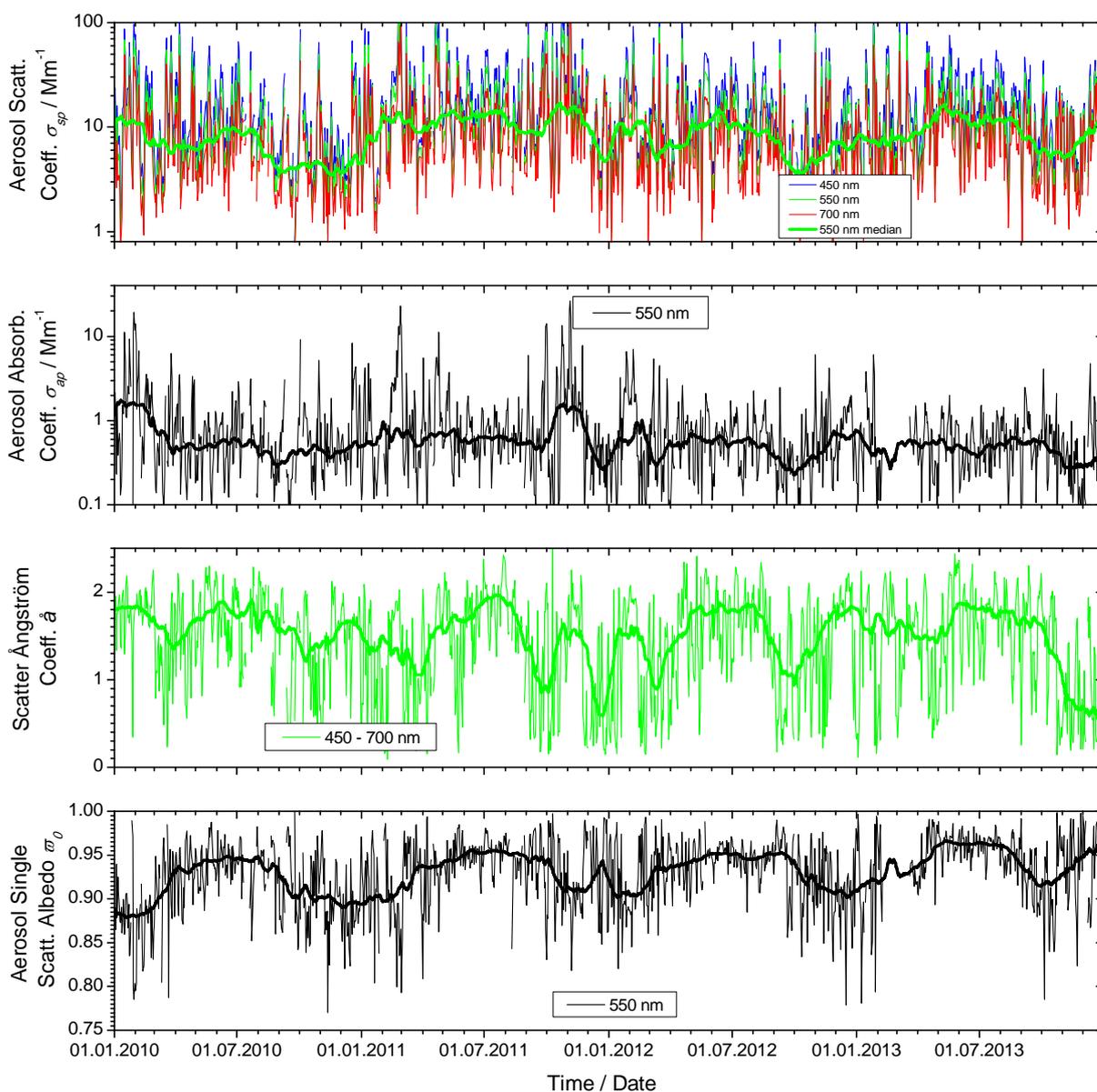
Figure 34: Time series of aerosol optical properties daily means measured for 2010 - 2013 at Birkenes. The top panel shows the aerosol scattering coefficient σ$_{sp}$ at 450, 550, and 700 nm wavelength measured by integrating nephelometer. The second panel depicts the aerosol absorption coefficient σ$_{ap}$ at 550 nm wavelength measured by filter absorption photometer, shifted from the instrument wavelength at 525 nm to 550 nm for consistent comparison assuming an absorption Ångström coefficient of -1. The third and forth panels show the scattering Ångström coefficient å$_{sp}$ and the single scattering albedo ϖ$_{0}$ as derived properties, respectively. All plots also depict the running 8-week medians of the respective properties as heavy lines to visualize seasonal variations.

The time series of surface aerosol optical properties at Birkenes now comprises 4 years, still too short for trend analysis. So far, the time series of σ_{sp} and $å_{sp}$ don't show any visible underlying trend, which is consistent with the findings for other European continental background stations at Jungfraujoch (Switzerland, mountain top), Hohenpeissenberg (Southern Germany, elevated boundary layer), and Pallas (Northern Finland, boreal background) (Coen et al, 2013). Also the range of σ_{sp} values encountered, 3 - 50 Mm^{-1} with an annual average of about 12.5 Mm^{-1}, is consistent with findings at comparable stations (Delene & Ogren, 2002). The variation of σ_{sp} and $å_{sp}$ is rather driven by synoptic scale transport patterns of the air masses arriving at Birkenes on a time scale of a few days, as discussed in detail in last year's report.

For $å_{sp}$ which varies between 1 and 2 over the year, a slight seasonal dependence can be detected, with a tendency for higher values in summer than in winter. This is due to a seasonal cycle in the concentration of fine-mode particles, with higher values in summer than in winter, which will be discussed below.

Also the variability of σ_{ap} and ϖ_0 are dominated by synoptic scale transport of air masses to Birkenes on the time scale of hours to days. The values of σ_{ap} fall in the range of 0.3 – 4 Mm^{-1} with annual means around 1 Mm^{-1}, whereas ϖ_0 varies between 0.86 – 0.96. Both properties characterizing aerosol absorption show in Birkenes an annual cycle and a tendency towards an underlying trend, as far as possible to detect this with a time series of 4 years duration. Both features are visible best in the time series of ϖ_0, which shows a clear annual cycle with lower values (more aerosol absorption) in winter due to black carbon (BC) emissions from domestic heating with wood stoves as discussed in detail in last year's report. Underlying the annual cycle, ϖ_0 shows a tendency to higher values, i.e. decreasing aerosol absorption. Such a tendency has so far not been observed for other European stations, only for stations in the continental U.S. and Alaska (Barrow) (Coen et al, 2013). If found to be persistent in the forthcoming years, this tendency to decreasing aerosol absorption would most likely be caused by decreasing BC emissions due to stricter regulations for both traffic emissions and those from domestic heating.
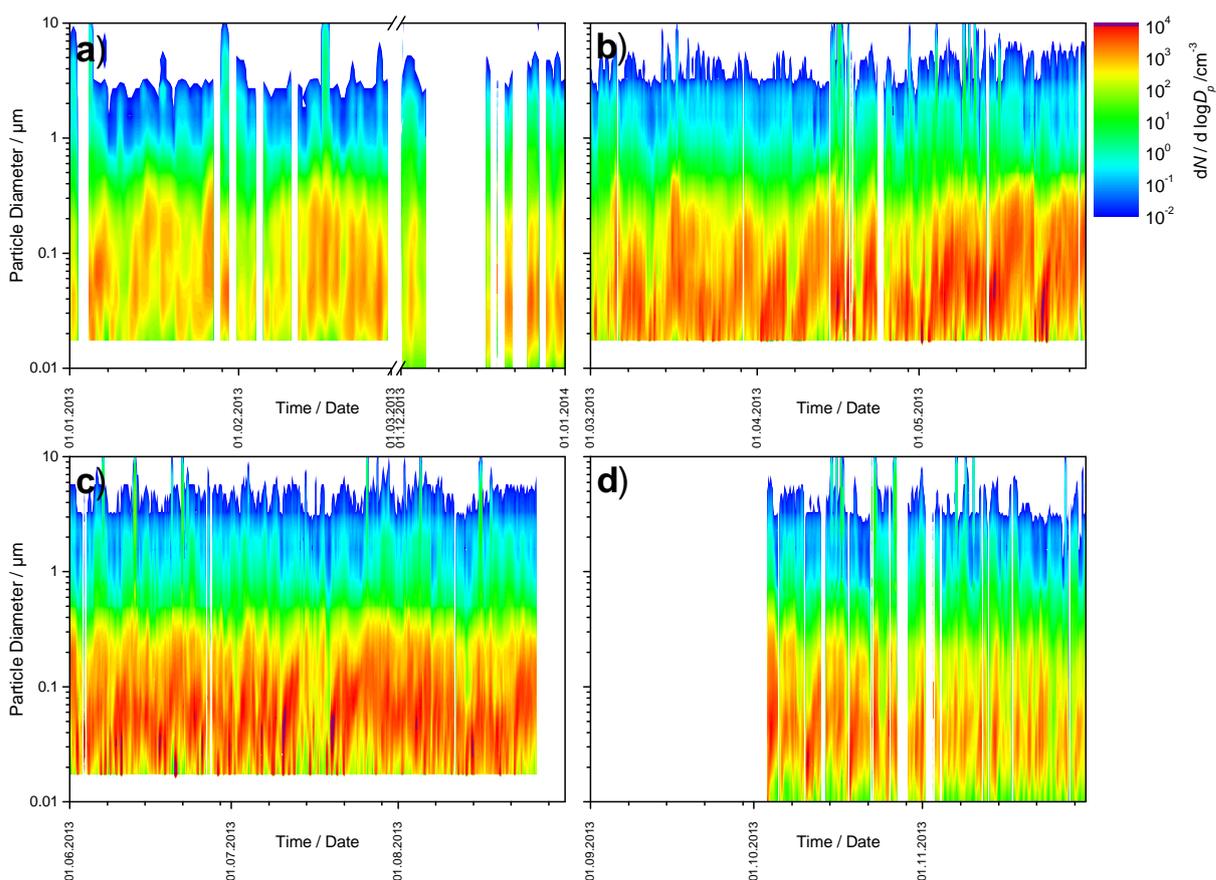
Figure 35: 2013 time series of particle number size distribution at Birkenes, panel a) winter, panel b) spring, panel c) summer, panel d) autumn
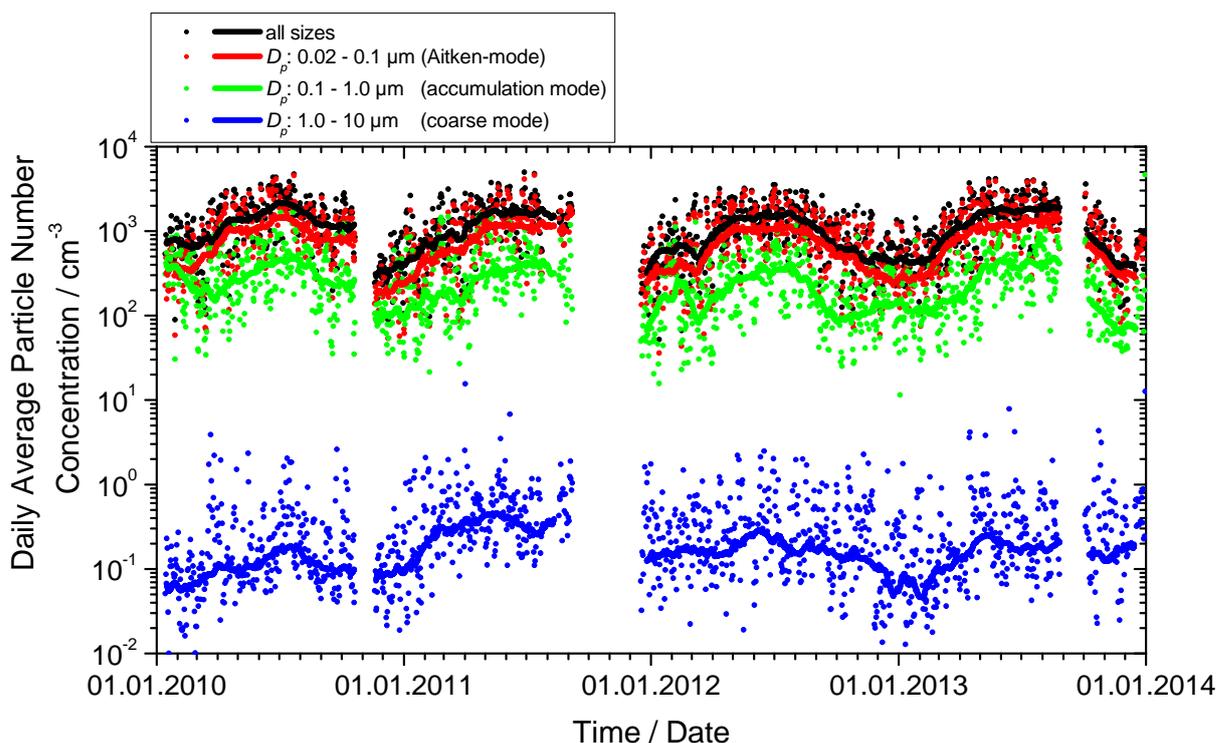
Figure 36: 2010-2013 time series of particle number concentration integrated over selected size ranges representing the different physical processes governing the atmospheric aerosol. The dotted graphs represent daily averages of the respective size range, the solid lines the respective running 8-weekly medians to highlight the seasonal variation

Figure 35 shows the time series of the particle number size distribution (PNSD) measured at Birkenes in 2013, separated into 4 different panels by season. In this plot type, the x-axis holds the time of the observation, whereas the y-axis holds the particle diameter D_p on a logarithmic scale. The logarithmic colour scale holds the particle concentration, normalised to the logarithmic size interval, dN / dlog D_p. The use of logarithmic axis is common when displaying PNSD information since both particle diameter and particle concentration tend to span several orders of magnitude while containing relevant information over the whole scale. In this report, the PNSD reported for Birkenes covers for the first time the whole size range between 0.01 – 10 μm by combining the information of two instruments, one each focussing on the fine and coarse size ranges, into a common PNSD product (see appendix for details). Where existing, operating procedures and quality standards defined by the WMO Global Atmosphere Watch Programme and the European research infrastructure ACTRIS have been used (Wiedensohler et al., 2012).

Even though the PNSD isn't uniquely connected to a specific air mass type, it is normally fairly characteristic for the air mass, and can serve, together with the single scattering albedo ϖ_0, as valuable indication of air mass origin, which at Birkenes shifts with the synoptic weather situation. Though the information content of a PNSD time series plot is too high to be discussed in detail here. The PNSD and ϖ_0 observations reconfirm previous findings on the dominant air mass types at Birkenes, which consist of: 1) clean Arctic background aerosol; 2) continental aerosol; 3) Arctic haze; 4) biogenic aerosol, i.e. vegetation emitted precursor gases condensing to the particle phase by photooxidation; 5) wood combustion aerosol from domestic heating. A detailed analysis of the predominant air mass types at Birkenes and their occurrence is currently

ongoing in the base-funded project "Strategic Aerosol Observation and Modelling Capacities for Northern and Polar Climate and Pollution" (SACC).

Year	Season	N_{ait} / cm^{-3}	N_{acc} / cm^{-3}	N_{coarse} / cm^{-3}	N_{total} / cm^{-3}	σ_{sp} (550 nm) / Mm^{-1}	σ_{ap} (550 nm) / Mm^{-1}	ϖ_0 (550 nm)
2009/10	Winter	440	384	0.087	824	16.82	3.09	0.88
2010	Spring	1030	324	0.311	1354	12.33	0.78	0.93
2010	Summer	1511	488	0.323	1999	11.30	0.70	0.94
2010	Autumn	835	299	0.260	1135	7.26	0.71	0.90
2010	Whole Year	973	362	0.256	1336	11.52	1.24	0.91
2010/11	Winter	454	285	0.311	739	16.96	2.18	0.89
2011	Spring	1127	369	0.639	1496	18.67	1.26	0.93
2011	Summer	1391	438	0.572	1829	15.43	0.74	0.95
2011	Autumn	1594	464	0.966	2059	29.74	2.87	0.92
2011	Whole Year	1047	371	0.565	1418	20.26	1.69	0.93
2011/12	Winter	424	213	0.305	637	11.29	1.00	0.91
2012	Spring	1107	271	0.386	1378	15.10	0.86	0.93
2012	Summer	1314	392	0.485	1706	12.62	0.67	0.95
2012	Autumn	661	152	0.365	814	9.80	0.65	0.92
2012	Whole Year	889	263	0.375	1152	12.22	0.83	0.92
2012/13	Winter	383	183	0.183	566	12.48	0.92	0.90
2013	Spring	1190	352	0.411	1543	17.03	0.68	0.95
2013	Summer	1519	447	0.467	1967	13.81	0.56	0.96
2013	Autumn	701	162	0.417	864	8.89	0.64	0.91
2013	Winter	453	135	0.465	588	17.67	0.87	0.94
2013	Whole Year	1020	304	0.391	1324	13.73	0.67	0.94

Table 7: 2010 - 2013 seasonal and annual means of size distribution integrals, scattering coefficient, absorption coefficient, and single scattering albedo.

In order to condense the information in the PNSD time series, Figure 36 shows the time series of selected PNSD integrals, i.e. the concentration of particles falling into selected size intervals. The size intervals are chosen to represent characteristic processes governing the

atmospheric aerosol (see appendix for more details): 1) the Aitken-mode size range, 0.02 – 0.1 µm; 2) the accumulation mode size range, 0.1 – 1 µm; 3) the coarse mode size range, 1 - 10 µm. The time series in Figure 36 represent daily averages over these PNSD integrals for the whole period since the Birkenes station upgrade in 2010. Also included are the running 8-weekly medians for highlighting seasonal variations. The respective size range integral particle concentrations, N_{ait} for the Aitken mode, N_{acc} for the accumulation mode, and N_{coa} for the coarse mode, are also included in Table 7 to show the respective seasonal and annual average concentrations. As to be expected, the particle concentration in the Birkenes aerosol in absolute terms is dominated by the Aitken mode particles, followed by the accumulation mode. Also the most prominent feature in Figure 36 is exhibited by the particle concentrations in these 2 modes, a clear annual cycle caused by the same underlying physical process. In summer, the vegetation emits gaseous aerosol precursors, which are photooxidised and condense onto Aitken-mode particles or form those directly. These particles coagulate, increasing the concentration of accumulation mode particles. The processes controlling N_{coa} are decoupled from those controlling N_{ait} and N_{acc}. Coarse mode particles are mainly formed from bulk material, their concentration is affected by wind speed (levitating dust, spores, pollen, sea salt), snow cover, and rain (both inhibiting dust levitation). In addition, particles containing long range transport of secondary organic and inorganic aerosols (SIA and SOA) may partly be in the coarse fraction depending on the atmospheric chemical processes.

4.1.2 Column Integrated Properties Measured In Situ by Remote Sensing from the Surface

Ground-based remote sensing of the optical characteristics of aerosols in the atmospheric total column is conducted with multi-wavelength sun-photometers. A sun-photometer is oriented towards the sun to detect the solar radiation attenuated along the slant path from the top-of-atmosphere to the ground. The atmospheric aerosol load leads to a decrease in the solar radiation transmitted through the atmosphere. This decrease depends on the aerosol optical depth (AOD), which is given by the integral of the volume aerosol extinction coefficient along the vertical path of the atmosphere. The wavelength dependence of AOD, described by the Ångström exponent (Å) is a qualitative indicator of the particle size and contains information about the aerosol type. The larger the Ångström exponent, the smaller the size of the particles measured.

Photos of instruments used for monitoring of spectral resolved AOD at Birkenes and Ny-Ålesund (see below), their main characteristics are given in Appendix II, and detailed Tables with monthly data for all years are given in Appendix I.

AOD measurements started at the Birkenes Observatory in spring 2009, utilizing an automatic sun and sky radiometer (CIMEL type CE-318, instrument #513). The retrieval method is that of the AERONET version 2 direct sun algorithm (for details: http://aeronet.gsfc.nasa.gov). Quality assured (Level 2) data are available for the first four years of operation, 2009 - 2012. In 2013, the measurements started after receiving the instrument back from the Spanish GOA-UVA AERONET-EUROPE Calibration Service Centre in June. Raw data area available for the time period June - December 2013. The 2013 data are AERONET level 1.5 data, which implies that they have been automatically cloud cleared, but have not yet been post field calibrated. An additional manual cloud-screening has been performed by NILU as an initial quality assurance. The Cimel instrument has been sent for calibration to GOA-UVA in October 2014, thus AERONET level 2 data for 2013 will become available after post calibration in 2014.

Figure 37: 2009 - 2013 time series of aerosol optical depth (AOD) at 550 nm wavelength in the atmospheric column above Birkenes (upper panel) and Ångström coefficient describing the AOD wavelength dependence (lower panel). Mean values and standard deviations are given.

The AOD and Å time series and seasonal variations are shown in Figure 37 and Figure 38. The 2013 monthly mean and mean values for all years are shown in Table 8. Data for all years are given in Appendix I. There is no obvious trends seen within the five years of observations. The data gaps seen are mainly caused by the calibration periods and less sun-light hours during the winter months between November and February. In general, AOD measured at Birkenes are relative low, compared to central European observations (e.g. AERONET gives climatological values for Cabauw in the Netherlands vary between 1.2 ± 0.06 in December and 3.1 ±0.19 in April). The highest AOD have been observed in April (~0.16) and July (~0.13), both months show a large spread of values, AOD is considerable lower during the winter months. The lower scatter of the data during winter can be a combination of both, lower variability of the column aerosol load and lower sampling during the darker seasons. AOD values for 2013 are within the spread observed during the years 2009 - 2013. Also in the rest of Southern Scandinavia, AOD is higher during the summer months (Toledano et al., 2012). The larger Ångström exponent
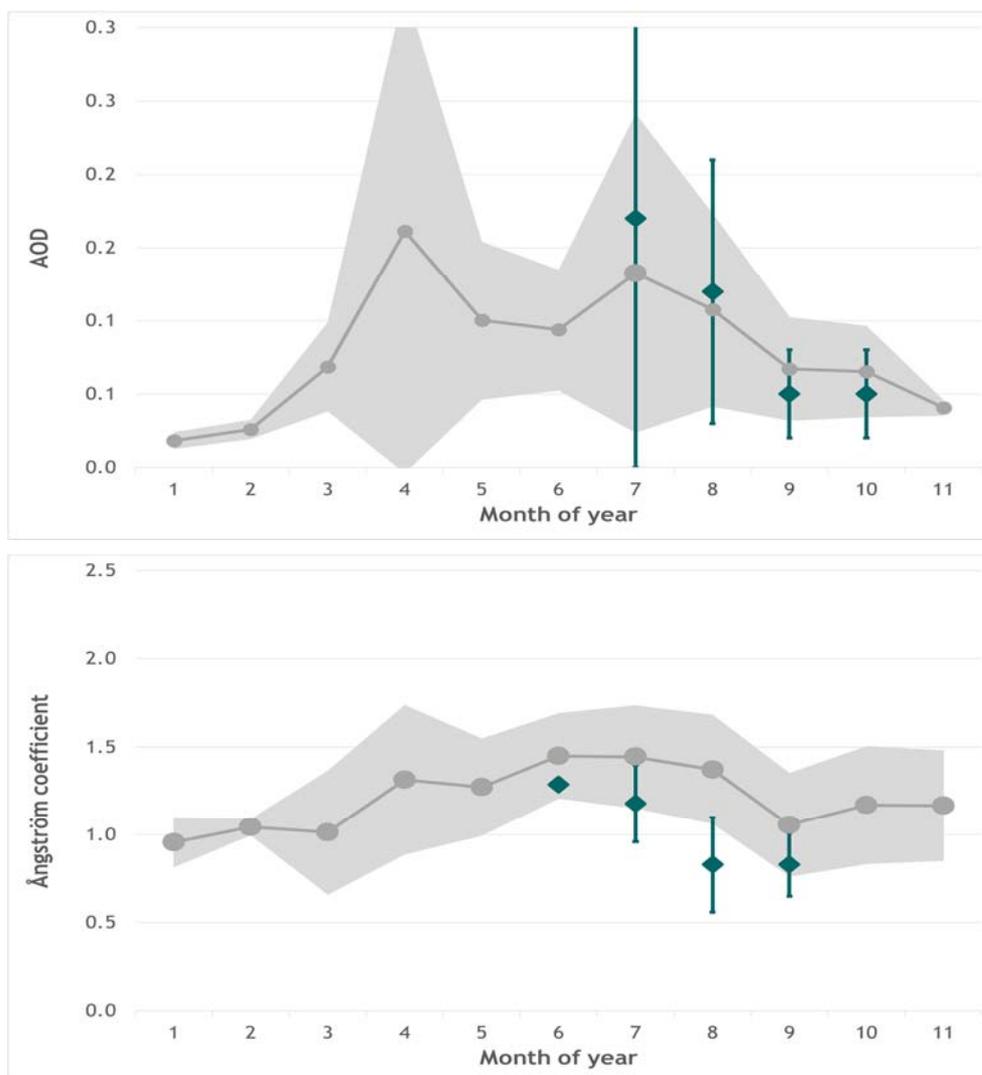
Figure 38: Seasonal variation of the aerosol optical depth (AOD) (upper panel) and Ångström coefficient (lower panel) observed at Birkenes Observatory. Values marked in grey are the mean and standard deviations for the time period 2009-2013; the 2013 monthly mean and standard deviations are shown in green.

between June and August indicate a predominance of finer particulates in Southern Norway during summer. The Ångström exponent decreased towards winter-time, indicating larger particles. The annual cycle can be linked to long-range transport patterns from e.g. the European continent.

4.2 Optical, column-integrated aerosol properties at Zeppelin Observatory

In 2002, Physikalisch-Meteorologisches Observatorium Davos/*World Radiation Center* (PMOD/WRC) in collaboration with NILU, started AOD observations in Ny-Ålesund (at the Sverdrup station, 46 m a.s.l.) as part of the global AOD network on behalf of the WMO GAW program. A precision filter radiometer (PFR) measures the extinction in four narrow spectral bands at 368 nm, 415 nm, 500 nm and 862 nm. Data quality control includes instrumental

Table 8: Monthly mean values for 2013 and mean for the time period 2009-2013, plus standard deviations, for aerosol optical depth (AOD) and Ångström coefficient observed in Birkenes. In addition, the number of days with cloud free and quality assured observations are given.

Month/Year	Jan	Feb	Mar	Apr	May	Jun	Jul	Aug	Sep	Oct	Nov
Aerosol optical depth (AOD)											
2013							0.17 ±0.17	0.12 ±0.09	0.05 ±0.03	0.05 ±0.03	
Mean 09-13	0.02 0.01	0.03 ±0.01	0.07 ±0.03	0.16 ±0.17	0.10 ±0.05	0.09 ±0.04	0.13 ±0.11	0.11 ±0.07	0.07 ±0.04	0.07 ±0.03	0.04 ±0.01
Ångström coefficient (Å)											
2013							1.3 ± 0.2	1.2 ±0.3	0.8 ±0.2	0.8 ±0.3	
Mean 09-13	1.0 ±0.1	1.0 ±0.0	1.0 ±0.4	1.3 ±0.4	1.3 ±0.3	1.5 ±0.2	1.4 ±0.3	1.4 ±0.3	1.1 ±0.3	1.2 ±0.3	1.2 ±0.3
Number of days with cloud-free and quality assured observations (lev 2; lev 1.5 for 2013)											
2013							26	18	13	7	
Total 09-13	7	2	31	36	63	68	86	77	53	41	8

control like detector temperature and solar pointing control as well as objective cloud screening. Ångström coefficients are derived for each set of measurements using all four PFR channels. Calibration is performed annually at PMOD/WRC. Near Real Time data are displayed at www.pmodwrc.ch/worcc. Quality assured data are available at the World Data Center of Aerosols (WDCA), hosted at NILU (see https://ebas.nilu.no).

In Ny-Ålesund, the sun is below 5° between 10 October and 4 March, limiting the period with suitable sun-photometer observations to the spring-summer seasons (NILU contributes to an initiative to fill the gap in the winter-time AOD climatology, see Appendix I). In 2013, sun-photometer observations were made between March and September and for 62 days AOD values are available. The AOD and Å time series and seasonal variations are shown in Figure 39 and Figure 40. The 2013 monthly mean and mean values for all years are shown in Table 9. Data for all years are given in Appendix I.

The data reveal the expected pattern, high aerosol load with larger AOD (~0.10 from March to May) during the Arctic haze season, and lower summer values, ~0.06 in June-July to less than 0.05 in September, with standard deviation equal to 0.04 in spring and 0.03 in summer and
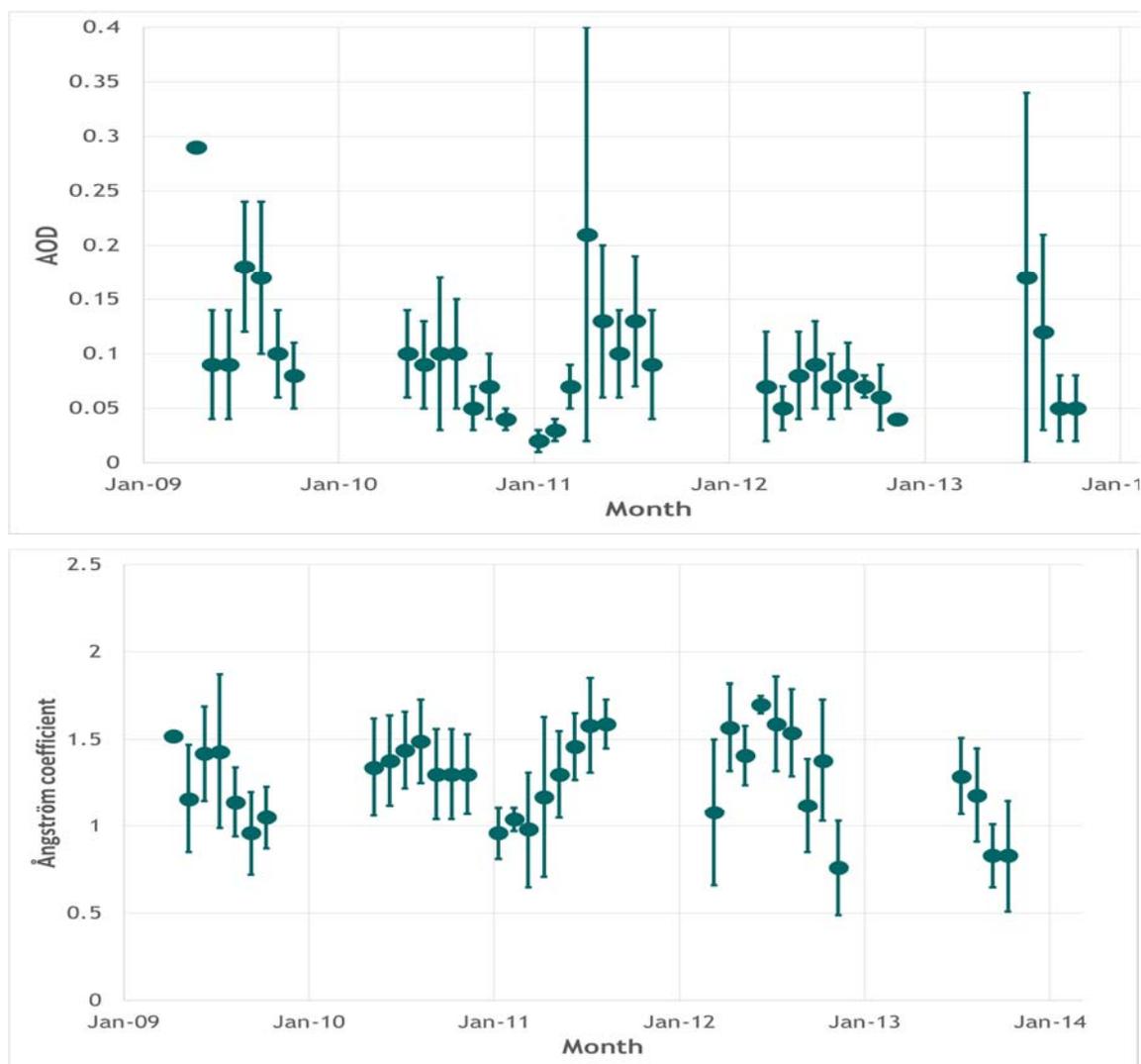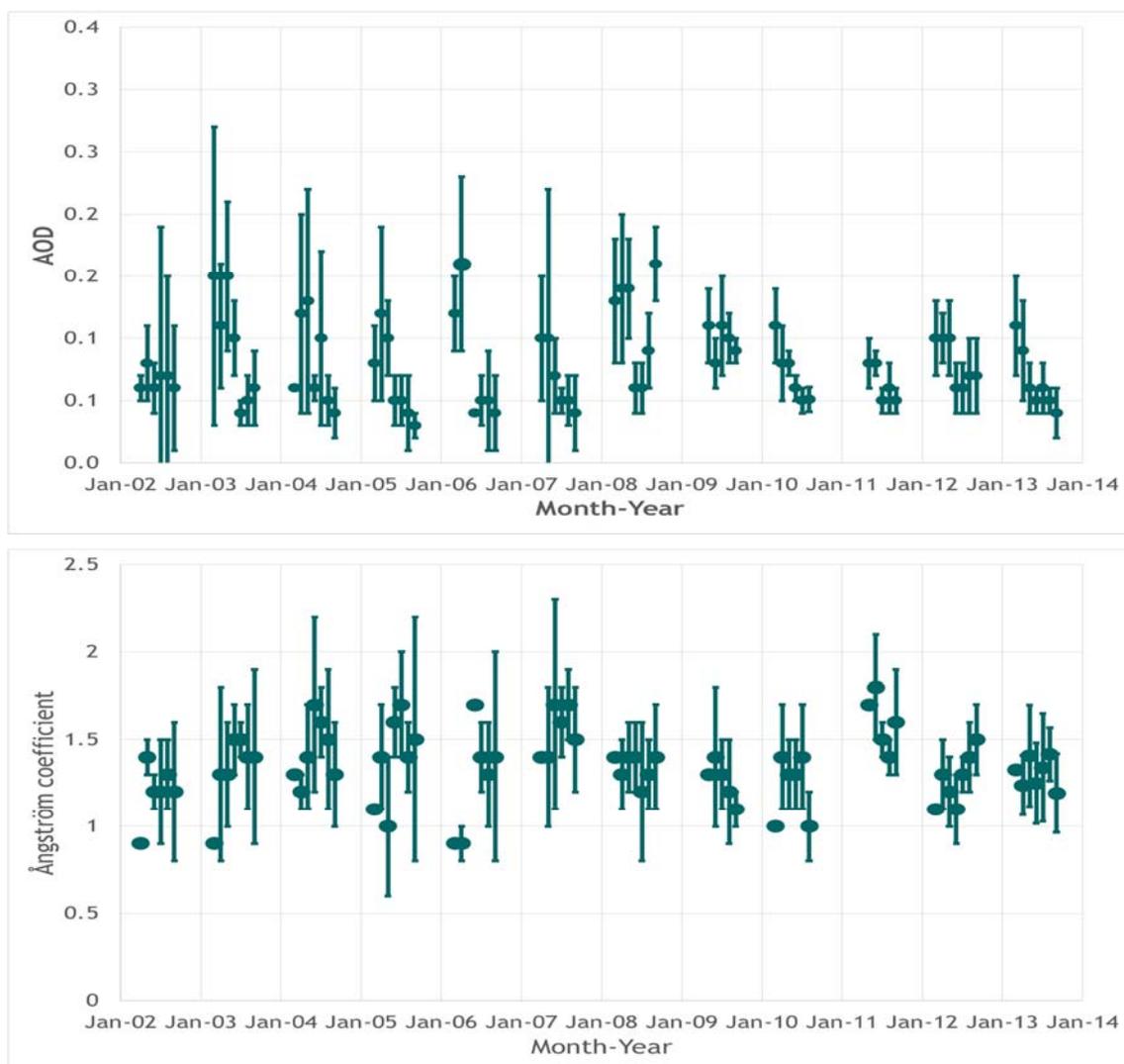
Figure 39: 2002 - 2013 time series of aerosol optical depth (AOD) at 550 nm wavelength in the atmospheric column above Ny-Ålesund (upper panel) and Ångström coefficient (lower panel). Mean values and standard deviations are given.

autumn. Å increased slowly from 1.3 in March to 1.6 in June, and slowly decreased to ~1.5 in August, with standard deviation of ~0.3 in all months. In 2013 the AOD was comparable to the multi-annual average except in May where values were considerable lower. The Ångström exponents was ~0.1 below the multi-annual mean. The low AOD in May 2013 may reveal a slightly earlier onset of the summer season, but the non-homogeneous sampling due to sunlit conditions, from the sun-photometer data alone, this cannot be concluded. The multi-annual monthly mean of Å is around 1.5, thus indicating dominance of fine particles, with on average slightly larger aerosols in the total column seen in 2013. Variability of Å in winter-spring is given presumably due to the larger variability of fine and coarse particle concentrations during the frequent Arctic haze episodes and the summer-autumn values are caused by the larger variability of the fine particle mode atmospheric content (mainly related to boreal forest fire smoke particle transport) with respect to that of accumulation/coarse mode particles (mainly of oceanic origin).
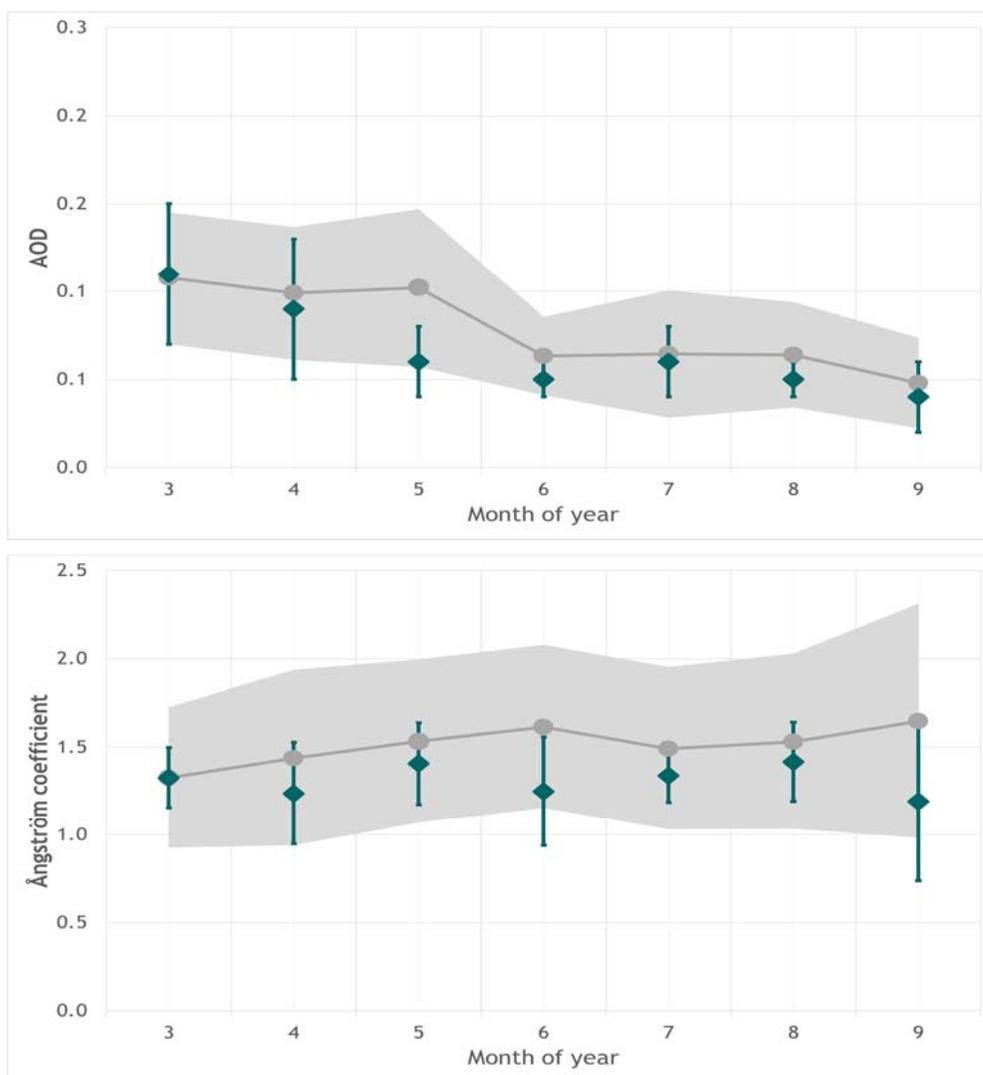
Figure 40: Seasonal variation of the aerosol optical depth (AOD) (upper panel) and Ångström coefficient (lower panel) observed in Ny-Ålesund. Values marked in grey are the mean and standard deviations for the time period 2009-2013; the 2013 monthly mean and standard deviations are shown in green.

The observations made by NILU are in good agreement with sun-photometer measurements performed by the Alfred-Wegener Institute (Bremerhaven, Germany) at a closely location in Ny-Ålesund (Tomasi et al., 2014). The authors give an updated comprehensive review of aerosol remote sensing in polar regions, including the sun-photometer observations in Ny-Ålesund.

Table 9: Monthly mean values for 2013 and mean for the time period 2002-2013, plus standard deviations, for aerosol optical depth (AOD) and Ångström coefficient observed in Ny-Ålesund. In addition, the number of days with cloud free and quality assured observations are given.

Month/Year	Mar	Apr	May	Jun	Jul	Aug	Sep
Aerosol optical depth (AOD)							
2013	0.11±0.04	0.09±0.04	0.06±0.02	0.05±0.01	0.06±0.02	0.05±0.01	0.04±0.02
Mean 2002-13	0.11±0.04	0.10±0.04	0.10±0.04	0.06±0.02	0.06±0.04	0.06±0.03	0.05±0.03
Ångström coefficient (Å)							
2013	1.3±0.2	1.2±0.3	1.4±0.2	1.6±0.3	1.3±0.2	1.4±0.2	1.2±0.5
Mean 2002-13	1.3±0.4	1.4±0.5	1.5±0.5	1.6±0.5	1.5±0.5	1.5±0.5	1.7±0.7
Number of days with cloud-free and quality assured observations							
2013	5	13	10	10	8	7	9
Total 2002-13	44	113	105	112	131	98	90

5. References

Aas, W., Solberg, S., Yttri, K.E. (2014) Monitoring of long-range transported air pollutants in Norway, annual report 2013. Kjeller, NILU (Miljødirektoratet rapport, M-203/2014) (NILU OR, 30/2014).

Asmi, A., Collaud Coen, M., Ogren, J. A., Andrews, E., Sheridan, P., Jefferson, A., Weingartner, E., Baltensperger, U., Bukowiecki, N., Lihavainen, H., Kivekäs, N., Asmi, E., Aalto, P. P., Kulmala, M., Wiedensohler, A., Birmili, W., Hamed, A., O'Dowd, C., G Jennings, S., Weller, R., Flentje, H., Fjaeraa, A. M., Fiebig, M., Myhre, C. L., Hallar, A. G., Swietlicki, E., Kristensson, A., Laj, P. (2013) Aerosol decadal trends - Part 2: In-situ aerosol particle number concentrations at GAW and ACTRIS stations. *Atmos. Chem. Phys.*, *13*, 895-916. doi:10.5194/acp-13-895-2013.

Coen, M.C., Andrews, E., Asmi, A., Baltensperger, U., Bukowiecki, N., Day, D., Fiebig, M., Fjaeraa, A. M., Flentje, H., Hyvärinen, A., Jefferson, A., Jennings, S. G., Kouvarakis, G., Lihavainen, H., Myhre, C.L, Malm, W. C., Mihapopoulos, N., Molenar, J. V., O'Dowd, C., Ogren, J. A., Schichtel, B. A., Sheridan, P., Virkkula, A., Weingartner, E., Weller, R., Laj, P. (2013) Aerosol decadal trends - Part 1: In-situ optical measurements at GAW and IMPROVE stations. *Atmos. Chem. Phys.*, *13*, 869-894. doi:10.5194/acp-13-869-2013.

Delene, D.J., Ogren, J.A. (2002) Variability of aerosol optical properties at four North American surface monitoring sites. *J. Atmos. Sci., 59,* 1135-1150.

IPCC (2013) Summary for policymakers. In: *Climate Change 2013: The Physical Science Basis. Contribution of Working Group I to the Fifth Assessment Report of the Intergovernmental Panel on Climate Change*. Ed.by Stocker, T.F., Qin, D., Plattner, G.-K., Tignor, M., Allen, S.K., Boschung, J., Nauels, A., Xia, Y., Bex, V., Midgley, P.M. Cambridge, Cambridge University Press. pp. 3-29.

Hartmann, D.L., Klein Tank, A.M.G., Rusticucci, M., Alexander, L.V., Brönnimann, S., Charabi, Y., Dentener, F.J., Dlugokencky, E.J., Easterling, D.R., Kaplan, A., Soden, B.J., Thorne, P.W., Wild, M., Zhai, P.M. (2013) Observations: atmosphere and surface. In: *Climate Change 2013: The Physical Science Basis. Contribution of Working Group I to the Fifth Assessment Report of the Intergovernmental Panel on Climate Change*. Ed.by Stocker, T.F., Qin, D., Plattner, G.-K., Tignor, M., Allen, S.K., Boschung, J., Nauels, A., Xia, Y., Bex, V., Midgley, P.M. Cambridge, Cambridge University Press. pp. 159-254.

Isaksen, I.S.A., Hov, Ø. (1987) Calculation of trends in the tropospheric concentration of O_3, OH, CO, CH_4 and NO_x. *Tellus*, *39B*, 271-285.

Myhre, G., Myhre, C. E.L., Samset, B. H., Storelvmo, T. (2013a) Aerosols and their relation to global climate and climate sensitivity. *Nature Education Knowledge*, *4,* 5,7. **URL:** http://www.nature.com/scitable/knowledge/library/aerosols-and-their-relation-to-global-climate-102215345

Myhre, G., Shindell, D., Bréon, F.-M., Collins, W., Fuglestvedt, J., Huang, J., Koch, D., Lamarque, J.-F., Lee, D., Mendoza, B., Nakajima, T., Robock, A., Stephens, G., Takemura, T., Zhang, H. (2013b) Anthropogenic and natural radiative forcing. In: *Climate Change 2013: The Physical Science Basis. Contribution of Working Group I to the Fifth Assessment Report of the Intergovernmental Panel on Climate Change*. Ed.by Stocker,

T.F., Qin, D., Plattner, G.-K., Tignor, M., Allen, S.K., Boschung, J., Nauels, A., Xia, Y., Bex, V., Midgley, P.M. Cambridge, Cambridge University Press. pp. 659-740.

Prather, M., Ehhalt, D., Dentener, F., Derwent, R.G., Dlugokencky, E., Holland, E., Isaksen, I.S.A., Katima, J., Kirchhoff, V., Matson, P., Midgley, P.M., Wang, M. (2001) Atmospheric chemistry and greenhouse gases. In: *Climate Change 2001: The Scientific Basis, Contribution of Working Group I to the Third Assessment Report of the Intergovernmental Panel on Climate Change.* Ed. by: Houghton, J.T., Ding, Y., Griggs, D.J., Noguer, M., van der Linden, P.J., Dai, X., Maskell, K., Johnson, C.A. Cambridge, Cambridge University Press. pp. 239-287.

Repo, M.E., Susiluoto, S., Lind, S.E., Jokinen, S., Elsakov, V., Biasi, C., Virtanen, T., Pertti, J., Martikainen, P.J. (2009) Large N_2O emissions from cryoturbated peat soil in tundra. *Nature Geosci., 2*, 189-192.

Simmonds, P.G., Manning, A.J., Cunnold, D.M., Fraser, P.J., McCulloch, A., O'Doherty, S., Krummel, P.B., Wang, R.H.J., Porter, L.W., Derwent, R.G., Greally, B., Salameh, P., Miller, B.R., Prinn, R.G., Weiss, R.F. (2006) Observations of dichloromethane, trichloroethene and tetrachloroethene from the AGAGE stations at Cape Grim, Tasmania, and Mace Head, Ireland. *J. Geophys. Res., 111*, D18304, doi:10.1029/2006JD007082.

Svendby, T.M., Edvardsen, K., Stebel, K., Myhre, C.L., Dahlback, A. (2014) Monitoring of the atmospheric ozone layer and natural ultraviolet radiation. Annual report 2013. Kjeller, NILU (Miljødirektoratet rapport, M-201/2014) (NILU OR, 28/2014).

Stebel, K., Vik, A.F., Myhre, C.L., Fjæraa, A.M., Svendby, T., Schneider, P. (2013) Towards operational satellite based atmospheric monitoring in Norway SatMoNAir. Kjeller, NILU, (NILU OR, 46/2013).

Toledano, C., Cachorro, V., Gausa, M., Stebel, K., Aaltonen, V., Berjón, A., Ortiz de Galisteo, J.P., de Frutos, A.M., Bennouna, Y., Blindheim, S, Myhre, C.L., Zibordi, G., Wehrli, C., Kratzer, S., Hakansson, B., Carlund, T., de Leeuw, G., Herber, A., Torres, B. (2012) Overview of sun photometer measurements of aerosol properties in Scandinavia and Svalbard. *Atmos. Environ., 52*, 18-28. doi: 10.1016/j.atmosenv.2011.10.022.

Tomasi, C., Kokhanovsky, A. A., Lupi, A., Ritter, C., Smirnov, A., O'Neill, N. T., Stone, R. S., Holben, B. N., Nyeki, S., Wehrli, C., Stohl, A., Mazzola, M., Lanconelli, C., Vitale, V., Stebel, K., Aaltonen, V., de Leeuw, G., Rodriguez, E., Herber, A. B., Radionov, V. F., Zielinski, T., Petelski, T., Sakerin, S. M., Kabanov, D. M., Xue, Y., Mei, L., Istomina, L., Wagener, R., McArthur, B., Sobolewski, P. S., Kivi, R., Courcoux, Y., Larouche, P., Broccardo, S., Piketh, S. J. (2014) Aerosol remote sensing in polar regions. *Earth Science Reviews*, accepted. doi:10.1016/j.earscirev.2014.11.001.

Thompson, R. L., Dlugockenky, E., Chevallier, F., Ciais, P., Dutton, G., Elkins, J. W., Langenfelds, R. L., Prinn, R. G., Weiss, R. F., Tohjima, Y., Krummel, P. B., Fraser, P., Steele, L. P. (2013) Interannual variability in tropospheric nitrous oxide. *Geophys. Res. Lett, 40*, 4426–4431, doi:10.1002/grl.50721.

Tørseth, K., Aas, W., Breivik, K., Fjæraa, A. M., Fiebig, M., Hjellbrekke, A. G., Lund Myhre, C., Solberg, S., Yttri, K. E. (2012) Introduction to the European Monitoring and Evaluation Programme (EMEP) and observed atmospheric composition change during 1972–200. *Atmos. Chem. Phys., 12,* 5447-5481, doi:10.5194/acp-12-5447-2012.

Vik, A.F., Myhre, C.L., Stebel, K., Fjæraa, A.M., Svendby, T., Schyberg, H., Gauss, M., Tsyro, S., Schulz, M., Valdebenito, A., Kirkevåg, A., Seland, Ø., Griesfeller, J. (2011) Roadmap towards EarthCARE and Sentinel-5 precursor. A strategy preparing for operational application of planned European atmospheric chemistry and cloud/aerosol missions in Norway. Kjeller, NILU (NILU OR, 61/2011).

Wiedensohler, A., Birmili, W., Nowak, A., Sonntag, A., Weinhold, K., Merkel, M., Wehner, B., Tuch, T., Pfeifer, S., Fiebig, M., Fjäraa, A.M., Asmi, E., Sellegri, K., Depuy, R., Venzac, H., Villani, P., Laj, P., Aalto, P., Ogren, J.A., Swietlicki, E., Williams, P., Roldin, P., Quincey, P., Hüglin, C., Fierz-Schmidhauser, R., Gysel, M., Weingartner, E., Riccobono, F., Santos, S., Grüning, C., Faloon, F., Beddows, D., Harrison, R., Monahan, C., Jennings, S.G., O'Dowd, C.D., Marinoni, A., Horn, H.-G., Keck, L., Jiang, J., Scheckman, J., McMurry, P.H., Deng, Z., Zhao, C.S., Moerman, M., Henzing, B., de Leeuw, G., Löschau, G., Bastian, S. (2012) Mobility particle size spectrometers: harmonization of technical standards and data structure to facilitate high quality long-term observations of atmospheric particle number size distributions. *Atmos. Meas. Tech.*, 5, 657 – 685, doi:10.5194/amt-5-657-2012.

WMO (2014) Greenhouse Gas Bulletin. The state of greenhouse gases in the atmosphere using global observations through 2013. Geneva, World Meteorological Organization (GHG Bulletin No. 10, 9 September 2014). **URL:** http://library.wmo.int/opac/index.php?lvl=notice_display&id=16396#.VGHPz5-gQtK

WMO (2013) Greenhouse Gas Bulletin. The state of greenhouse gases in the atmosphere using global observations through 2012. Geneva, World Meteorological Organization (GHG Bulletin No. 9, 6 November 2013). **URL:** http://www.wmo.int/pages/prog/arep/gaw/ghg/documents/GHG_Bulletin_No.9_en.pdf

WMO (2012) Greenhouse Gas Bulletin. The state of greenhouse gases in the atmosphere using global observations through 2011. Geneva, World Meteorological Organization (GHG Bulletin No. 8, 19 November 2012). **URL:** http://www.wmo.int/pages/prog/arep/gaw/ghg/documents/GHG_Bulletin_No.8_en.pdf

WMO (2011) Scientific assessment of ozone depletion: 2010. Geneva, World Meteorological Organization (Global ozone research and monitoring project, Report No. 52).

Xiong, X., Barnet, C. D., Maddy, E., Sweeney, C., Liu, X., Zhou, L., Goldberg, M. (2008) Characterization and validation of methane products from the atmospheric infrared sounder AIRS. *J. Geophys. Res., 113,* G00A01, doi:10.1029/2007JG000500.

APPENDIX I: Data Tables

Table A1: Annual mean concentration for all greenhouse gases included in the programme at Zeppelin and Birkenes. All concentrations are mixing ratios in ppt, except for methane and carbon monoxide (ppb) and carbon dioxide (ppm). The annual means are based on a combination of the observed methane values and the modelled background values; during periods with lacking observations, we have used the modelled background mixing ratios in the calculation of the annual mean. All underlying measurement data can be downloaded directly from the database: http://ebas.nilu.no/

Component	2001	2002	2003	2004	2005	2006	2007	2008	2009	2010	2011	2012	2013
Carbondioxide - Zeppelin	-	-	-	-	-	-	-	-	-	-	-	394.8	393.1
Carbondioxide - Birkenes	-	-	-	-	-	-	-	-	-	393.7	396.5	397.9	400.7
Methane - Zeppelin	1846.6	1842.9	1855.1	1852.3	1851.6	1853.1	1863.6	1873.5	1888.4	1881.2	1879.6	1891.8	1897.8
Methane - Birkenes	-	-	-	-	-	-	-	-	-	1885.3	1895.5	1900.5	1902.3
Carbon monoxide	123.3	126.0	140.4	131.7	128.4	126.8	120.0	119.6	117.7	126.8	115.4	120.6	113.1
Nitrous oxide	-	-	-	-	-	-	-	-	-	-	324.2	325.0	326.1
Chlorofluorocarbons													
CFC-11*	258.9	257.2	255.3	253.6	251.4	249.4	246.7	244.7	242.7	240.7	238.3	236.6	234.9
CFC-12*	547.1	547.7	547.9	546.0	547.2	546.4	542.5	541.6	537.7	534.5	531.5	528.3	525.2
CFC-113*	81.5	80.8	80.0	79.4	78.7	77.9	77.4	76.8	76.2	75.5	74.6	74.1	73.4
CFC-115*	8.23	8.19	8.24	8.28	8.41	8.39	8.38	8.40	8.43	8.42	8.42	8.44	8.43
Hydrochlorofluorocarbons													
HCFC-22	159.4	164.3	170.0	175.2	181.0	188.8	196.1	204.6	212.6	220.0	225.9	231.5	236.6
HCFC-141b	16.6	17.9	18.8	19.4	19.6	20.0	20.5	21.0	21.5	22.1	23.0	24.0	25.0
HCFC-142b*	14.5	15.0	15.7	16.5	17.1	18.2	19.3	20.4	21.3	22.1	22.7	23.1	23.3
Hydrofluorocarbons													
HFC-125	2.24	2.96	3.56	4.32	4.89	5.62	6.45	7.47	8.58	10.01	11.77	13.55	15.60
HFC-134a	20.8	26.0	30.8	35.6	40.0	44.2	48.6	53.4	57.8	63.5	68.5	73.6	78.9
HFC-152a	2.81	3.48	4.18	4.92	5.65	6.78	7.75	8.65	9.05	9.57	10.04	10.34	10.22
Halons													
H-1211*	4.39	4.44	4.49	4.53	4.52	4.48	4.43	4.39	4.33	4.26	4.18	4.09	3.99
H-1301	2.99	3.07	3.13	3.18	3.21	3.24	3.26	3.27	3.28	3.30	3.32	3.35	3.38
Other halocarbons													
Methylchloride	504.6	521.7	528.6	524.5	520.8	521.4	523.3	523.9	525.9	520.1	509.5	513.4	540.5
Methylbromide	8.88	9.08	8.97	8.94	8.63	8.61	8.34	7.74	7.36	7.28	7.20	7.04	7.02
Dichloromethane	30.6	31.2	32.5	32.5	31.9	33.1	35.0	36.8	37.9	41.4	42.1	45.4	54.1
Chloroform	10.9	10.6	10.8	10.5	10.5	10.5	10.6	10.4	10.8	11.4	11.9	12.1	12.7
Methylchloroform	38.3	32.1	27.2	22.8	19.1	15.9	13.3	11.1	9.2	7.8	6.5	5.4	4.5
Trichloroethylene	0.67	0.59	0.40	0.45	0.39	0.39	0.29	0.33	0.52	0.53	0.54	0.52	0.57
Perchloroethylene	4.63	4.10	3.70	3.68	3.10	2.81	3.01	2.64	2.92	3.04	2.80	2.71	2.54
Sulphurhexafluoride*	4.96	5.14	5.37	5.61	5.82	6.08	6.31	6.63	6.93	7.19	7.50	7.79	8.12

Table A 2: All calculated trends per year, standard error and regression coefficient for the fit. The trends are all in pptv per year, except for CH_4 N_2O, and CO which are in ppbv.

Component	Formula	Trend /yr	Standard errors	R^2
Carbon dioxide - Zeppelin	CO_2	-	-	-
Carbon dioxide - Birkenes		-	-	-
Methane - Zeppelin	CH_4	4.54	0.073	0.776
Methane - Birkenes		-	-	-
Carbon monoxide	CO	-1.28	0.070	0.808
Nitrous oxide	N_2O	-	-	-
Chlorofluorocarbons				
CFC-11*	CCl_3F	-2.07	0.007	0.985
CFC-12*	CF_2Cl_2	-1.9	0.017	0.895
CFC-113*	CF2ClCFCl2	-0.67	0.002	0.981
CFC-115*	CF_3CF_2Cl	0.020	0.001	0.375
Hydrochlorofluorocarbons				
HCFC-22	$CHClF_2$	6.785	0.008	0.997
HCFC-141b	$C_2H_3FCl_2$	0.608	0.002	0.981
HCFC-142b*	CH_3CF_2Cl	0.819	0.001	0.996
Hydrofluorocarbons				
HFC-125	CHF_2CF_3	1.052	0.001	0.998
HFC-134a	CH_2FCF_3	4.746	0.004	0.999
HFC-152a	CH_3CHF_2	0.680	0.002	0.987
Halons				
H-1211*	$CBrClF_2$	-0.037	0.000	0.964
H-1301	$CBrF_3$	0.028	0.000	0.726
Halogenated compounds				
Methylchloride	CH_3Cl	-0.01	0.079	0.882
Methylbromide	CH_3Br	-0.196	0.002	0.858
Dichloromethane	CH_2Cl_2	1.62	0.012	0.942
Chloroform	$CHCl_3$	0.135	0.003	0.747
Methylchloroform	CH_3CCl_3	-2.684	0.002	0.999
Trichloroethylene	$CHClCCl_2$	0.002	0.002	0.331
Perchloroethylene	CCl_2CCl_2	-0.139	0.006	0.322
Sulphurhexafluoride*	SF_6	0.265	0.000	0.996

Table A 3: Monthly means and standard deviation of aerosol optical depth (AOD) at 500 nm at Ny-Ålesund.

Month/Year	Mar	Apr	May	Jun	Jul	Aug	Sep
Aerosol optical depth (AOD)							
2002		0.06±0.01	0.08±0.03	0.06±0.02	0.07±0.12	0.07±0.08	0.06±0.05
2003	0.15±0.12	0.11±0.05	0.15±0.06	0.10±0.03	0.04±0.01	0.05±0.02	0.06±0.03
2004	0.06±0.00	0.12±0.08	0.13±0.09	0.06±0.01	0.10±0.07	0.05±0.02	0.04±0.02
2005	0.08±0.03	0.12±0.07	0.10±0.03	0.05±0.02	0.05±0.02	0.04±0.03	0.03±0.01
2006	0.12±0.03	0.16±0.07		0.04±0.00	0.05±0.02	0.05±0.04	0.04±0.03
2007		0.10±0.05	0.10±0.12	0.07±0.03	0.05±0.01	0.05±0.02	0.04±0.03
2008	0.13±0.05	0.14±0.06	0.14±0.04	0.06±0.02	0.06±0.02	0.09±0.03	0.16±0.03
2009			0.11±0.03	0.08±0.02	0.11±0.04	0.10±0.02	0.09±0.01
2010	0.11±0.03	0.08±0.03	0.08±0.01	0.06±0.01	0.05±0.01	0.05±0.01	
2011			0.08±0.02	0.08±0.01	0.05±0.01	0.06±0.02	0.05±0.01
2012	0.10±0.03	0.10±0.02	0.10±0.03	0.06±0.02	0.06±0.02	0.07±0.03	0.07±0.03
2013	**0.11±0.04**	**0.09±0.04**	**0.06±0.02**	**0.05±0.01**	**0.06±0.02**	**0.05±0.01**	**0.04±0.02**
Mean (02-13)	**0.11±0.04**	**0.10±0.04**	**0.10±0.04**	**0.06±0.02**	**0.06±0.04**	**0.06±0.03**	**0.05±0.03**

Table A 4: Monthly means and standard deviation of the Ångström coefficient (Å) at Ny-Ålesund.

Month/Year	Mar	Apr	May	Jun	Jul	Aug	Sep
Ångström coefficient (Å)							
2002		0.9±0.1	1.4±0.1	1.2±0.3	1.2±0.2	1.3±0.4	1.2±0.5
2003	0.9±0.5	1.3±0.3	1.3±0.2	1.5±0.1	1.5±0.3	1.4±0.5	1.4±0.3
2004	1.3±0.1	1.2±0.3	1.4±0.5	1.7±0.2	1.6±0.4	1.5±0.3	1.3±0.3
2005	1.1±0.3	1.4±0.4	1.0±0.2	1.6±0.3	1.7±0.2	1.4±0.7	1.5±0.4
2006	0.9±0.1	0.9±0.3		1.7±0.2	1.4±0.3	1.3±0.6	1.4±0.3
2007		1.4±0.4	1.4±0.6	1.7±0.2	1.6±0.2	1.7±0.3	1.5±0.4
2008	1.4±0.2	1.3±0.2	1.4±0.2	1.4±0.4	1.2±0.2	1.3±0.3	1.4±0.3
2009			1.3±0.4	1.4±0.2	1.3±0.3	1.2±0.1	1.1±0.1
2010	1.0±0.3	1.4±0.2	1.3±0.2	1.3±0.3	1.4±0.2	1.0±0.1	
2011			1.7±0.3	1.8±0.1	1.5±0.1	1.4 ±0.3	1.6±0.2
2012	1.1±0.2	1.3±0.2	1.2±0.2	1.1±0.1	1.3±0.2	1.4±0.2	1.5±0.2
2013	**1.3±0.2**	**1.2±0.3**	**1.4±0.2**	**1.6±0.3**	**1.3±0.2**	**1.4±0.2**	**1.2±0.5**
Mean (02 -13)	1.3±0.4	1.4±0.5	1.5±0.5	1.6±0.5	1.5±0.5	1.5±0.5	1.7±0.7

Table A 5: Number of days with AOD observations at Ny-Ålesund made within the months.

Month/Year	Mar	Apr	May	Jun	Jul	Aug	Sep
Number of days with cloud-free and quality assured observations							
2002		4	15	11	6	9	14
2003	3	12	16	8	15	17	12
2004	2	8	13	9	5	12	12
2005	12	17	24	15	10		11
2006	6	12			5	12	4	13
2007		16	9	12	17	10	9
2008	15	12	14	20	16	13	2
2009				7	10	17	8	8
2010	7	18	7	10	12	3	1
2011			2	2	7	4	6
2012	6	18	12	15	16	11	4
2013	**5**	**13**	**10**	**10**	**8**	**7**	**9**
Total (02-13)	**56**	**130**	**129**	**127**	**141**	**98**	**101**

Month/Year	Mar	Apr	May	Jun	Jul	Aug	Sep

Table A 6: Monthly means and standard deviation of aerosol optical depth (AOD) at 500 nm at Birkenes.

Month/ Year	Jan	Feb	Mar	Apr	May	Jun	Jul	Aug	Sep	Oct	Nov
Aerosol optical depth (AOD)											
2009				0.29 ±0.00	0.09 ±0.05	0.09 ±0.05	0.18 ±0.06	0.17 ± 0.07	0.10 ± 0.04	0.08 ±0.03	
2010					0.10 ±0.04	0.09 ±0.04	0.10 ±0.07	0.10 ±0.05	0.05 ±0.02	0.07 ±0.03	0.04 ±0.01
2011	0.02 ±0.01	0.03 ±0.01	0.07 ±0.02	0.21 ±0.19	0.13 ±0.07	0.10 ±0.04	0.13 ±0.06	0.09 ±0.05			
2012			0.07 ±0.05	0.05 ±0.02	0.08 ±0.04	0.09 ±0.04	0.07 ±0.03	0.08 ±0.03	0.07 ±0.01	0.06 ±0.03	0.04 ±0.00
2013							**0.17 ±0.17**	**0.12 ±0.09**	**0.05 ±0.03**	**0.05 ±0.03**	
Mean 09-13	**0.02 0.01**	**0.03 ±0.01**	**0.07 ±0.03**	**0.16 ±0.17**	**0.10 ±0.05**	**0.09 ±0.04**	**0.13 ±0.11**	**0.11 ±0.07**	**0.07 ±0.04**	**0.07 ±0.03**	**0.04 ±0.01**

Table A 7: Monthly means and standard deviation of the Ångström coefficient (Å) at Birkenes

Month/ Year	Jan	Feb	Mar	Apr	May	Jun	Jul	Aug	Sep	Oct	Nov
Ångström coefficient (Å)											
2009				1.5 ±0.0	1.2 ±0.3	1.4 ±0.3	1.4 ±0.4	1.1 ±0.2	1.0 ±0.2	1.1 ±0.2	
2010					1.3 ±0.3	1.4 ±0.3	1.4 ±0.2	1.4 ±0.2	1.3 ±0.3	1.3 ±0.3	1.3 ±0.23
2011	1.0 ±0.2	1.0 ±0.1	1.0 ±0.3	1.2 ±0.5	1.3 ±0.3	1.5 ±0.3	1.6 ±0.3	1.6 ± 0.1			
2012			1.1 ±0.4	1.6 ±0.3	1.4 ±0.4	1.7 ±0.1	1.6 ±0.3	1.5 ±0.3	1.1 ±0.3	1.4 ±0.4	0.8 ±0.3
2013							**1.3 ± 0.2**	**1.2 ±0.3**	**0.8 ±0.2**	**0.8 ±0.3**	
Mean 09-13	**1.0 ±0.1**	**1.0 ±0.0**	**1.0 ±0.4**	**1.3 ±0.4**	**1.3 ±0.3**	**1.5 ±0.2**	**1.4 ±0.3**	**1.4 ±0.3**	**1.1 ±0.3**	**1.2 ±0.3**	**1.2 ±0.3**

Table A 8: Number of days with AOD observations at Birkenes made within the months.

Month/Year	Jan	Feb	Mar	Apr	May	Jun	Jul	Aug	Sep	Oct	Nov
Number of days with cloud-free and quality assured observations (lev 2; lev 1.5 for 2013)											
2009				1	22	25	11	13	15	12	
2010					13	16	18	15	16	10	6
2011	7	2	20	23	18	20	15	13			
2012			11	12	10	7	16	18	9	12	2
2013							26	18	13	7	
Total	**7**	**2**	**31**	**36**	**63**	**68**	**86**	**77**	**53**	**41**	**8**

APPENDIX II

Description of instruments and methodologies

In this appendix are the instrumental methods used for the measurements of the various greenhouse gases presented. Additionally we explain the theoretical methods used in the calculation of the trends.

Details about greenhouse gas measurements and recent improvement and extensions

Table A 9: Instrumental details for greenhouse gas measurements at Zeppelin and Birkenes.

Component		Instrument and method	Time res.	Calibration procedures	Start - End	Comment
Methane (Birkenes)	CH_4	Picarro CRDS G1301 CO2/CH4/H2O	5 s	Working std. calibrated against GAW stds at EMPA	19. May 2009 ->	Data coverage in 2013 was 97%
Methane (Zeppelin)	CH_4	GC-FID/	1 t	NOAA reference standards	Aug 2001-Apr 2012	
Methane (Zeppelin)	CH_4	Picarro CRDS	5 sec	NOAA reference standards	20.Apr. 2012 ->	Data coverage 2013: 97%
Nitrous oxide (Zeppelin)	N_2O	GC-FID	30 min	Hourly, working std. calibrated vs. NOAA stds		Data coverage 2013 96%
Carbon monoxide (Zeppelin)	CO	GC-HgO/UV	20 min	Every 20 min, working std. calibrated vs. GAW std.	15.Sep.20 012012	Data coverage 2012: discontinued after 2012
Carbon monoxide (Zeppelin)	CO	Picarro CRDS	5 sec	NOAA reference standards.	20.Apr 2012 ->	Data coverage 2013: 97%
Carbon dioxide (Zeppelin)	CO_2	LI-COR Picarro CRDS from 20.4.2012	1 h 5 sec	NOAA reference standards	1989 - 2012 20.Apr. 2012 ->	CO_2 measurements in cooperation with ITM Stockholm University (SU). Data coverage 2013: 97%
Carbon dioxide (Birkenes)	CO_2	Picarro CRDS G1301 CO2/CH4/H2O	5 s	Working std. calibrated against GAW stds at EMPA		Measurements started 19 May 2009.
CFC-11 CFC-12 CFC-113 CFC-115 HFC-125 HFC-134a HFC-152a HFC-365mfc HCFC-22 HCFC-141b HCFC-142b H-1301 H-1211	$CFCl_3$ CF_2Cl_2 $CF_2ClCFCl_2$ CF_3CF_2Cl CHF_2CF_3 CH_2FCF_3 CH_3CHF_2 $CF_3CH_2CHF_2$ CH_3 CHF_2Cl CH_3CFCl_2 CH_3CF_2Cl CF_3Br CF_2ClBr	ADS-GCMS	4 h	Every 4 hours, working std. calibrated vs. AGAGE std.	4.Jan 2001-2010	This instrument was not in operation in 2012 (se next row). Data coverage 2011: no data reported from this instrument after 31.12.2010 The measurements of the CFCs have higher uncertainty and are not within the required precision of AGAGE. See next section for details.

Table cont.:

Component		Instrument and method	Time res.	Calibration procedures	Comment
Methyl Chloride	CH_3Cl				
Methyl Bromide	CH_3Br				
Methylendichloride	CH_2Cl_2				
Chloroform	$CHCl_3$				
Methylchloroform	CH_3CCl_3				
TriChloroethylene	$CHClCCl_2$				
Perchloroethylene	CCl_2CCl_2				
Sulphurhexafluoride	SF_6				
Tetrafluormethane	CF_4	Medusa-GCMS No. 19	2 h	Every 2 hours, working std. calibrated vs. AGAGE std	Data coverage 2012: 70% .
PFC-116	C_2F_6				
PFC-218	C_3F_8				
PFC-318	$c-C_4F_8$				
Sulphurhexafluoride	SF_6				
Sulfuryl fluoride	SO_2F_2				
HFC-23	CHF_3				
HFC-32	CH_2F_2				
HFC-125	CHF_2CF_3				
HFC-134a	CH_2FCF_3				
HFC-143a	CH_3CF_3				
HFC-152a	CH_3CHF_2				
HFC-227ea	CF_3CHFCF_3				
HFC-236fa	$CF_3CH_2CF_3$				
HFC-245fa	$CF_3CH_2CHF_2$				
HFC-365mfc	$CF_3CH_2CHF_2CH_3$				
HCFC-22	CHF_2Cl				
HCFC-124	$CHClFCF_3$				
HCFC-141b	CH_3CFCl_2				
HCFC-142b	CH_3CF_2Cl				
CFC-11	$CFCl_3$				
CFC-12	CF_2Cl_2				
CFC-113	$CF_2ClCFCl_2$				
CFC-114	CF_2ClCF_2Cl				
CFC-115	CF_3CF_2Cl				
H-1211	CF_3Br				
H-1301	CF_2ClBr				
H-2402	CF_2BrCF_2Br				
Methyl Chloride	CH_3Cl				
Methyl Bromide	CH_3Br				
Methyl Iodide	CH_3I				
Methylendichloride	CH_2Cl_2				
Chloroform	$CHCl_3$				
Methylchloroform	CH_3CCl_3				
Dibromomethane	CH_2Br_2				
Bromoform	$CHBr_3$				
TriChloroethylene	TCE				
Perchloroethylene	PCE				
Ethane	C_2H_6				
Benzene	C_6H_6				
Carbonyl Sulfide	COS				
Ozone	O_3		5 min		

Data quality and uncertainties

Halocarbons

In 2001 – 2010 measurements of a wide range of hydrochlorofluorocarbons, hydrofluorocarbons (HCFC-141b, HCFC-142b, HFC-134a etc.), methyl halides (CH_3Cl, CH_3Br, CH_3I) and the halons (e.g. H-1211, H-1301) were measured with good scientific quality by using ADS-GCMS. The system also measured other compounds like the chlorofluorocarbons, but the quality and the precision of these measurements was not at the same level. Table A 10 shows a list over those species measured with the ADS-GCMS at Zeppelin Observatory. The species that are in blue are of acceptable scientific quality and in accordance with recommendations and criteria of the AGAGE network for measurements of halogenated greenhouse gases. Those listed in red have higher uncertainty and are not within the required precision of AGAGE. There are various reasons for this increased uncertainty; unsolved instrumental problems e.g. possible electron overload in detector (for the CFC's), influence from other species, detection limits (CH_3I, $CHClCCl_2$) and unsolved calibration problems ($CHBr_3$). Since 1.September 2010 the ADS-GCMS was replaced by a Medusa-GCMS system. The uncertainty improved for almost all species (table 9 for details), but there are periods where measurements of the CFC's are still not satisfactory. This is an unsolved problem within the AGAGE network.

Table A 10: ADS-GCMS measured species at Zeppelin from 4.January 2001 to 1. September 2010. Good scientific quality data in Blue; Data with reduced quality data in Red. The data are available through http://ebas.nilu.no. Please read and follow the stated data policy upon use.

Compound	Typical precision (%)	Compound	Typical precision (%)
SF_6	1.5	H1301	1.5
HFC134a	0.4	H1211	0.4
HFC152a	0.6	CH_3Cl	0.6
HFC125	0.8	CH_3Br	0.8
HFC365mfc	1.7	CH_3I	5.1
HCFC22	0.2	CH_2Cl_2	0.4
HCFC141b	0.5	$CHCl_3$	0.3
HCFC142b	0.5	$CHBr_3$	15
HCFC124	2.3	CCl_4	0.5
CFC11	0.3	CH_3CCl_3	0.6
CFC12	0.3	$CHClCCl_2$	1.2
CFC113	0.2	CCl_2CCl_2	0.7
CFC115	0.8		

Table below gives an overview over the species measured with the Medusa-GCMS systems at the AGAGE stations and the typical precision with the different instruments. The Medusa-GCMS instrument at the Zeppelin Observatory meet the same criteria as shown in the table.

Table A 11: AGAGE measured species.

Compound	Typical precision (%)	Compound	Typical precision (%)
CF4	0.15	H1301	1.5
C2F6	0.9	H1211	0.5
C3F8	3	H2402	2
SF6	0.4	CH3Cl	0.2
SO2F2	1.6	CH3Br	0.5
HFC23	0.7	CH3I	2
HFC32	5	CH2Cl2	0.8
HFC134a	0.4	CHCl3	0.6
HFC152a	1.2	CHBr3	0.6
HFC125	1	CCl4	1
HFC143a	1.2	CH3CCl3	0.7
HFC365mfc	10	CHClCCl2	2.5
HCFC22	0.3	CCl2CCl2	0.5
HCFC141b	0.4	C2H2	0.5
HCFC142b	0.6	C2H4	2
HCFC124	2	C2H6	0.3
CFC11	0.15	C6H6	0.3
CFC12	0.05	C7H8	0.6
CFC13	2		
CFC113	0.2		
CFC114	0.3		
CFC115	0.8		

Methane

Harmonisation of historic concentration measurements (http://www.ingos-infrastructure.eu/) during 2012. All original measurement signals have been processed with new improved software to recalculate every single measurement over the last 12 years. This new software facilitates systems for QA/QC and detection of measurement errors. The data series has got a clean-up and the precision of existing measurements has improved.Over the last 12 years period a selected number of working standards have been stored and in 2012 it was analysed against new reference standards using new improved instrumentation. All other working standards are linked to these through comparative measurements. Hence, all calibrations over the 12 year period have been recalculated and the whole time series adjusted accordingly.

There were two instruments, the GC-FID and a new Picarro (Cavity Ring-Down Spectrometer) run in parallel in 2012. The Picarro also participated in a GAW audit during autumn 2012 with

good results. Comparisons of the data from the two instruments are shown below. The revised data series I reported to InGOS and also available in http://ebas.nilu.no.

N₂O measurements

N_2O is measured using a gas chromatograph with an electron capture detector. The instrument has performed well during the period, but have a gap in measurements late fall 2012 due to problems with delivery of carrier gas. The instrument needs a special gas mixture to perform well. This special gas has long delivery times from the producer. When the gas purchased turned out to be the wrong mixture it took two months to get a new batch delivered, resulting in a data coverage of only 68% for the year 2012.
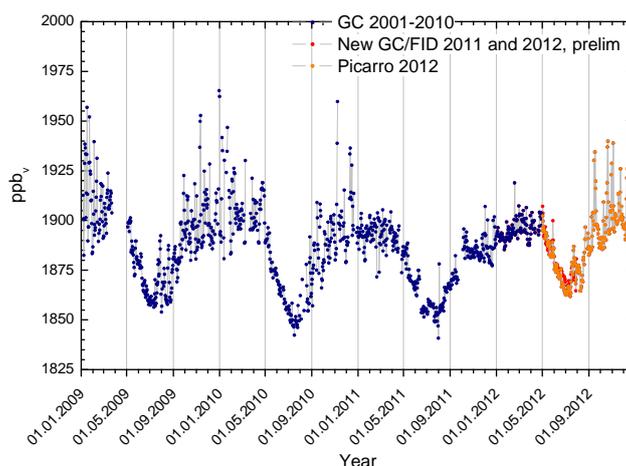

Figure 41: Daily mean of methane measured with the old GC (2001-2010), new GC-FID in 2011 -> and a new Picarro (Cavity Ring-Down Spectrometer) run in parallel in 2012.

CO₂ measurements

At the Zeppelin station carbon dioxide (CO_2) is monitored in cooperation withStockholm University (Institute of Applied Environmental Research, ITM). SU maintained a continuous infrared CO_2 instrument, which has been monitoring from 1989 to summer 2013. This instrument was run in parallel with NILUs new cavity ring down instrument for one year before it was stopped. Measurements are since then monitored by NILUs instrument and calibrated against SU-ITM's set of NOAA reference standards as a cooperation between the two institutes. Both methods were included in the GAW audit in September 2012, showing good results for both methods and good consistency between instruments.

The continuous data are enhanced by the weekly flask sampling programme in co-operation with NOAA CMDL. Analysis of the flask samples provides CH_4, CO, H_2, N_2O and SF_6 data for the Zeppelin Observatory.

Air inlet at Zeppelin

In 2011 the air inlet for the GHG measurements at Zeppelin were improved to reduce possible influence from the station and visitors at the station. The inlet was moved away from the station and installed in a 15 m tower nearby for the following components:

- N_2O
- CH_4
- CO_2
- CO
- Halogenated compounds
- NOAA flaks sampling program
- Isotope flask sampling of CO_2 and CH_4
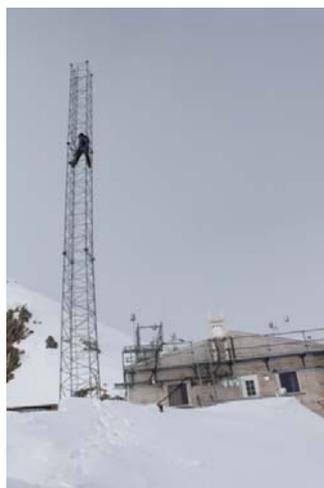
NILU engineer Are Bäcklund about to install a new air inlet for the Medusa instrument. Photo: Ove Hermansen, NILU

Calculation of trends for greenhouse gases

To calculate the annual trends the observations have been fitted as described in Simmonds et al. (2006) by an empirical equation of Legendre polynomials and harmonic functions with linear, quadratic, and annual and semi-annual harmonic terms:

$$f(t) = a + b\left(\frac{N}{12}\right)\cdot P_1\left(\frac{t}{N}-1\right) + \frac{1}{3}\cdot d\left(\frac{N}{12}\right)^2 \cdot P_2\left(\frac{t}{N}-1\right) + c_1 \cdot \cos\left(2\pi t\right) + s_1 \sin\left(2\pi t\right) + c_2 \cos\left(4\pi t\right) + s_2 \sin\left(4\pi t\right)$$

The observed *f* can be expressed as functions of time measures from the 2N-months interval of interest. The coefficient *a* defines the average mole fraction, *b* defines the trend in the mole fraction and *d* defines the acceleration in the trend. The *c* and *s* define the annual and inter-annual cycles in mole fraction. N is the mid-point of the period of investigation. P_i are the Legendre polynomials of order *i*.

Determination of background data

Based on the daily mean concentrations an algorithm is selected to find the values assumed as clean background air. If at least 75% of the trajectories within +/- 12 hours of the sampling day are arriving from a so-called clean sector, defined below, one can assume the air for that specific day to be non-polluted. The remaining 25% of the trajectories from European, Russian or North-American sector are removed before calculating the background.

On the surface in situ observations of aerosol microphysical and optical properties at Birkenes

With respect to microphysical aerosol properties, the particle number size distribution (PNSD) is observed at surface-level at Birkenes. The relevant and observed particle sizes cover a range of 0.01 µm – 10 µm in particle diameter. The diameter range of 1.0 µm – 10 µm is commonly referred to as coarse mode, the range $D_p < 1.0$ µm as fine mode. The fine mode is separated further into Aitken-mode (0.01 µm $< D_p <$ 0.1 µm) and accumulation mode (0.1 µm $< D_p <$ 1 µm). The distinction of these modes is justified by different predominant physical processes as function of particle size. In the Aitken-mode, particles grow by condensation of precursor gases from the gas-phase, and coagulate among themselves or with accumulation mode particles. Accumulation mode particles grow by taking up Aitken-mode particles or by mass uptake while being activated as cloud droplets, and they are removed by precipitation. Coarse mode particles in turn are formed by break-up of biological or crustal material, including pollen, bacteria, and fungus spores, and removed by gravitational settling and wet removal. The PNSD of an aerosol is needed for quantifying any interaction or effect of the aerosol since all of them depend strongly on particle size.

To measure the PNSD at Birkenes, 2 measurement principles are combined. A Differential Mobilty Particle Spectrometer (DMPS) measures the particle number size distribution, now in the range of 0.01 – 0.8 µm particle diameter after several improvements of the instrument. In a DMPS, the particles in the sample air stream are put into a defined state of charge by exposing them to an ionised atmosphere in thermal equilibrium. The DMPS uses a cylindrical capacitor to select a narrow size fraction of the particle phase. The particle size in the selected size fraction is determined by the voltage applied to the capacitor. The particle number concentration in the selected size fraction is then counted by a Condensation Particle Counter (CPC). A mathematical inversion that considers charge probability, diffusional losses of particles in the system, transfer function of the capacitor, and counting efficiency of the CPC is then used to calculate the particle number size distribution. The PNSD of particles with diameters 0.25 µm $< D_p <$ 30 µm is measured with an Optical Particle Spectrometer (OPS). In the OPS, the particles in the sample stream are focussed through a laser beam. The instrument registers number and amplitude of the pulses of light scattered by the particles. The particle pulses are sorted into a histogram by their amplitude, where the pulse amplitude yields the particle diameter and the pulse number the particle concentration, i.e. together the PNSD. Both, the DMPS and the OPS, yield method specific measures of the particle diameter, the electrical mobility and the optical particle diameter, respectively. When related to the spherical equivalent geometric particle diameter commonly referred to, both particle size measures depend on particle shape (causing a 5% systematic uncertainty in particle diameter), the optical particle diameter in addition on particle refractive index (causing a 20% systematic uncertainty in particle diameter). In this report, the PNSDs provided by DMPS and OPS are joined into a common PNSD. To quality assure this process, PNSDs are accepted only if DMPS and OPS PNSD agree within 25% in particle diameter in their overlap size range. Together, both

instruments provide a PNSD that spans over 3 orders of magnitude in particle diameter, and over 6 orders of magnitude in particle concentration.

Another microphysical property measured at Birkenes is the Cloud Condensation Nuclei (CCN) Concentration, i.e. the concentration of particles that could act as condensation nuclei for liquid-phase cloud droplets, which is a property depending on the water vapour supersaturation. The corresponding instrument, a Cloud Condensation Nucleus Counter (CCNC), exposes the aerosol sample to an "artificial cloud" of defined supersaturation, and counts the cloud activated particles optically. Observations of the CCN concentration are essential for quantifying the indirect aerosol climate effect. The CCNC at Birkenes has been in operation since 2012, but is currently not included in the monitoring programme.

Optical aerosol parameters quantify the direct aerosol climate effect. The observation programme at Birkenes includes the spectral particle scattering coefficient $\sigma_{sp}(\lambda)$ and the spectral particle absorption coefficient $\sigma_{ap}(\lambda)$. The scattering coefficient quantifies the amount of light scattered by the aerosol particle population in a sample per distance a light beam travels through the sample. The absorption coefficient is the corresponding property quantifying the amount of light absorbed by the particle population in the sample. An integrating nephelometer is used for measuring $\sigma_{sp}(\lambda)$ at 450, 550, and 700 nm wavelength. In this instrument, the optical sensors look down a blackened tube that is filled with aerosol sample. The tube is illuminated by a light source with a perfect cosine intensity characteristic perpendicularly to the viewing direction. It can be shown mathematically that this setup integrates the scattered light seen by the optical sensors over all scattering angles. The particle absorption coefficient $\sigma_{ap}(\lambda)$ is measured by 2 Particle Soot Absorption Photometers (PSAPs). A PSAP infers $\sigma_{ap}(\lambda)$ by measuring the decrease in optical transmissivity of a filter while the filter is loaded with the aerosol sample. The transmissivity time series is subsequently translated into an absorption coefficient time series by using Lamber-Beer's law, the same law also used in optical spectroscopy. The PSAPs deployed at Birkenes are a home-built 1 wavelength version that has received quality assurance by intercomparisons within the EU network and infrastructure projects EUSAAR (European Supersites for Atmospheric Aerosol Research) and ACTRIS (Aerosols, Clouds, and Trace gases Research InfraStructure Network), and a 3-wavelength version. Both instruments are interpreted in combination to benefit from both, quality assurance in a research network and spectral capabilities. For comparison with the nephelometer, the PSAP data has been transferred to a wavelength of 550 nm assuming an absorption Ångström coefficient åap of -1, adding 2% systematic uncertainty to the data. The correction factor found for one Birkenes PSAP during the recent intercomparison workshop has been included in the analysis.

All in situ observations of aerosol properties representing the ground-level are conducted for the aerosol at dry-state (RH < 40%) for obtaining inter-comparability across the network.

Details about aerosol optical depth measurements

The amount of particles in the air during sunlit conditions is continuous monitored by means of a Precision-Filter-Radiometer (PFR) sun photometer, located at the Sverdrup station in Ny-Ålesund and a Cimel instrument at Birkenes. The observations in Ny-Ålesund are performed in collaboration with PMOD/WRC (C. Wehrli), Davos, Switzerland. The main instrument characteristics are given below.
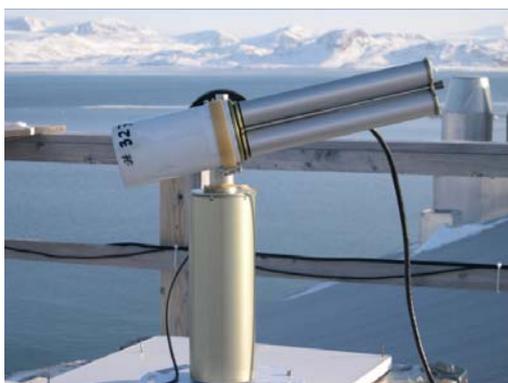
AERONET - Cimel C-318

- Sun (9 channels) and sky radiances
- Wavelength range: 340-1640 nm
- 15 min sampling
- No temperature stabilization
- AOD uncertainty: 0.01-0.02

PFR-GAW- Precision Filter Radiometer

- Direct sun measurements (4 channels)
- Wavelength range: 368 - 862 nm
- 1 min averages
- Temperature stabilized
- AOD uncertainty: 0.01

Figure 42: Photos and typical features of the standard instrument of the AERONET (left panel) and GAW PFR network instruments (right panel)

The sun-photometer measurements in Ny-Ålesund are part of the global network of aerosol optical depth (AOD) observations, which started in 1999 on behalf of the WMO GAW program. The instrument is located on the roof of the Sverdrup station, Ny-Ålesund, close to the EMEP station on the Zeppelin Mountain (78.9°N, 11.9°E, 474 m a.s.l.). The Precision Filter Radiometer (PFR) has been in operation since May 2002. In Ny-Ålesund the sun is below 5° of elevation from 10 October to 4 March, limiting the period with sufficient sunlight to the spring-early autumn season. However, during the summer months it is then possible to measure day and night if the weather conditions are satisfactory. The instrument measures direct solar radiation in four narrow spectral bands centered at 862 nm, 501 nm, 411 nm, and 368 nm. Data quality control includes instrumental control like detector temperature and solar pointing control as well as objective cloud screening. Measurements are made at full minutes are averages of 10 samples for each channel made over a total duration of 1.25 seconds. SCIAMACHY TOMSOMI ozone columns and meteorological data from Ny-Ålesund are used for the retrieval of aerosol optical depth (AOD).

Aerosol optical depth measurements started at the new Birkenes observatory in spring 2009, utilizing an automatic sun and sky radiometer (CIMEL type CE-318), with spectral interference filters centered at selected wavelengths: 340 nm, 380 nm, 440 nm, 500 nm, 675 nm, 870 nm, 1020 nm, and 1640 nm. The measurement frequency is approximately 15 minutes (this depends on the air-mass and time of day). Calibration was performed in Izaña in the period 13 May to 24 of July 2008 (RIMA-AERONET sub-network). Between 11 December 2009 and 26 January 2010 and between 16 September and November 2011, at Autilla del Pino (Palencia, Spain), the operational calibration platform managed by GOA for RIMA-AERONET sun photometers. In the context of ACTRIS (**A**erosols, **C**louds, and **T**race gases **R**esearch **I**nfra **S**tructure Network, an EU (FP7) project) Transnational Access instrument calibration has been completed 14 May 2013 at

the *GOA-UVA (Spain)* installation of the AERONET-EUROPE Calibration Service Centre. Raw data are processed and quality assured centrally by AERONET. The instrument has been sent for calibration to *GOA-UVA (Spain*) in October 2014. Data reported for 2009 - 2012 are quality assured AERONET level 2.0 data, which means they have been pre- and post field calibrated, automatically cloud cleared and have been manually inspected by AERONET. Observations in 3013 have been obtained in the time period between June and December. Data reported for 2013 are AERONET level 1.5 data, which implies that they have been automatically cloud cleared, but have not yet been post field calibrated. An additional manual cloud-screening has been performed to quality assure the dataset from the most recent year.

Outlook on observations of aerosol optical depth in Ny-Ålesund beyond 2013

Two observational initiatives and collaborations should be mentioned here:

1. Collaborative observations between NILU and the Alfred Wegener Institute (AWI, Germany) using a sun-photometer on top of the Zeppelin Mountain, which is a unique opportunity to separate the boundary layer contribution from the total column, and thereby get new insides into the contribution of local versus long-range transport of aerosols. AWI financed the instruments, NILU had ordered the a solar-tracker in 2012, but due to long delivery times, only in spring 2013, measurements on a more routine bases started. In 2013 an instrumental failure limited the observations to spring/early summer, a longer observational data set exists from 2014. The scientific evaluation of the data is ongoing and results will be reported in 2015.

2. Currently, a major obstacle to obtaining a complete year around AOD climatology in the Arctic arises from the long polar night. To fill gaps in the aerosol climatology plans are ongoing to deploy and test a lunar photometer to Ny-Ålesund in autumn 2014. This is a collaborative initiative between PMOD/WRC, ISAC-CNR, NILU and others. Seed money for this activity has been received from the Svalbard Science Forum. Initial results from the observations, e.g. lunar observations made during the night of the 5 and 6 November, are very promising.

APPENDIX III: Abbreviations

Abbreviation	Full name
ACTRIS	Aerosols, Clouds, and Trace gases Research InfraStructure Network
ADS-GCMS	Adsorption-Desorption System – Gas Chromatograph Mass Spectrometer
AERONET	Aerosol Robotic Network
AGAGE	Advanced Global Atmospheric Gases Experiment
AIRS	Atmospheric Infrared Sounder
AMAP	Arctic Monitoring and Assessment
AOD	Aerosol optical depth
AWI	Alfred Wegener Institute
BC	Black carbon
CAMP	Comprehensive Atmospheric Monitoring Programme
CCN	Cloud Condensation Nuclei
CCNC	Cloud Condensation Nucleus Counter
CFC	Chlorofluorocarbons
CLTRAP	Convention on Long-range Transboundary Air Pollution
CO	Carbon monoxide
CPC	Condensation Particle Counter
DMPS	Differential Mobility Particle
EMEP	European Monitoring and Evaluation Programme
ERF	Effective radiative forcing ERF
ERFaci	ERF due to aerosol–cloud interaction
EU	European Union
EUSAAR	European Supersites for Atmospheric Aerosol Research
GAW	Global Atmosphere Watch
GB	Ground based
GOA-UVA	Atmospheric Optics Group of Valladolid University
GOSAT	Greenhouse Gases Observing Satellite
GWP	Global Warming Potential
HCFC	Hydrochlorofluorocarbons
HFC	Hydrofluorocarbons
ICOS	Integrated Carbon Observation System
InGOS	Integrated non-CO2 Greenhouse gas Observing System

Abbreviation	Full name
IPCC	Intergovernmental Panel on Climate Change
ISAC-CNR	Institute of Atmospheric Sciences and Climate (ISAC) of the Italian National Research Council
ITM	Stockholm University - Department of Applied Environmental Science
MOCA	Methane Emissions from the Arctic OCean to the Atmosphere: Present and Future Climate Effects
NASA	National Aeronautics and Space Administration
NOAA	National Oceanic and Atmospheric Administration
OC	Organic Carbon
ODS	Ozone-depleting substances
OH	Hydroxyl radical
OPS	Optical Particle Spectrometer
OSPAR	Convention for the Protection of the marine Environment of the North-East Atlantic
PFR	Precision filter radiometer
PMOD/WRC	*Physikalisch-Meteorologisches Observatorium Davos/World Radiation Center*
PNSD	Particle number size distribution
ppb	Parts per billion
ppm	Parts per million
ppt	Parts per trillion
PSAP	Particle Soot Absorption Photometers
RF	Radiative forcing
RI	Research Infrastructure
RIMA	Red Ibérica de Medida fotométrica de Aerosoles
SACC	Strategic Aerosol Observation and Modelling Capacities for Northern and Polar Climate and Pollution
SCIAMACHY	SCanning Imaging Absorption spectroMeter for Atmospheric CHartographY
SIS	Strategisk instituttsatsing
SMPS	Scanning Mobility Particle
TES	Tropospheric Emission Spectrometer
TOA	Top Of Atmosphere
TOMS OMI	Total Ozone Mapping Spectrometer Ozone Monitoring instrument

Abbreviation	Full name
UN	United Nations
VOC	Volatile organic compounds
WDCA	World Data Centre for Aerosol
WDCS	World Data Centre of Aerosols
WMGHG	Well-mixed greenhouse gases
WMO	World Meteorological Organization

The Norwegian Environment Agency's primary tasks are to reduce greenhouse gas emissions, manage Norwegian nature, and prevent pollution.

We are under the Ministry of Climate and Environment and have over 700 employees at our two offices in Trondheim and Oslo and at the Norwegian Nature Inspectorate's more than sixty local offices.

Our principal functions include monitoring the state of the environment, conveying environment-related information, exercising authority, overseeing and guiding regional and municipal authorities, cooperating with relevant industry authorities, acting as an expert advisor, and assisting in international environmental efforts.